Characterization of Mge1, a nucleotide exchange factor of mitochondrial Hsp70, under oxidative and thermal stress

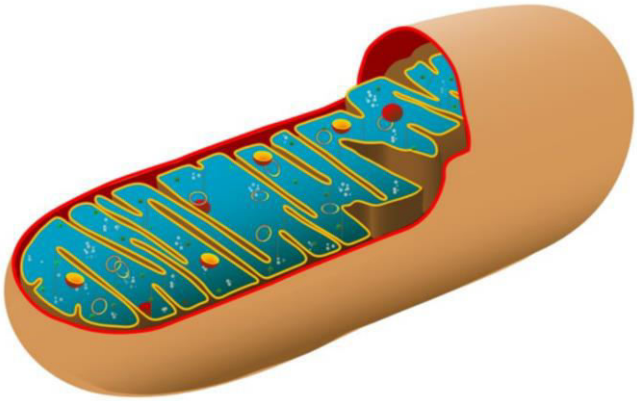

Thesis submitted for the degree of

DOCTOR OF PHILOSOPHY

By

Adinarayana Marada

(09LBPH02)

Department of Biochemistry

School of Life Sciences

University of Hyderabad-500046

India

Department of Biochemistry

School of Life Sciences

University of Hyderabad

Hyderabad 500 046

India

CERTIFICATE

This is to certify that this thesis entitled **"Characterization of Mge1, a nucleotide exchange factor of mitochondrial Hsp70, under oxidative and thermal stress"** submitted to the University of Hyderabad by **Mr. Adinarayana Marada**, for the degree of Doctor of Philosophy, is based on the studies carried out by him under my supervision. I declare to the best of my knowledge that this has not been submitted earlier for the award or diploma from any other University or Institution.

Dr. Naresh Babu V Sepuri

Supervisor

Head

Department of Biochemistry

Dean

School of Life Sciences

Department of Biochemistry

School of Life Sciences

University of Hyderabad

Hyderabad 500 046

India

DECLARATION

I hereby declare that the work presented in my thesis is entirely original and was carried out by me in the Department of Biochemistry, University of Hyderabad, under the supervision of **Dr. Naresh Babu V Sepuri.** I further declare that this work has not been submitted earlier for the award of degree or diploma from any other University or Institution.

Dr. Naresh Babu V Sepuri
Supervisor

Adinarayana Marada

Date:

Place: Department of Biochemistry
University of Hyderabad - 500 046

Acknowledgments

- First and foremost I offer my sincerest gratitude to my supervisor **Dr.Naresh Babu V Sepuri** for his continuous support throughout my research with his motivation, enthusiasm, immense knowledge, invaluable guidance, advice and ideas make my thesis possible here. I could not have imagined having a better advisor and mentor for my Ph.D thesis. He has been invaluable on both an academic and a personal level, for which I am extremely grateful. His attention, moral support and timely suggestions were useful in the preparation of my thesis. I am always grateful to my supervisor for everything

- I am always thankful to my doctoral committee members: Dr. Krishnaveni Mishra and Dr.Suresh Yenugu for their critical comments and invaluable suggestions on my PhD work.

- I would like to thank Heads of Department of Biochemistry (Prof. N. Siva Kumar, Prof. O.H. Setty, Prof. K.V.A Ramaiah) and Deans of School of Life Sciences (Prof. Pallu Reddanna, Prof. A.S Raghavendra, Prof. R.P. Sharma, Prof. Ramanadham) for allowing me to use all the central facilities of department and school.

- I express my gratitude to Dr. Bramanandam Manavathi, Dr. S. Rajagopal, Dr.Suresh Yenugu for moral support, inspiration and encouragement.

- I would like to specially acknowledge Dr. Thanuja Krishnamoorthy for the invaluable suggestions and sparing her valuable time in patiently reading my manuscripts and PhD thesis.

- I thank all faculty members of school of life sciences, I also thank all the non-teaching staff for their timely help.

- I sincerely acknowledge Dr. Mohammed for his help in CD analysis.

- I also thank my lab mates Dr. Pulla Reddy, Dr. Samuel, Dr. Anjaneyulu, Dr.Prasad, Madhavi, Praveen, Ramana, Srinivasu,Yerranna, Manoj, Fareed, Chandrasekhar, Viswamitra,Tejeswani,Sowmya,Naimisha, Yagna priya, Shubi, Ruthvik, Soumik, Nilam and Narasimha for making my stay in the lab wonderful. I particularly thank Praveen, Srinivas and Madhavi for all their help during my PhD.

- I have been really privileged to have friends; Suresh, Vijay N reddy,Ramana, Kiran,Madhu, Janardhan, Shanmuka Kumar, Verma, Surendra, Somusekhar,Tirupati and Chaitu. They literally supported me all through my ups and downs.

- I thank all my Friends for their love and affection

- I acknowledge UGC for my financial support through BSR-JRF and SRF.

- I also thank all the funding bodies (CSIR, UGC, ICMR, DBT, CREBB, DST, FIST, UPE, PURSE) for their financial assistance to the department and school.

- I would like to thank my family for all the love and support. Their love and care always made me happy and forget the bad times.

- Finally, I thank God Almighty for his blessings throughout.

..... Adinarayana Marada

Table of contents

Chapter 2: Characterization of yeast Mge1, a nucleotide exchange factor of mitochondrial Hsp70, under oxidative stress

2.1 Introduction

2.2 Methodology

- 2.2.1 Materials
- 2.2.2 cDNA synthesis
- 2.2.3 Polymerase chain reaction
- 2.2.4 Restriction Digestion
- 2.2.5 Ligation of yeast and human MGE1 with pET28 (a) /pTEF-LEU/URA vector
- 2.2.6 Site Directed Mutagenesis
- 2.2.7 Agarose Gel Electrophoresis
- 2.2.8 Bacterial Transformation
- 2.2.9 Bacterial expression and protein Purification
- 2.2.10 SDS-PAGE analysis
- 2.2.11 Western blot analysis
- 2.2.12 Antibody purification by affinity chromatography
- 2.2.13 Purification of polyclonal Antibodies
- 2.2.14 Preparation of H_2O_2 Solution
- 2.2.15 *In vitro* cross linking of recombinant proteins
- 2.2.16 Circular Dichorism Spectroscopy
- 2.2.17 Coimmuno-precipitation (co-IP)
- 2.2.18 Construction of MGE1 mutant strains
- 2.2.19 Yeast media
- 2.2.20 Serial dilution and H_2O_2 resistance assay
- 2.2.21 Isolation of yeast mitochondria

Chapter 3: Influence of Thermal stress on the structure & functional properties of Mge1, a Mitochondrial component of protein import motor

Acronyms

Acronyms used in this thesis

AAC	ATP/ADP carrier
APS	Ammonium per sulphate
ATP	Adenosine triphosphate
BSA	Bovine serum albumin
BS^3	Bis (sulfosuccinimidyl) suberate
CD	Circular Dichroism
CCPO	Cytochrome C peroxidase
CoxIV	Cytochrome oxidase subunit IV
co-IP	Co-immunoprecipitation
DEPC	Diethylpyrocarbonate
DMSO	Dimethylsulphoxide
SU9-DHFR	Subunit 9 – Dihydrofolate reductase
dNTP	Deoxyribonucleotide triphosphate
DSS	Di succinimidylsuberate
DTT	Dithiothreitol
DCF-DA	2′,7′-Dichlorodihydrofluorescein diacetate
ECL	Enhanced chemiluminescence
EDTA	Ethylene diamine tetra acetic acid
GST	Glutathione *S*-transferase
GROMACS	GROningen MAchine for Chemical Simulations
HEPES	(N-(2-Hydroxyethyl)-piperizine-N'-(2-ethane sulfonic acid)
H_2O_2	Hydrogen peroxide
IgG	Immunoglobulin G
IMS	Inter membrane space
IMM	Inner mitochondrial membrane
IPTG	Isopropyl β-D-thiogalactopyranoside
I-TASSER	Iterative Threading ASSEmbly Refinement
kDa	Kilo Dalton
M	Molar
$MgCl_2$	Magnesium chloride
MPP	Mitochondrial processing peptidase

mtDNA	Mitochondrial deoxyribonucleic acid
Mxrs	Methionine sulfoxide reductases
MAPSCI	Multiple Alignment of Protein Structures and Consensus Identification
HSP	Heat shock protein
NaCl	Sodium chloride
NADH	Nicotinamide adenine dinucleotide
NC	Nitrocellulose
NBD	Nucleotide binding domain
Ni-NTA	Nickel nitrilotriacetic acid
NEF	Nucleotide exchange factor
OD	Optical density
OXPHOS	Oxidative phosphorylation
PAGE	Polyacrylamide gel electrophoresis
PAM	Presequence translocase associated motor
PBS	Phosphate-buffered saline
PCR	Polymerase chain reaction
PDB	Protein data bank
PMSF	Phenyl methylsulfonyl fluoride
PME	Particle Mesh Ewald
ROS	Reactive oxygen species
Rpm	Rotations per minute
RMSD	Root mean square deviation
RMSF	Root mean square fluctuation
SBD	Substrate-binding domain
SAM	Sorting and assembly machinery
SEM	Sucrose-EDTA-MOPS
S. cerevisiae	Saccharomyces cerevisiae
SDS	Sodium dodecyl sulfate
SDS-PAGE	SDS-polyacrylamide gel electrophoresis
Ssc1	Stress-seventy subfamily C
Ssq1	Stess-seventy subfamily Q
Taq	Thermophilus aquaticus
TBS	Tris-buffered saline
TBST	Tris-buffered saline Tween20

TEMED	N,N,N‘,N‘-tetramethylethylene diamine
TIM	Translocase of inner mitochondrial membrane
TOM	Translocase of outer mitochondrial membrane
Tris	Tris-(Hydroxymethyl) aminoethane
ΔΨm	Mitochondrial inner membrane potential
YPD	Yeast Extract, Peptone, Dextrose

Chapter 1

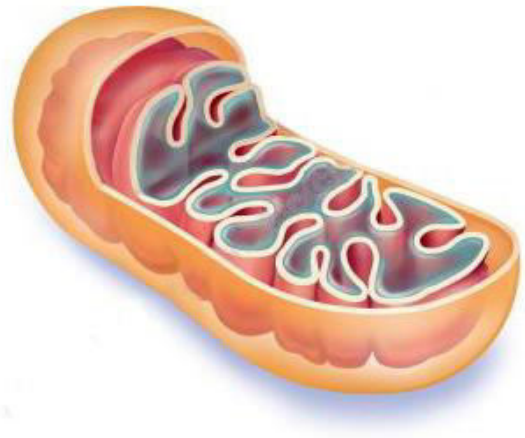

INTRODUCTION

1.1 Mitochondria

The mitochondrion is a membrane bound organelle found in almost all eukaryotic cells [1]. It is typically round or oval in shape, 0.5 to 1.5 μM wide and 1-2 μM long in size. Depending on the organism, tissue type and level of cellular metabolic activity, a cell may contain just one or several mitochondria. Mitochondria are considered as “the powerhouse of the cell" because they are the main sites of adenosine triphosphate (ATP) production in cells through the process known as oxidative phosphorylation (OXPHOS). Besides ATP production, mitochondria also play an important role in lipid, carbohydrate, nucleotide and amino acid metabolism, cellular calcium homeostasis, apoptosis, heme synthesis and Fe/S cluster biogenesis [2]–[5].

1.2 Structure of mitochondria

Mitochondria are surrounded by two membranes. The two membranes, outer and inner membrane, divide the mitochondrion into two separate aqueous compartments, the intermembrane space (IMS), the space between outer and inner membrane, and the mitochondrial matrix (Fig.1). The membranes are made up of phospholipids and proteins [6]. The outer membrane (OM) is smooth and composed of phospholipids and proteins in a ratio of 1:1. The outer membrane is permeable to ions, water, nutrients, energy molecules (ADP, ATP), metabolites and proteins that are less than10 kDa. The permeability of outer membrane is mainly due to the presence of large pore like structures called porins. Porins are beta barrel proteins that forms large aqueous channels across the lipid bilayer of the membrane [7], [8]. Outer membrane contains protein import receptors and enzymes that are involved in lipid synthesis, and the machinery for the division and fusion of the mitochondrion [9].

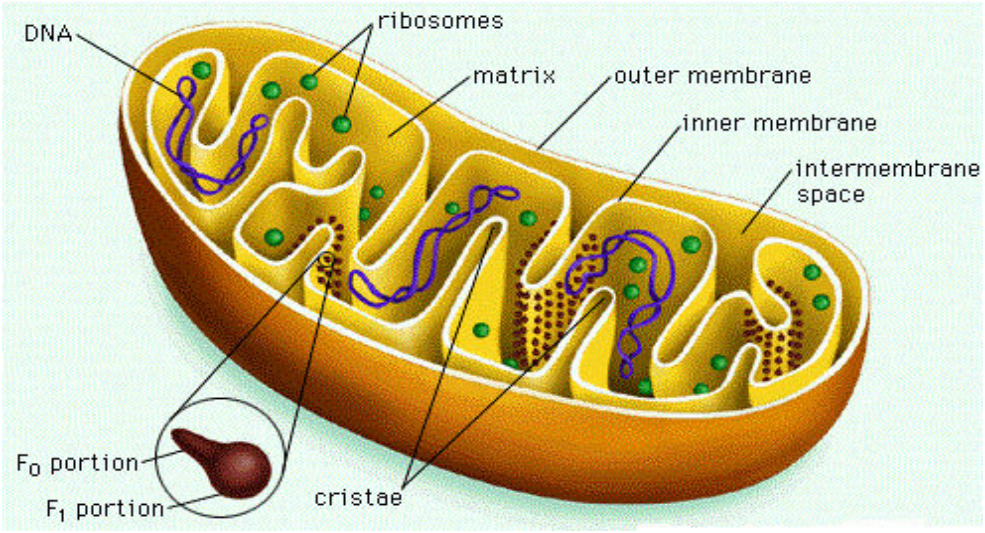

Figure 1.1 The general organization of mitochondrion

Figure shows the major compartments of mitochondria: the outer membrane,the inter membrane space , inner membrane folded into cristae and mitochondrial matrix.
(Image source from of http://uhscellprojects2010.wikispaces.com/Mitochondria)

The inner membrane (IM) is a more complex structure and impermeable to metabolites and ions. Inner membrane contains transporters to facilitate the movement of molecules in and out of the matrix [10], [11]. In addition, inner membrane contains the electron transport chain (ETC) complexes, ATP synthase and protein import machineries [12]. The inner membrane is folded into cristae that project into the matrix in order to increase the surface area of the membrane.The amount of folding of the inner membrane is determined by the energy requirements of the cell [13]. The inter mitochondrial space is located in between the outer and inner membrane that facilitates the transfer of ATP molecules out of the matrix and into the cytosol [14].

The mitochondrial matrix is enclosed within the inner membrane.It contains enzymes required for several metabolic pathways that includes tricarboxylic acid cycle (TCA), fatty acid oxidation, heme synthesis and Fe/S cluster biogenesis [6]. The matrix also contains ribosomes, tRNAs, mtDNA and enzymes required for mitochondrial gene expression.

Mitochondria import most of their phospholipids from the cytoplasm to maintain their membranes [15]. Cardiolipin is an acidic and hydrophobic phospholipid required for the function of many mitochondrial proteins such as cytochrome *c* oxidase. The amount of Cardiolipin in mitochondrial inner membrane is changed in response to the level of thyroid hormones [16]–[18].

1.3 Mitochondrial DNA

In mammalian cells, each mitochondrion harbors 2–10 copies of mtDNA, which is a circular double strand DNA molecule [19]. The replication of mtDNA occurs predominantly in the late S and G2 phases of the cell cycle, but may also occur throughout the cell cycle [20]. In addition, it has been shown that the mtDNA replication does not occur simultaneously with the growth and division of the organelle. Thus, mtDNA replication may not be coupled with mitochondrial proliferation. In humans, the copy number of mtDNA varies with cell type and tissue [21]. Under normal physiological conditions, mtDNA molecules double in each cell cycle to maintain a constant amount of mtDNA after the cell division.

Mitochondrial DNA encodes 13 polypeptides, including seven subunits of NADH dehydrogenase (ND1, ND2, ND3, ND4, ND4L, ND5, and ND6), three subunits of cytochrome *c* oxidase (COI, COII, and COIII), two subunits of F_0F_1ATPase (ATPase 6 and ATPase 8), and cytochrome *b.* Mammalian mtDNA also codes for two rRNAs and a set of 22 tRNAs that are essential for protein synthesis in mitochondria [22]. The assembly and functioning of the respiratory enzyme complexes in mammalian cells require coordinated expression and interaction between gene products of the mitochondria and nuclear genomes [23].

1.4 Protein targeting

Eukaryotic cells are divided into numerous organelles, compartments that are surrounded by membranes. The vast majority of proteins, however, is synthesized in a single compartment, the cytosol. About half of these proteins have to be transported into or across at least one cellular membrane to reach their functional destination [24]–[26]. For example, the budding yeast *Saccharomyces cerevisiae* synthesizes about 6000 different proteins with about 3000 of these proteins directed to various cell organelles. However, it raises several fundamental questions such as a) how do precursor proteins targeted to the correct organelle? b) how do they translocate across the hydrophobic membranes? and c) how do they sorted and assembled into their final functional forms?. Decades of continuous research reveals that specific sequences within nascent protein acts as a targeting signal for transport and assembly in a specific compartment of various organelles.

1.5 Mitochondrial biogenesis

Mitochondria are essential organelle involved in many cellular processes, including cellular respiration and energy production, lipid metabolism, free radical production, biosynthesis of heme and iron-sulfur (Fe-S) clusters. Mitochondria contain about approximately 500–1400 different proteins [27]–[29]. However, only handful of proteins, 13 in humans are encoded by mitochondrial genome and most of the proteins are encoded by nuclear genes and synthesized on cytosolic ribosomes and hence biogenesis of mitochondrial proteiome require contributions from mitochondria and the nuclear genome. Nuclear encoded proteins are imported to differrent compartments of mitochondria by a complex regulated pathways.

1.6 Mitochondrial protein import

The mitochondrial protein import machinery has been extensively studied in yeast *S. Cerevisiae* and *Neurospora crassa* using both biochemical and genetic methods. Protein translocation into mitochondria is complicated by the fact that mitochondria contain four subcompartments: two membranous compartments, the outer and the inner membrane, and two aqueous compartments, the intermembrane space (IMS) and the matrix. Nascent mitochondrial membrane proteins that are synthesized in the cytosol, not only have to reach mitochondria but have to be integrated into the right mitochondrial membrane [30], [31].

Precursors of mitochondrial proteins, also termed preproteins, are released from the ribosomes into the cytosol upon termination of translation. These precursor proteins imported into mitochondria in a post-translational manner [27], [32], [33]. Targeting signals that are present at the N-terminus or mature part of the protein target these proteins into different sub-compartments of mitochondria. Although several reports suggest that the contribution of a cotranslational import to the biogenesis of mitochondria [34]–[36], however definite evidence is still lacking to support the co-translational import. In the cytosol, newly synthesized preproteins interacts with chaperones like Hsp70 and Hsp90 to prevent their degradation and aggregation [37], [38]. Preproteins in a complex with cytosolic chaperones are delivered to receptors that are present on the outer membrane of mitochondria.

In most cases, presequence containing proteins (also called as precursors or preproteins) are targeted to the mitochondrial matrix. Presequences, the N-terminal cleavable amphipathic sequences, 15-100 amino acid residues in length, represent the most abundant and well-defined type of the signal [39]. After the import into the matrix, presequence is removed by a metalloprotease, a mitochondrial processing peptidase (MPP).

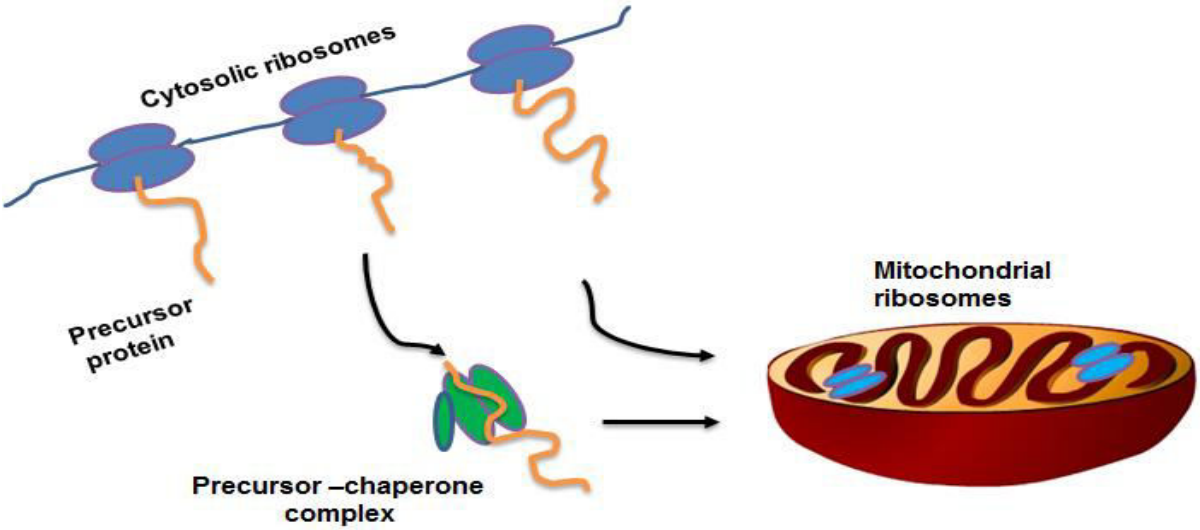

Figure 1.2 Biogenesis of mitochondrial proteins

Most mitochondrial proteins are synthesized on cytosolic ribosomes and are imported into the organelle. Approximately 1% of mitochondrial proteins are synthesized inside the organelle.

Transport of presequence containing precursor proteins to mitochondrial matrix is mediated by the Translocase of Outer Membrane (TOM) complex, followed by the Translocase of Inner Membrane (TIM) complex or TIM23 complex. However, in some proteins non-cleavable hydrophobic sorting signal followed by presequence causes translocation arrest of the precursor protein at the TIM23 complex. These precursor proteins are subsequently inserted into the membrane by a different mechanism. For few inter membrane space (IMS)-targeted proteins, additional cleavage event mediated by an inner membrane peptidase releases the mature protein into IMS from the membrane [31]. Although presequences are the most common targeting signals, most of the inner and outer membrane proteins do not contain any cleavalble pressequence. These proteins contain signals in their mature part of the protein. These signals are poorly defined and not completely characterized. However, these proteins can be divided into several classes [30], [31]**.** Outer membrane proteins that never contain presequences uses signals of two types: (1) a C-terminal β-signal, utilized by β-barrel outer membrane proteins and are recognized by TOM and Sorting and Assembly Machinery (SAM), (2) α-helical-type signals, utilized by the α-helical outer membrane proteins, which

are inserted via Mim1 pathway [31], [40]. Finally, multispanning inner membrane proteins, such as the members of the metabolite carrier family, have multiple internal signals distributed over the entire protein sequence. These proteins utilize the TOM and TIM22 complex for their targeting and insertion into the inner membrane [31], [41].

1.6.1 TOM complex

The Translocase of the Outer mitochondrial Membrane (TOM) is the general entry gate for mitochondrial proteins. It consists of a channel-forming subunit Tom40, presequence receptors Tom20, Tom22 and Tom70, and three small Tom proteins (Tom5, Tom6 and Tom7). Tom40 is a beta-barrel protein, together with other small Tom's forms the protein-conducting channel. The TOM complex also known as the general import pore [42]. Tom20 and Tom70 act as primary receptors for the incoming precursor proteins, while the former being responsible predominantly for presequence recognition, the latter recognizing the hydrophobic internal targeting signals. Tom22 plays an important structural role in the TOM complex and responsible for binding preproteins on both sides of the outer mitochondrial membrane [43], [44]. β-barrel proteins of the outer membrane are first imported by TOM complex into the IMS. In the IMS they are chaperoned by the essential small Tim's, Tim9-Tim10 and Tim8-13, which form two hexameric complexes [45]. Further insertion of outer membrane proteins into the membrane is done by the sorting and assembly machinery of the outer mitochondrial membrane, the SAM complex (also known as the translocase of outer membrane beta-barrel proteins (TOB). TOB complex contains Sam50, the pore-forming subunit, and two peripheral components, Sam35 and Sam37 [40], [44], [46]. Small Tim proteins that are present in IMS are mainly involved in the import pathway mediated by Tim23 and Tim22 complex [45] .

The majority of Inter Membrane Space (IMS) proteins are imported by the Mitochondrial Intermembrane space Assembly (MIA) pathway. The intermembrane space of mitochondria is considered to be equivalent to the periplasm of the ancestral α-proteobacterium. Similar to the bacterial periplasm and in contrast to the predominantly reducing cytosol, IMS provides oxidative environment to the imported proteins [47], [48]. The MIA pathway utilizes cysteine residues for protein import into the IMS. The precursor proteins that are transferred through the Tom40 channel in a reduced state. Mia40 harbours six conserved cysteine residues that are clustered in the form of one CPC and two CX_9C motifs. The CPC motif of Mia40 is redox sensitive and is involved in the formation of transient disulfide mediated intermediates. The CPC motif interacts with the cysteine motifs of proteins in their reduced form that are targeted to the intermembrane space. Mia40 through its CPC motif promotes the oxidative folding of precursor proteins by drawing electrons from them. The resulting reduced form of Mia40 is re-oxidized by transferring electrons to Erv1, a sulfahydral oxidase. In contrast, the CX_9C motifs are involved in creating intra-molecular disulphide bonds for stabilizing the structure of Mia40. Erv1, a sulfhydryl oxidase of the intermembrane space, reoxidizes by transferring electrons to respiratory chain via cytochrome *c* [45], [49].

Non-cleavable multispanning inner membrane proteins are inserted into the membrane by the TIM22 complex. Chaperoning of these proteins through the IMS requires action of the small Tim proteins, which are also needed for the SAM-mediated insertion of outer membrane proteins. The TIM22 complex itself consists of the following components: Tim54, Tim22, Tim18, and Sdh3.This complex also associated with small Tim's (Tim9, Tim10 and Tim12) [41].

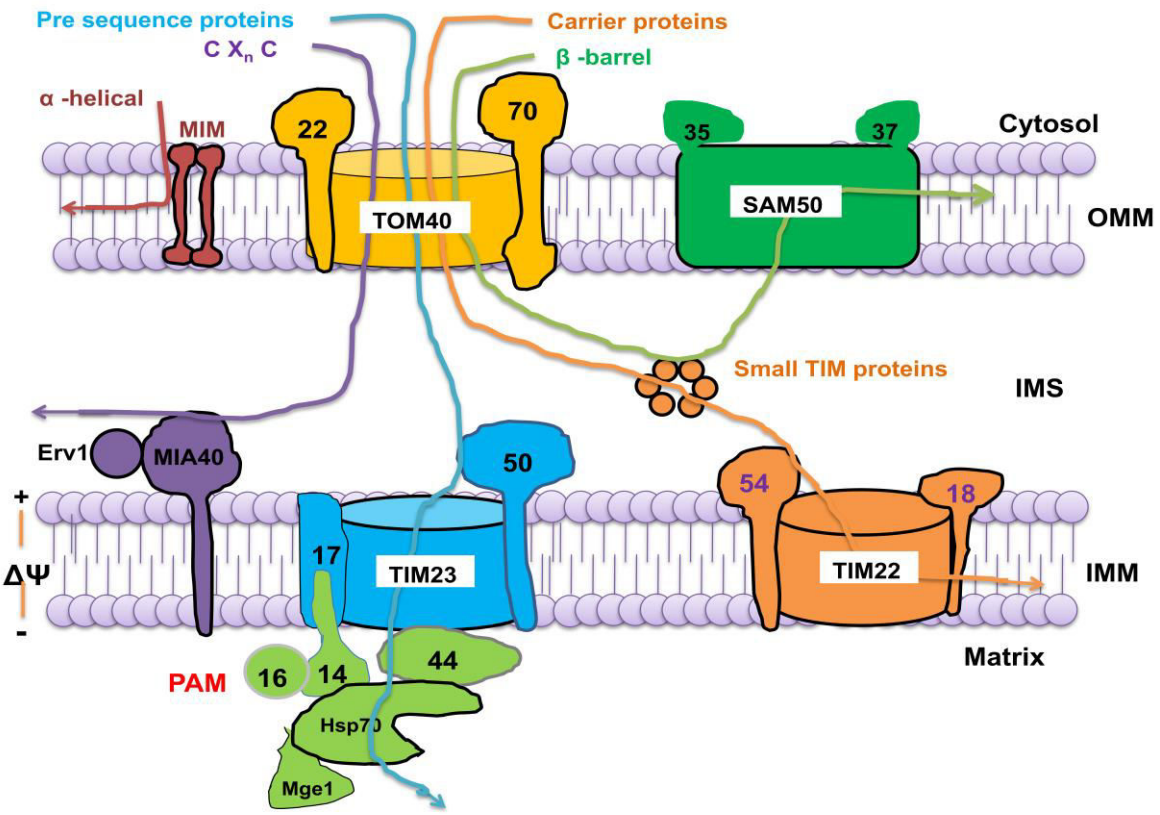

Figure 1.3 Schematic representation of the mitochondrial protein import pathways: The membrane potential (ΔΨ) across the mitochondrial inner membrane is generated by the electron transport chain.. α-helical proteins are transported in a TOM independent manner using the MIM complex. All other precursor proteins uses the TOM complex as a general entry gate. CX_9C motif containing precursors are imported by the MIA complex into the IMS. The small Tim proteins as well as the SAM complex facilitate β-barrel protein insertion into the outer membrane. Additionally, the small Tim proteins participate in the import of carrier proteins mediated by TIM22 translocase. Complete matrix translocation of precursors occurs through The TIM23 complex that requires the import motor (PAM) and Hsp70/Mge1 complex.

1.6.2 TIM23 complex

The TIM23 complex is the main translocase in the inner membrane of mitochondria. It is an entry gate for a vast majority of preproteins targeted to the matrix and inner membrane. The majority of preproteins imported via the TIM23 translocase contain cleavable N-terminal matrix targeting sequence (MTS). The import is driven by the energy from ATP hydrolysis

and the difference in membrane potential ($\Delta\Psi$) across the inner membrane. $\Delta\Psi$ is necessary for the translocation of the positively charged residues of the MTS on the matrix side of the translocase. Further import of the preprotein requires energy in the form of ATP hydrolysis for mtHsp70 mediated import.

The TIM23 translocase is further subdivided into two divisions: a membrane embedded part and the import motor. Membrane embedded part of the complex contains the receptor Tim50 and the translocation channel formed by Tim23 and Tim17 proteins. The import motor consists of Tim44, chaperone mtHsp70 and several of its Co chaperones: Tim14, Tim16, and Mge1 [26].

The core of the TIM23 complex is formed by three essential inner membrane proteins: Tim50 with a receptor function in the intermembrane space [50], [51], the channel-forming protein Tim23 [52], [53], and Tim17, which is involved in motor recruitment and lateral sorting of preproteins [54], [55]. Tim50 and Tim23, as well as the fourth subunit, Tim21 have exposed domains in the intermembrane space. These domains are involved in the transient interaction of the TIM23 complex with the TOM complex and thus facilitate preprotein translocation from the outer to the inner membrane [50], [51], [54]. Tim21 also participates in the transient coupling of the TIM23 complex with the respiratory chain complexes III and IV, and thereby supports the membrane potential ($\Delta\psi$) driven import step [56]–[58].

The membrane potential plays a dual role in preprotein import: $\Delta\psi$ activates the Tim23 channel and exerts an electrophoretic effect on the positively charged presequences ($\Delta\psi$ is negative on the matrix side) [52], [59], [60].

Table 1.1: Subunits of the presequencetranslocase (TIM23 complex)

Subunit	Function	Essential
Tim23	ΔΨ and presequence dependent protein channel, recognizes presequence, binds to Tim17, Tim21 and Tim50	Yes
Tim17	Involved in gating and sorting, tethers Pam18	Yes
Tim50	binds to presequence precursor, transfer from TOM toTIM23, induces channel closure under resting conditions	Yes
Tim21	Couples $TIM23^{SORT}$ to complex III	No

1.6.3 The transport pathway for matrix targeted precursors

The current model of presequence containing protein import across the TIM23 complex starts with transfer of presequence bound to $Tom22^{IMS}$ to the TIM23 complex. This is most likely mediated by either an indirect competition of $Tim21^{IMS}$ with $Tom22^{IMS}$ or a direct competition of $Tim50^{IMS}$ and $Tom22^{IMS}$ for the presequence [54], [61], [62]. Subsequently, the precursor binds to Tim50 [63], [64] and then transferred to $Tim23^{IMS}$, which binds to the presequence with its C-terminal half of the IMS domain, and guided into the channel of the TIM23 complex [65], [66]. The transport across the inner membrane is driven by the ΔΨ acting on the net positively charged presequence (electrophoretic effect) [59], [67]. Besides Tim23, no other presequence receptor in the TIM23 complex was identified so far. However, Tim50 is assumed to fulfill partially the presequence receptor function. Even though $Tim50^{IMS}$ induces closure of the Tim23 channel, presequence peptides can open it again indicating a recognition event [52]. However, it is unclear whether this is solely due to the recognition of the presequence by $Tim23^{IMS}$. Recent atomic structure of the inter membrane space domain of Tim50 revealed a negatively charged groove, which was proposed to be responsible for presequence binding [68].

1.6.4 The sorting pathway

Despite the channel forming activity, both Tim23 and Tim17 was shown to be actively involved in the sorting process [54]. After the presequence is transported across the inner membrane the Tim23 translocase can engage a stop transfer signal present in the precursor [69]–[71]. The hydrophobic (TMD) part of the sorting signal is arrested in the channel [72], and afterwards the substrate partitions into the lipid bilayer. Sorting into the inner membrane was demonstrated with the $TIM23^{SORT}$ complex [60]. The coupling of the translocase to the respiratory chain by Tim21 makes the sorting process more resistant to changes in the membrane potential [56]. Interestingly, the sorting and matrix transport mediated by TIM23 seems to be inversely regulated as overexpression of Tim21 reduces matrix import [54]. This is most likely due to a reduction of PAM subunits at TIM23 [73]**.** Additionally, Tim17 mutants defective in motor association, or Pam18 mutants deficient in association with Tim17 lead to an increased sorting efficiency [54], [73], [74]. Interestingly, the import motor components Pam16 and Pam18 were found in close vicinity to laterally sorted substrates and they may affect the efficiency of insertion independent of the ATPase activity of the import motor [74]. However, it remains elusive whether $\Delta\Psi$ dependence on the sorting process is only due to transport of the presequence across the membrane or the lateral release itself.

1.6.5 Complete matrix translocation of precursor is powered by the PAM complex

Complete translocation of precursor proteins into the mitochondrial matrix depends on the presequence translocase associated motor (PAM complex). This ATP dependent import motor is one of the most complex Hsp70 based systems in the cell [75].

Hsp70 systems Hsp70 class of proteins are involved in protein folding, prevention of protein aggregation, remodelling of protein complexes and associated with protein translocation machineries in different cellular compartments like ER, chloroplasts or mitochondria [31],

[76], [77]. Hsp70 chaperones share a conserved structural domain: an N-terminal nucleotide binding domain (NBD) followed by an interdomain linker and the C-terminal peptide binding domain [78]. The mechanism of Hsp70 function in protein folding is well studied in the bacterial DnaK system [79]–[81]. In the ATP bound state, the affinity of the peptide binding domain for substrate peptides is low. The substrate binding and release rate is high in the ATP bound state (on-off rate), enabling the chaperone to bind rapidly to new substrates. In contrast, the ADP bound state has high affinity for substrate results in tight association of chaperone with substrate. The ATPase activity of Hsp70 converts ATP to ADP. However, the intrinsic ATPase activity of Hsp70 is usually low and requires external stimulation by DnaJ (Hsp40) class of proteins.

J-proteins posses a typical four helical fold with a conserved HPD motif in the loop between helix II and III. Parts of helix II, the HPD motif and helix III of Hsp40 are involved in interaction with interdomain linker and proximal residues of Hsp70 [82], [83]. Binding of a J-protein to ATP bound Hsp70 alters the conformation of the interdomain linker. This conformational change is transmitted to the active site in the NBD domain leading to an enhanced ATP hydrolysis [83], [84]. In the ADP bound state the peptide binding domain of Hsp70 has a high affinity for its substrate with a slow on-off rate. In this state, the Hsp70 assists in protein folding or generates vectorial protein translocation. For the recycling of Hsp70, the bound ADP needs to be released. The conserved GrpE/Mge1 class proteins facilitate the exchange of ATP for ADP on Hsp70 thereby facilitates the release of nascent protein from Hsp70. In yeast, mitochondria contain three different members of Hsp70s (Ssc1, Ssq1, Ssc3). The main Hsp70 (Ssc1) is involved in the import and folding of nascent proteins.

The dynamics of Ssc1 (Hsp70) conformation have been studied extensively in yeast [85], [86]. In the substrate free state, Ssc1 can fluctuate between an ATP state with an open substrate binding domain lid and an ADP or nucleotide free state with a flexible lid [86]. ATP bound Ssc1 can bind to its substrate tightly upon Mdj1 stimulated ATP hydrolysis that induces closure of the lid of the substrate binding domain. The association of Mdj1 with substrate bound ADP-Ssc1-complex is relatively stable. Mdj1 slowly releases from the complex with a half life of ~5 min in the absence of nucleotide exchange factor and ATP. Binding of Mge1 to Ssc-ADP-substrate complex, accelerates the release of ADP and thereby facilitate the binding of ATP. Binding of ATP triggers the release of Mge1 within milliseconds. These events followed by conformational changes in Ssc1 causing the release of bound peptide and Mdj1[86].

Interestingly, mitochondrial Hsp70 depends on itself for its biogenesis with the help of additional chaperones. After import motor dependent import into the mitochondrial matrix, Hsp70 exists in an unfolded state. Although folding of the peptide binding domain does not require any additional cochaprones or factors, folding of the NBD domain requires Hep1 (Tim15) chaperone [87]–[89]. Hep1 is a zinc finger protein and requires Zn^{2+} for its own folding [90]. The binding of Hep to Hsp70 results in formation of intermediate Hsp70-Hep1 complex. This complex can facilitate the binding of nucleotides to the NBD domain, stabilizing its fold and subsequently releases Hep1 [91]. Further, Hep1 also prevents the formation of nucleotide free aggregation prone intermediate of Hsp70 during its biogenesis [92].

T**he PAM complex** The import motor promotes ATP dependent translocation of precursors into the matrix. Pam complex also required for the sorting of proteins in particular when sorting signal is not adjacent to the presequence (e.g. Cox5a) [93]. These precursors are

initially imported in a motor dependent manner, but are sorted as soon as the sorting signal is presented to the TIM23 complex.

The initial steps of presequence transfer across the inner membrane depend on Tim17 mediated recruitment of Motor complex at the TIM23 complex [94], [95]. Later, Pam17 initiates the assembly of the J-module at the translocase This assembly step required for the regulation in conversion of the TIM23 translocase either the matrix transport or lateral insertion mode [94]–[97]. As presequence emerges on the matrix side of the inner membrane, Tim44 binds to the precursor [98]. Tim44 is an inner membrane protein and has affinity to specific phospholipid, Cardiolipin [99], [100]. Further, Tim44 associates with components of TIM23 complex, such as Tim23 and Tim17 [101]. This initial binding of Tim44 with emerging preproteint traps the precursor and prevents backsliding. This Tim44-precursor complex is then engaged by Hsp70 at the exist site of the TIM23 complex [96], [102], [103]. Continuous binding of Hsp70 to the precursor in part due to stimulation of ATPase activity by a J-protein, Pam18 [104], [105]. It clearly serves in recruitment of Pam18 to close vicinity of the exit site of TIM23, which together with Hsp70 recruitment is important for an efficient and spatially controlled activation of the ATPase activity. The J-module of Pam18 also interacts with the respiratory chain, just like $TIM23^{SORT}$, however independent of Tim21 [57]. This function might be a coordinated switch from $TIM23^{SORT}$ to $TIM23^{MOTOR.}$ function. Pam18 is an inner membrane protein with its C-terminal J-domain being exposed on the matrix side. It is recruited to the TIM23 complex through interaction of TMD domain and N-terminal IMS domain with Tim17 as well as in a complex of J-domain with J-like domain of Pam16 [54], [106]–[108]. Pam16 does not possess the ATPase stimulating activity on Hsp70, [109], [110]. Pam16 bound to the inner membrane through interaction of hydrophobic N-terminus domain with N-terminal region of Tim44 [111]. This interaction of N-terminal of Tim44 and Pam16 may modulate the relative positioning of Pam18 and Hsp70 to each other

[111], [112]. This would imply a mechanism for Tim44 or Pam16 to sense the incoming polypeptide from the TIM23 complex.

Table 1.2: Subunits of the presequencetranslocase associated import motor (PAM complex)

Subunit	Function	Essential
Tim44	Binds to precursor, tethers Hsp70 to exit the site	Yes
Hsp70 (Ssc1)	ATP dependent precursor binding, generates vectorial movement	Yes
Pam16	Tethers Pam18 to the exit site of the translocase, binds with N-terminus to Tim44 N-terminus	Yes
Pam 18	J-protein, activates ATPase activity of Hsp70, tethered by Pam16 and the interactions of its IMS domain with Tim17	Yes
Tim 17	Assembly of Pam16-Pam18 complex, involved in initial transfer steps	No
Mge1	Nucleotide exchange factor of Hsp70	Yes
Hep1	Assists folding and stability of Hsp70	Yes

Vectorial movement of the precursor: Two major models for the generation of vectorial movement of precursor during mitochondrial import have been proposed: the Brownian ratchet mechanism" [104], [113] and the Power stroke mechanism" [114], [115]. The hallmark of the power-stroke model" is that mtHsp70 undergoes a conformational change, which is powered by the ATP hydrolysis and uses Tim44 as a support to generate a force directed into the matrix. However, this hypothesis lacks a direct experimental evidence.

The ratchet or trapping mechanism functions by traping and preventing backslinding of precursor through several rounds of mtHsp70 binding to the precursor emerging from the translocation pore. The import is therefore driven by the Brownian thermal motion of the precursor in the translocation channel. As the bound Hsp70 prevents the backsliding of

precursor, it can only move into the mitochondrial matrix, thereby exposing another segment of precursor that can be engaged by a new Hsp70 molecule. Hence, the asymmetric distribution of mtHsp70 molecules with respect to the inner membrane and ATP mediated binding of mtHsp70 to the substrate contribute to the movement of precursor into the matrix. However, the import efficiency is determined by the unfolding of tightly folded domains of precursors on the surface of mitochondria [116]–[120].

This model was recently extended to thermodynamic aspects of the translocation of precursor (Entropic pulling) [121]. Binding of the mtHsp70 molecules to the substrate decreases the available diffusion volume of mtHsp70 as membrane proximal regions are excluded. Hence diffusion is directed towards the matrix providing a force to unfold protein domains on the mitochondrial surface.

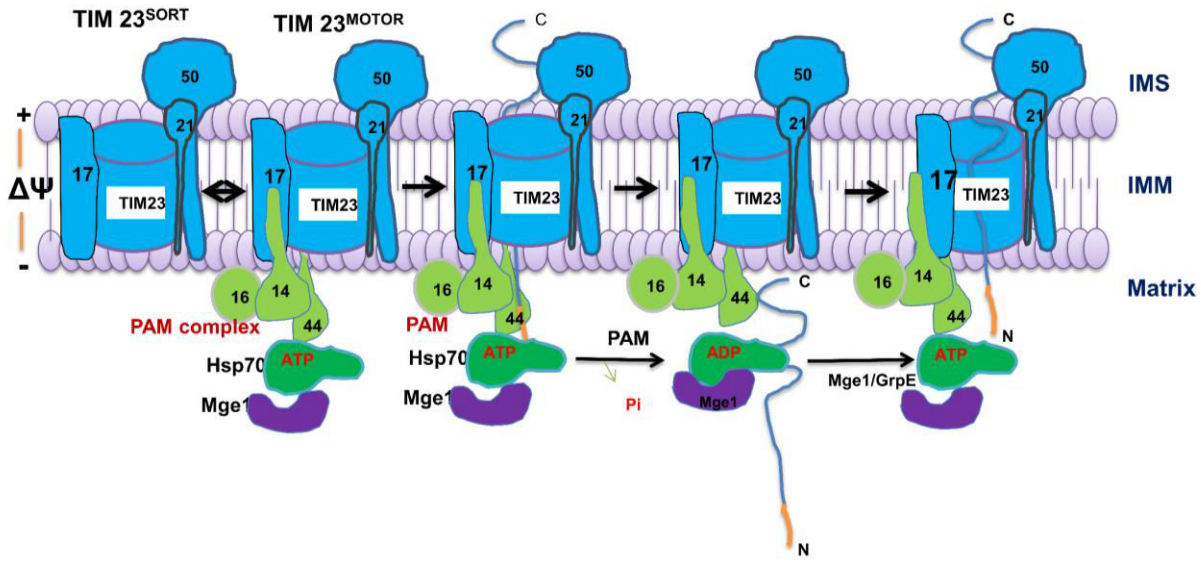

Figure 1.4: The translocase of the inner mitochondrial membrane TIM23 complex and the Hsp70/Mge1 cycle during protein import.

Schematic representation of the TIM23 complex and their subunits. The import of precursors into the mitochondrial matrix is mediated by Hsp70/Mge1 chaperone cycle in an ATP dependent manner. Tight binding of Hsp70 to the substrate at the translocase is triggered by Pam18 mediated stimulation. Mge1 facilitates the dissociation of Hsp70-ADP complex and allows the binding of Hsp70-ATP to the free Tim44. Release of the ADP from the Hsp70 is

mediated by the nucleotide exchange factor, Mge1 leading to a dissociation of the Hsp70 from its substrate thereby facilitates the translocation of substrate into the mitochondrial matrix.

The current accepted model is rachet and entropic pulling based on the experimental evidences as shown in the Figure 1.4. The first critical step in the import process is the recruitment of ATP-bound mtHsp70 to Tim44. This step is also stimulated by nucleotide exchange factor, Mge1 [117], [119]. Once positioned correctly at the translocase, Hsp70-ATP engages with the precursor. ATP hydrolysis in close vicinity to the exit site of the translocase is triggered by Pam18 [105], [122], [123]. However, it is not known whether a successful binding of the substrate by Hsp70 is stimulated by this mechanism or whether this is solely regulated by the positioning of the subunits in the first place. The hydrolysis of ATP followed by the dissociation of Hsp70-ADP from Tim44 are facilitated by Mge1 [117]. At this step the vectorial movement of precursor takes place as rebinding of the Hsp70-ADP complex to Tim44 is very inefficient and hence the precursor diffuses away into the matrix [117], [119], [123]. The free Tim44 can bind another Hsp70-ATP that can then efficiently trap the newly exposed segment of the precursor [124]. The first cycle high affinity substrate binding Hsp70-ADP complex releases ADP by the action of Mge1 [117], [125], [126]. Due to high ATP concentration in the matrix, ATP binds to Hsp70 causing the release of substrate and ATP-Hsp70 ready for a new cycle. The step-size of Hsp70 can vary between 20 to 60 residues, depending on the unfolding rate of the precursor protein [120]. It is not known so far whether any other PAM subunits follow the cyclic recruitment like Hsp70, or whether subunits are firmly engaged with the translocase during translocation of one precursor. Successive rounds of this cycle will eventually complete matrix translocation of the precursor. The import rates can reach 10-15 pmol imported protein/ min /mg mitochondria *in vitro*, meaning that one TIM23 takes about 1 min to transport one precursor [127], [128].

1.7 Mitochondrial ROS production

The term reactive oxygen species (ROS) are usually used to signify any oxygen-containing molecule (radical or non-radical) capable of initiating some kind of deleterious reaction. These include superoxide anion (O_2^-), hydrogen peroxide (H_2O_2), hydroxyl radical (HO), peroxyl radical (RO_2^-), alkoxyl radical (RO^-), hydroperoxyl radical (HO_2^-), hypochlorous acid (HOCl), and singlet oxygen (O) [129]. O_2^- is the major ROS produced due to the single electron reduction of O_2. $O_2^-$is then dismutased to H_2O_2 in a reaction catalyzed by the superoxide dismutases (SOD).

$$\mathbf{2\ O_2^- + 2\ H_2O \rightarrow O_2 + H_2O_2 + 2\ OH^-}$$

H_2O_2 is scavenged by catalase (CAT) in the cytosol or glutathione peroxidase (GPx) and decomposes into water.

$$\mathbf{2\ H_2O_2 \rightarrow 2\ H_2O + O_2}$$

The primary role of mitochondria is the generation of ATP through oxidative phosphorylation (OXPHOS). Mitochondrial complex I and complex III are the major sites of ROS production. [2], [130]–[132] Mitochondrial ROS (reactive oxygen species) production accounts for approximately 90% of the total ROS production in a cell [133] . Complex II has also been reported as a site of O_2^- production, however, its contribution to the overall ROS levels is minimal [134].

Mammalian complex I is the entry point for electrons from NADH into the respiratory chain and is a ~1 MDa complex comprising 45 polypeptides [135], [136]. The first demonstration of ROS production by complex I was in SMPs (submitochondrial particle) where reduction of CoQ pool and generation of a large Δp by succinate led to uncoupler-sensitive H_2O_2 production [137]**.** Subsequently, it was shown that isolated complex I in the presence of

NADH produces $O_2^-$and that this generation is enhanced by the inhibitor rotenone, which binds to the CoQ-binding site [2].

Complex III funnels electrons from the CoQ pool to cytochrome *c*. The monomer is ~240 kDa and comprises 11 polypeptides,and it interacts transiently with CoQ during the Q-cycle at the Qi and Qo sites [138]. Complex III has for a long time been regarded as a source of O_2^- with in mitochondria [139]. When supplied with $CoQH_2$ and when the Q_i site is inhibited by Antimycin A, complex III produces large amounts of O_2^- by the reaction of O_2 with a ubisemiquinone bound to the Q_o site [2], [139]–[141]. This O_2^- is released from complex III to both sides of the inner membrane [142]. Further, Rotenone, Antimycin A and paraquat are also producers of H_2O_2.

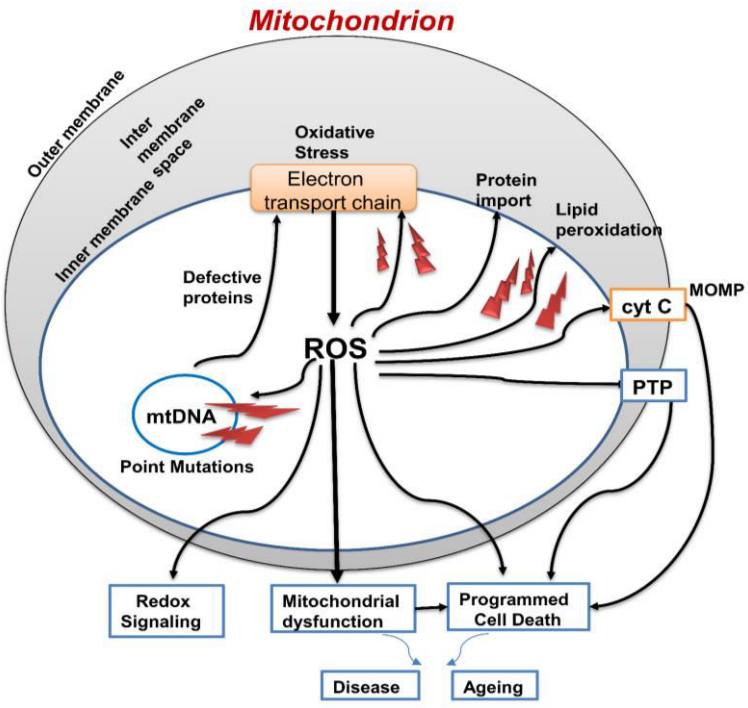

Figure 1.5 Overview of mitochondrial ROS production: Mitochondrial ROS causes the oxidative damage to mitochondrial DNA and impairs the ATP synthesis, pProtein import and numerous metabolic pathways. Mitochondrial ROS triggers the release of pro apoptotic proteins such as cytochrome c (cytc) to the cytosol by mitochondrial outer membrane permeabilization (MOMP) and activates the apoptotic machinery. In addition, mitochondrial ROS production leads to induction of the mitochondrial permeability transition pore (PTP),

which reduces the inner membrane permeable to small molecules. Consequently, mitochondrial oxidative damage contributes to a wide range of pathologies. In addition, mitochondrial ROS may act as a modulatable redox signal, reversibly affecting the activity of a range of functions in the mitochondria, cytosol and nucleus *(Image source from Murphy et al., 2009).*

1.8 Reactive oxygen species and mitochondrial dysfunction

Mitochondrial ROS induces oxidative damage to the OXPHOS machinery and leads to lots of mitochondrial associated disorders. A primary defect in oxidative phosphorylation may increase superoxide production, thereby increasing oxidative stress. ROS generated by mitochondria has been implicated in the pathogenesis of diverse chronic neurodegenerative diseases, diverse chronic neurodegenerative diseases, including Parkinson disease (PD), Alzheimer's disease (AD), amyotrophic lateral sclerosis (ALS), Huntington's disease (HD), and Friedreich's ataxia (FA).

Increased ROS production in neurodegenerative processes may affect normal mitochondrial parameters like ATP production, membrane potential, permeability transition pore activation, and calcium uptake. These changes can lead to neuronal death, mainly through excitotoxic pathways, involving oxidation of macromolecules and apoptosis [143] .

1.9 Oxidation of sulfur containing amino acids in recombinant proteins

Oxidation is one of the prevalent forms of chemical modification and sulfur containing amino acids, methionine and cysteine are susceptible to modification by a wide range of oxidants. Of the twenty amino acids, methionine and cysteine contain sulfur. Methionine is a un branched, non-polar amino acid that contains a thioether side chain and cysteine is a polar amino acid that contains a thiol side chain. The susceptibility of these amino acids to oxidation is a function of their biochemical properties and their locations within a particular

protein tertiary structure. Methionine and cysteine residues of proteins are particularly sensitive to oxidation [144].

1.10 Methionine oxidation

Oxidation of methionine may or may not affect a protein's biological activity or structural stability. Reactive oxygen species (ROS) can oxidize methionine (Met) residues of proteins to methionine sulfoxide (MetO). The formation of methionine sulphoxide is a reversible process. The forward reaction leads to the formation of both R- and S-stereoisomers of product. The backward reaction is catalyzed by methionine sulfoxidereductases (Mxrs) and back to methionine residues. Methionine sulfoxide affects many mechanisms like an increase in the rate of ROS generation, a decrease in the antioxidant capacity, a decrease in proteolytic activities which preferentially degrade oxidized proteins.

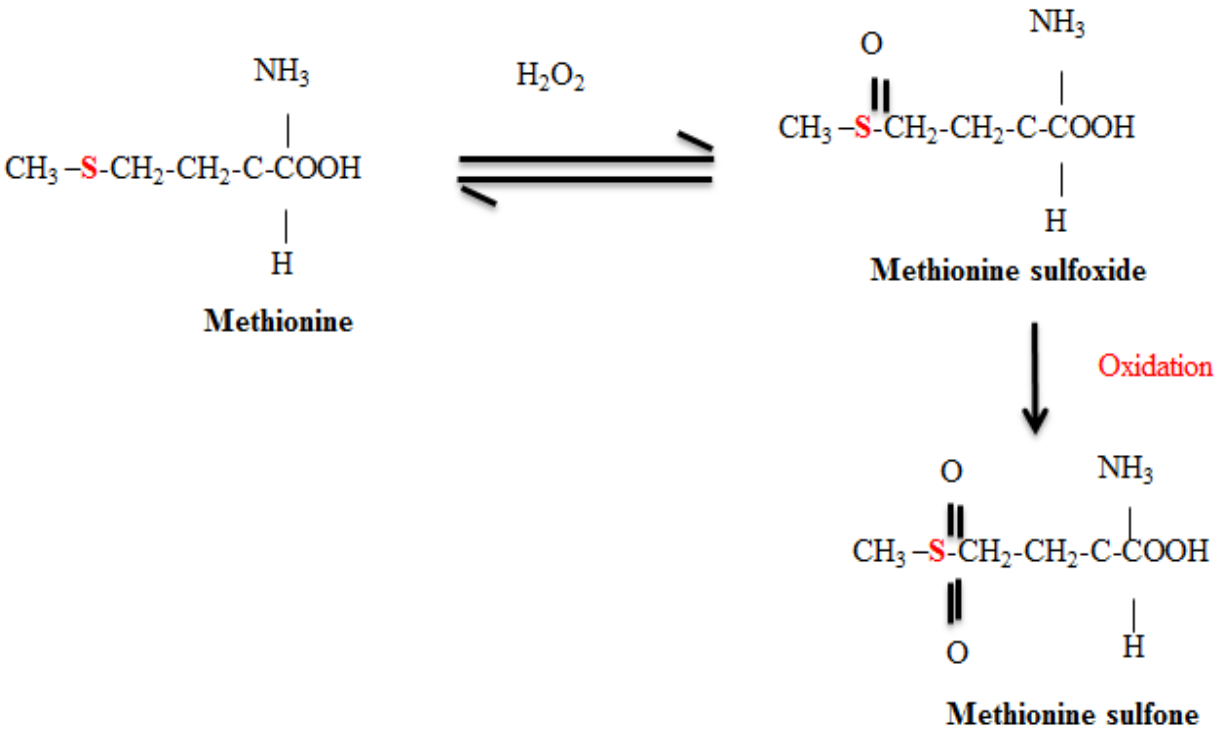

1.11 Scope of the thesis

Presequence contain proteins targated to mitochondrial matrix through TIM23 complex. Targeting of precursor protein to the matrix involve an interplay among many proteins, however final step of this process is mediated by Tim44 and a translocation motor which contains heat shock protein, mHsp70, Pam16, Pam18 and the nucleotide exchange factor Mge1[57], [107], [145], [146]. Hsp70, in combination with Tim44, binds to the emerging end of transit peptide from TIM channel in a ATP-dependant manner and ATPase cycle of mHsp70 leads to pulling or vectorial translocation of preproteins across the inner mitochondrial membrane [118], [119], [147]. Mge1, a component of this translocation motor, accelerates the exchange of ATP for ADP on mHsp70 and promotes changing the high substrate affinity conformation of mHsp70 to lower substrate affinity form with a concomitant release of precursor protein from mHsp70 thereby begins the next cycle of translocation [117], [126], [148], [149]. Mge1 acts as a thermo-sensor in bacteria and yeast [150]–[152]. At high temperatures, Mge1 exists as a monomer and fails to interact with mHsp70 [150], [153]. Further, temperature sensitive mutants of Mge1 accumulate precursors in the cytosol, aggregate proteins in the matrix and have reduced nucleotide dependent dissociation of mHsp70 from Tim44 [154]. It is also involved in maintenance of mitochondria during heat stress, sorting of proteins, degradation of misfolded proteins and the formation of iron sulfur clusters [155], [156].

Reactive oxygen species has been implicated in ageing besides a host of other diseases [157]. Electron transport chain present in mitochondria is the major source for the generation of reactive oxygen species and there has been an increased focus on identifying the protein(s) that have altered activity during oxidative stress to understand mitochondria mediated ROS signalling and diseases [130], [158] . Decreased import of mitochondrial DNA repair enzyme in aged samples [159], and reduced import of pre-proteins under pro-oxidant conditions

directly implicate a role for ROS in mitochondrial protein import [160]. ROS also reduces the activity of several mitochondrial proteins, such as aconitase, α-ketoglutarate dehydrogenase, and succinate dehydrogenase in mammalian cells [161]. Further, it is known that oxidative stress impairs growth of yeast [162]. However, no protein import factor or receptor of mitochondria has been implicated in the oxidative stress response either in lower or higher eukaryotes. This work focuses on the identification and characterization of import receptor Mge1 as an oxidative and thermal sensor.

Based on the above rationale, the objectives of the present study are as follows:

1. Characterization of yeast Mge1, a nucleotide exchange factor of mitochondrial Hsp70, under oxidative stress.

2. Influence of Thermal stress on the structure & functional properties of Mge1, a mitochondrial component of protein import motor.

Chapter 2

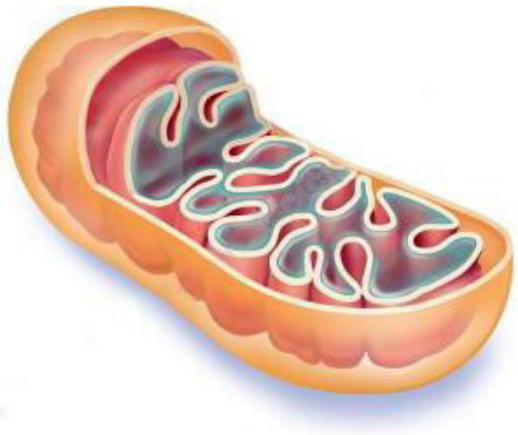

Characterization of yeast Mge1, a nucleotide exchange factor of mitochondrial Hsp70, under oxidative stress

2.1 INTRODUCTION

GrpE (for *GroP*-like gene *E*) was identified in a genetic screen for mutants that failed to propagate bacteriophage λ in *Escherichia coli* [163]. Homologues of *E.coli* GrpE in different species include mammalian mitochondrial GRPEL, *Saccharomyces cerevisiae* Mge1 and *D. melanogaster* Droe1p. Mge1,an essential protein of the mitochondrial matrix of *Saccharomyces cerevisiae,* is a sequence and functional homolog of *E. Coli* GrpE [164], [165]. GrpE/Mge1 plays a prominent role in mitochondria, chloroplasts, and bacterial cytoplasm. Functional Mge1 exists as dimer and this dimerization seems to be critical for its interaction with mHsp70 as monomeric form of Mge1 fails to interact with mHsp70.

Mge1 functions as nucleotide release factors for Hsp70 family of proteins in the mitochondrial matrix. Mge1p promotes the ADP release from Ssc1p (Hsp70) in the import motor complex, allowing the cycle of ATP-dependent protein translocation to proceed .The eukaryotic cytosol does not contain GrpE/Mge1 protein because GrpE-like function is provided by BAG1 protein. Mge1 in a complex with Ssc1p and the J-protein Mdj1p play a role in the refolding of proteins in the mitochondrial matrix [125], [166], [167]. In addition, Mge1 is involved in Fe-S cluster biogenesis as it acts as nucleotide release factor for Ssq1p, a Hsp70 homologue present in the mitochondrial matrix [168].

The structure of *E. coli* GrpE has been determined through X-ray crystallography. Further, GrpE was co-crystallized with the ATPase domain of DnaK. Each monomer of GrpE consists of a long N-terminal α-helix followed by short α-helix, and a compact β-sheet domain at the C- terminus. Thus it forms an asymmetric dimer consisting of two long N-terminal helices that lead to a four-helix bundle and two small β-sheet domains near the C-terminus. The N-terminal helices of GrpE are involved in its dimerization while the four-helix bundle and β-sheet domains of GrpE are involved in its interaction with DnaK [169].

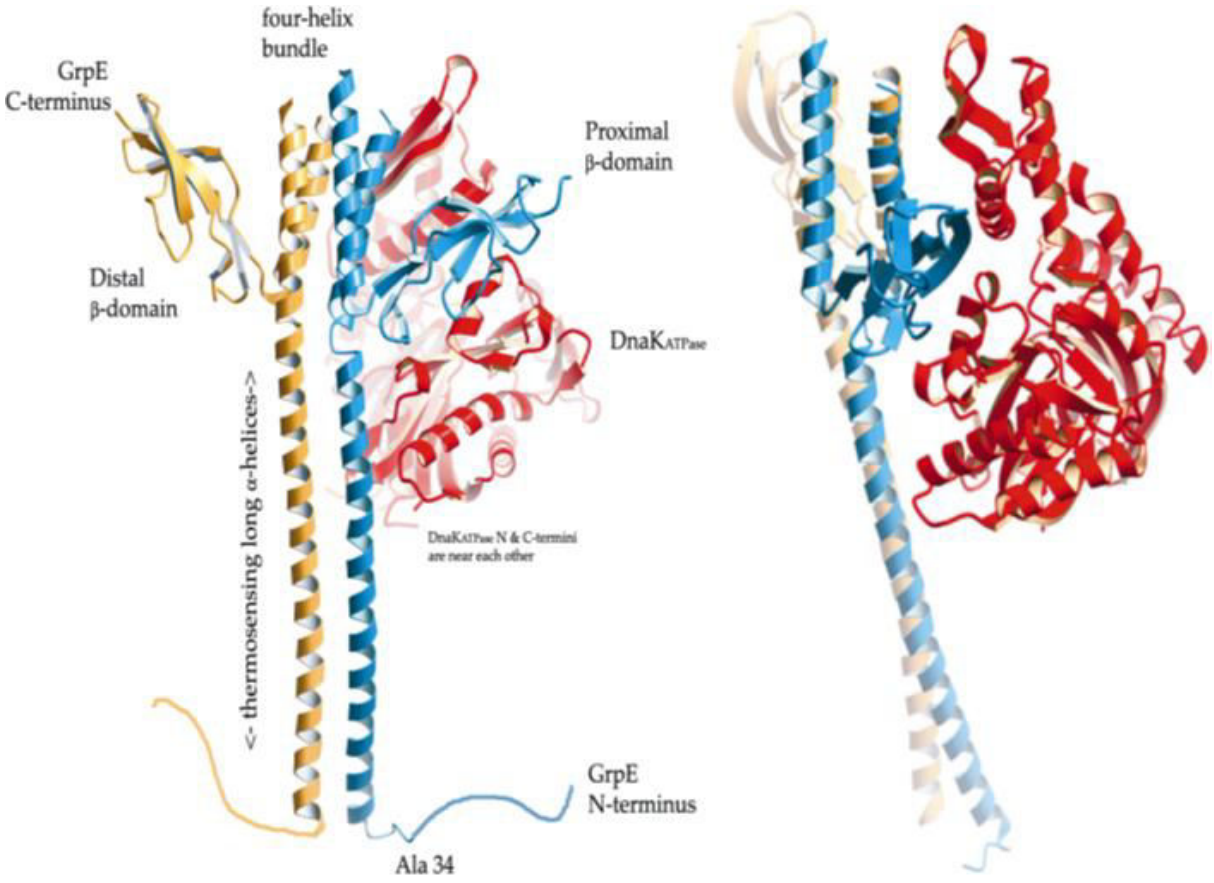

Ribbon drawing of the complex of Dimeric GrpE and the ATPase domain of DnaK: Ribbon diagram of the GrpE dimer (amino acids 34-197). A ribbon diagram shows the structure for the GrpE dimer. The three regions of the GrpE protein: the NH_2-terminal α-helical "tail" portion composed of amino acids 34-89 from each monomer, the four-helix bundle motif composed of amino acids 90-138 from each monomer , and the COOH-terminal β-sheet domain composed of amino acids 139-197 from each monomer. Most of the DNAK binding sites are present at the C-terminal end the GrpE *(Image source from Celia Harrison et al., 2003).*

In this study, by using Saccharomyces cerevisiae as a model system, we show that oxidative stress reduces protein import into mitochondria and is found to be correlated with reduced interaction of Hsp70 with Mge1. Most importantly, we find that dimeric yeast and human Mge1 acts like an oxidative sensor by dissociating into a monomer. As a result of this monomerization, it has reduced ability to interact with Hsp70 both *in vitro* and *in vivo*. In addition, a Mge1 M155L substitution mutant is resistant to oxidative stress. We find that

yeast cells expressing Mge1 M155L besides exhibiting normal growth in the presence of H_2O_2, have normal protein import activity in mitochondria along with stable Mge1-Hsp70 complex formation. Our studies provide mechanistic insights into the regulation of oxidative stress response by mitochondria.

2.2 Methodology

2.2.1 Materials

Hydrogen peroxide H_2O_2 was purchased from Amresco to use as a oxidative inducer.

Antimycin A, Paraquat (*N*, *N*′-dimethyl-4,4′-bipyridiniumdichloride) and

2`,7`-Dichlorofluorescindiacetate (DCFDA) was purchased from Sigma Aldrich.

BS^3 (Bis [sulfosuccinimidyl] suberate) and DSS (Disuccinimidylsuberate) cross linkers was purchased from Pierce.

MitoSOX™ Red Mitochondrial Superoxide Indicator was purchased from Life Technologies.

Radiolabel ^{35}**S** methionine, [ϒ-$P^{32]}$ ATP was purchased from Jonaki, CCMB-Hyderabad.

Rabbit reticulocyte lysate for *in vitro* translation was purchased from Promega.

All reagents and chemicals used in the study were purchased from Sigma-Aldrich, Amresco and Hi-Media.

METHODS

Cloning of Yeast and Human Mge1

2.2.2 cDNA synthesis

HeLa cell total RNA (3 µg) (Bangalore GeNei) was used to clone the Human *MGE1* gene. In brief, the following components were added in the following order:

1.3 µg of total RNA

1 µl of random hexamer primer

8 µl of DEPC water

The contents were mixed and incubated at 65^0C for 10 min.

Then the reaction was chilled on ice and the following components were added: 4 µl of 5X Reaction buffer, 1 µl of RNase Inhibitor, 2 µl of 10 mM dNTP Mix and 2 µl of M-MuLV Reverse Transcriptase. A total volume of 20 µl of reaction mixture was mixed and incubated at room temperature for 2 min followed by 60 min incubation at 37 ^{0}C. Finally, the reaction was terminated by heating at 95 ^{0}C for 2 min.

2.2.3 Polymerase chain reaction (PCR)

The complete coding sequence of yeast MGE1 was amplified without the mitochondrial targeting sequence (Δ43) from genomic DNA as a template. The reaction was carried out in a final volume of 50 µl with 10 pM of each NB18 Fwp: 5'CCC G▾AATT▴C ACC ATG GAT GAA GCC AAA AGT GAA GAA TCC 3'-(*E.CoR1)* and NB19 Revp : 5'ATT C▾TCGA▴G TTA GTT CTC TTC GCC CTT AAC AAT TCC 3'-*Xho1* primers, 2.5 mM each of the four dNTPs ,0.5U of Taq DNA polymerase enzyme, 500 ng of genomic DNA as template. The amplification was performed in PCR (Eppendorf) with an initial temperature step at 95^0C for 4 min, followed by 35 cycles of 94^0C: 30 sec, 48^0C: 30 sec and 72^0C: 2min; and a final extension at 72^0C for 7 min. The amplified product was visualized by 1% agarose gel electrophoresis and the amplified product was purified by gel extraction method (QUIAGEN). For the yeast expression of full length yeast MGE1, we amplified MGE1 by using NB187 Fwp: 5' CCCA G▾AATT▴C ACC ATG AGA GCT TTT TCA GCA GCC 3'-*E. CoR1* and NB19 Rev P: 5'ATT C▾TCGA▴G TTA GTT CTC TTC GCC CTT AAC AAT TCC 3'-*Xho1* primers. The PCR product was digested with *EcoRI / XhoI* restriction enzymes and cloned into high copy URA3 and high copy LEU2 plasmids under TEF promoters at the similar restriction sites to generate mutants of MGE1-M155L, H130L, H167L and H184L

respectively. Site directed mutagenesis was used to create MGE1-M155L, H130L, H167L and H184L harbouring MGE1 mutants respectively from Wild type MGE1. Human MGE1 without mitochondrial targeting sequence was amplified using Hela cells cDNA as a template by using NB202 Fwp: 5'CAAA G▼GATC▲C ACC ATG TCT CCC CGG TTG TTG 3'-*BamH1* and NB 201 Revp: 5'ACCC C▼TCGA▲G CTA AGC TTC CTT CAC CAC CCC 3'-*Xho1* primers.

2.2.4 Restriction Digestion

The amplified yeast and human MGE1 and pET28 (a) / pTEF-LEU/URA vectors were subjected to double digestion with *E.coR1* and *Xho1* restriction enzymes in a 50 µl reaction separately {(Insert 30 µl; 10X Tango Buffer 10 µl; Milli Q water 9 µl; *E.coR1* 0.5 U; *Xho1* 0.5 U) and (pET 28 (a) / pTEF-LEU/URA vector 30 µl; 10X Tango Buffer 10 µl; Milli Q water 9 µl *E.coR1* 0.5 U; *Xho1* 0.5 U)} at 37 ^{0}C for overnight. The digested products were visualized by 1% Agarose gel electrophoresis and the products were excised and gel purified by the QUIAGEN gel extraction method.

2.2.5 Ligation of yeast and human MGE1 with pET28 (a) /pTEF-LEU/URA vector

The digested yeast and human MGE1 fragment was ligated into a vector (pET 28 (a) / pTEF-LEU/URA) by using T4 DNA Ligase (Fermentas). The reactions were carried out in a final volume of 15 µl with 150 ng of vector, 3 fold excess of insert, 1 µl of T4 DNA Ligase and 1.5 µl of 10X T4 DNA Ligase Buffer. The reaction mixture was incubated at 16^{0}C for overnight and ligated product was transformed into DH5α cells.

2.2.6 Site Directed Mutagenesis

For the creation of mutations in the yeast MGE1 we employed site directed mutagenesis by using pfu DNA polymerase. The amplified DNA was treated with Dpn1 enzyme at 37 °C for 2 hrs in order to digest the parental, methylated DNA. Then the *Dpn1* treated plasmid was transformed into DH5α Cells. The clones were confirmed through the restriction digestion and sequencing. The primers used in the study were listed below.

Primers for creation of mutants in yeast MGE1:

NB188 Fwp: 5' GGG GTT AGA CTC ACA AGA GAT 3' (MGE1 M155L)

NB189 Revp: 5' ATC TCT TGT GAG TCT AAC CCC 3' (MGE1 M155L)

NB339 Fwp: 5' AAC TTT GGT CTT GCT TTG AAT 3' (MGE1 H130L)

NB340 Revp:5' ATT CAA AGC AAG ACC AAA GTT 3' (MGE1 H130L)

NB341 Fwp: 5' CTA AGA AAG CTC GGT ATT GAA 3' (MGE1 H167L)

NB342 Revp:5' TTC AAT ACC GAG CTT TCT TAG 3' (MGE1 H167L)

NB228 Fwp: 5' CCA AAT AAA CTC GAA GCA ACG 3'(MGE1 H184L)

NB229 Revp:5' CGT TGC TTC GAG TTT ATT TGG 3' (MGE1 H184L)

2.2.7 Agarose Gel Electrophoresis

Agarose gel electrophoresis was used to isolate DNA fragments made by PCR as well as to monitor the success of enzymatic digestion of DNA out of plasmid. Agarose gels were prepared by using 1-1.5 % (w/v) in 1X TAE buffer (40 mM TRIS buffer, 20 mM Acetate and 1 mM EDTA pH 8.0) containing 200 ng/ml ethidium bromide. The DNA samples were diluted with 6X DNA loading dye (30% Glycerol and 0.25% Bromophenol Blue) and separated on agarose gel. Electrophoresis was carried out by using fresh 1X TAE buffer at 100V. Subsequently, the DNA was detected by using UV light.

2.2.8 Bacterial Transformation

Competent cells of the E.coli DH5α / Rosetta gammie were used for plasmid preparation or protein expression respectively. About 10 µl of ligated product / 100 ng of pure plasmid was added to DH5α competent cells and incubated on ice for 30 min; heat shock was given at 42^0C for 1.3 min and chilled on ice for 2 min. Then 1 ml of LB medium was added to the cells and incubated at 37^0C shaker incubator for 60 min and the culture was plated on LB agar plate containing antibiotic (Kanamycin / Ampicillin). Further the colonies were screened for a clone with restriction digestion and sequence was confirmed by automated sequencer (Xcleris) .

Mitochondrial HSP70 plasmid in pET21b vector was a kind gift from Dr. Debkumar Pain (UMNDJ, USA).

2.2.9 Bacterial expression and protein Purification

Expression of His tagged human MGE1, YeastMGE1 and its mutantsand Hsp70 purification by Ni-NTA column

The plasmid pET28(a) harbouring yeast and human MGE1 and yeast MGE1 mutants or pET21b harbouring Hsp70 were transformed in to *E.coli* Rosetta gammei strain. A colony carrying the pET-MGE1 plasmid DNA was grown for overnight in LB medium containing kanamycin at 37^0C shaker incubator. The primary culture was diluted in to 1:50 in 500 ml fresh LB medium, grown with vigorous agitation to mid logarithmic phase ($OD_{600\ nm}$: 1.0), and incubated at 37^0C by addition of 1 mM IPTG (Isopropyl-β-D-thiogalactopyranoside) for 3 hrs. Further the culture was centrifuged at 10,000 rpm for 10 min to pellet down the bacterial cells. The pellet was suspended in 50 mM Tris-HCl pH 8.0 by $1/20^{th}$ volume. The suspended bacterial cells were ruptured by sonication. Then soluble (Supernatant) and insoluble (inclusion bodies) fractions were separated by centrifugation at 10,000 rpm for 10 min. The expressed recombinant proteins were present in soluble form. The soluble

recombinant proteins (yeast and human MGE1, MGE1 mutants and Hsp70) were purified on a Ni-NTA affinity column (Clontech). Sometimes, the expressed protein were present in inclusion bodies. If the expressed recombinant proteins were present in inclusion bodies, the inclusion bodies were solubilised in Urea buffer containing 8M Urea and 50 mM Tris-HCl pH 8.0. The insoluble recombinant proteins (Mitochondrial HSP70) were purified on a Ni-NTA affinity column (Clontech). Soluble proteins were eluted in soluble buffer A (0.4M imidazole, 100 mM Nacl, 20 mM Tris-HCL pH 7.5 and 5 mM β-mercaptoethanol) and the eluted fractions were dialyzed in buffer B (20%glycerol, 100 mM NaCl, 20 mM sodium phosphate pH 7.5). Insoluble proteins were eluted with Buffer C (0.4 M imidazole, 8M Urea, 20 mM Tris-HCL pH 7.5 and 5 mM β-mercaptoethanol) and eluted fractions were dialyzed by slowly removing urea concentration step by step until urea concentration to reach 0.1M. The final fraction was dialyzed with Buffer B. The protein concentration was measured by Bradford reagent assay and kept stored at -20^{o}C.

2.2.10 SDS-PAGE analysis

Purified recombinant proteins, mitochondrial lysate and the yeast cell lysate were separated on 10-12% SDS-PAGE [170]. Recombinant proteins were resolved on 10-12% SDS-PAGE followed by gel was stained with staining solution.

2.2.11 Western blot analysis

The proteins were resolved on 10% SDS-PAGE as described above and were transferred to a Nitrocellulose membrane (NC membrane) overnight at 40 volts. The membrane was blocked with TBST (20 mM Tris-HCl pH 7.5, 150 mM NaCl and 0.05% Tween20) containing 5% milk powder for 1 hr at room temperature. The membrane was incubated with primary antibody (Rabbit Mge1 1:1000 dilution and Rabbit mtHsp70, 1:2000 dilution) in TBST solution at room temperature for 2 hours followed by washing with a TBST solution for three

times. The blot was further incubated with HRP-conjugated secondary antibody (anti rabbit, 1:10000 dilution) for 2 hrs at room temperature. The membrane was washed three times with TBST solution for 15 min at room temperature followed by developing the blot using ECL reagents (GE Health care, USA) and Biorad Imaging system.

2.2.12 Antibody purification by affinity chromatography

The polyclonal antibodies for yeast Mge1 recombinant protein were raised in rabbit. The soluble recombinant protein was mixed either with Freund complete adjuvant or incomplete adjuvant (Bangalore Genei) for subsequent booster doses and injected into the rabbit. After subsequent booster doses, serum was collected from the rabbit blood. Yeast Mge1 polyclonal antibodies were purified by using antigen coupled CNBr Sepharose beads (GE Healthcare).

2.2.13 Purification of polyclonal Antibodies

The recombinant purified antigen (Mge1 protein) was dialyzed against the coupling buffer overnight (0.1 M NaHCO3 pH 8.0 and 0.5 M NaCl) at 4 ^{0}C. The dialyzed antigen in coupling buffer was mixed with CNBr activated Sepharose 4B beads and kept on rotisserie for 1 hour at room temperature or overnight at 4^{0}C. The beads were washed with coupling buffer and block the remaining active groups with the addition of 0.1 M Tris-HCl, pH 8.0 and incubated at room temperature for 2 hrs. Further, the column was washed 3 times by alternating pH cycle. Each cycle consist of a wash with 0.1 M Acetate buffer pH 4.0 containing 0.5 M NaCl followed by wash with 0.1 M Tris-HCl, pH 8.0 containing 0.5 M NaCl. Finally, the beads were kept in 1X PBS buffer pH 7.2 and stored at 4 ^{0}C. The dialyzed serum against 1X PBS pH 7.2 buffer was mixed with the ligand coupled CNBr activated sepharose beads and kept on a rotisserie for 2 hrs at 4^{0}C followed by centrifugation at 5000 rpm for 5 min to pellet down the sepharose beads. The beads were washed with 1X PBS, pH 7.2 for 3 times. The bound Mono-specific antibodies were eluted by using 0.1 M Glycine pH 2.5. The eluted

antibodies were neutralized with Tris buffer, concentrated and kept frozen at -20^{0}C for further use.

2.2.14 Preparation of H_2O_2 Solution

Initially a stock of 1 M H_2O_2 was prepared from commercially available 30% (v/v) H_2O_2 (Merck) by taking 102.14µl of H_2O_2 and diluting it to 1ml with de-ionized water. The concentration of H_2O_2 was measured spectrophotometrically at OD_{240} nm by placing 1ml of a 10 mM solution in a quartz cuvette. The concentration of H_2O_2 was calculated by using its extinction coefficient value (E_{240} = 43.6/M/cm).

2.2.15 In vitro cross linking of recombinant proteins

Cross linking of purified recombinant human MGE1,yeast Mge1 and its mutations (M155L,H130L,H167L and H184L) was performed with bis (sulfosuccinimidyl) suberate (BS^3; Pierce) at room temperature in 20 mM sodium phosphate (pH 7.4), 150 mMNaCl, 20mM HEPES and 50 mM Borate. 2.5 µg of purified proteins were pre-incubated with increasing concentrations of H_2O_2 (0.5, 1 and 2 mM) at room temperature for 20 min and BS^3 was added to a final concentration of 0.1 mM. The reaction was left for 30 min at the indicated temperature and quenched by addition of 40 mMTris–HCl (pH 7.5). Samples were analyzed by SDS-PAGE.

2.2.16 Circular Dichorism Spectroscopy

In general the CD spectroscopy used to study the secondary structure of proteins and their conformational changes. Circular dichroism spectra and oxidative denaturation curves were obtained in a Jasco J-810 spectropolarimeter, using a 2 mm path-length cuvette. Samples were prepared by dialysis against 20 mM sodium phosphate (pH 7.5). Four spectra were recorded between 260 nm and 190 nm and averaged.The secondary structure was determined

using CDNN 2.1, software for protein secondary structure analysis. For CD studies, the final concentration of Mge1 was 0.04 mM.

2.2.17 Coimmuno-precipitation (co-IP)

Purified recombinant wild type Mge1 or human Mge1 (20µM) and mutant Mge1-M155L (20µM) were pre-incubated with 1mM H_2O_2 at room temperature for 20 min. To this recombinant mHsp70 (7.5 mM) Hepes pH 7.6, 50 mM Nacl, 10 µM ADP) was added. Total lysates were incubated with Mge1 antibody for 2 hr at 4ºC on a rotator. Protein A beads were added to the lysates and further incubated for another 4hr at 4ºC. The beads were washed three times with (20 mM Hepes pH 7.6, 50 mM Nacl) buffer. Samples were resolved on SDS–PAGE, western transferred and probed with antibodies specific to mHsp70 and Mge1.

2.2.18 Construction of MGE1 mutant strains

Heterozygous diploid strain of MGE1,yNB39 (Euroscarf, Germany), a derivative of BY4743 was used for making haploid strains expressing either wild type or MGE1 mutants for *in vivo* studies .Yeast strain yNB39 was transformed with pNB185 (MGE1-pTEF-2µURA) to generate strain yNB59. yNB59 strain was grown in 2% KOAc with minimal amino acids to induce sporulation. Random sporulation analysis was carried out after zymolyase treatment and haploid yNB65 was selected from SC-Ura-Lys with G418 supplemented plates. PCR using primers for KanMX4 presence was done using genomic DNA from NB65 strain to confirm chromosomal deletion of MGE1.

The high copy URA3 plasmid in NB65 strain was replaced with either pNB186 (WT MGE1-pTEF-2µLEU) or pNB188 (MGE1-H130L-pTEF-2µLEU) or pNB187(MGE1-M155L-pTEF-2µLEU) or pNB189 (MGE1-H167L-pTEF-2µLEU) by plasmid shuffling to generate yNB67 or yNB 68 or yNB69 or yNB70 strains carrying wild type MGE1 or MGE1 H130L or MGE1

M155L or MGE1 H167L mutants respectively. These strains were treated with 5-FOA for two generations to remove URA3 borne wild type copy and the loss of URA3 plasmid was confirmed by lack of growth on SC-Ura plate. The resulting strains yNB 67 (WT MGE1), yNB 68 (H130L MGE1), yNB 69 (M155L MGE1) and yNB70 (H167L MGE1)were used for further analysis.

Table 2.1 :Yeast Strains are used in this study

Strain	Genotype	Resource
BY4741	*MAT*a, *his3*Δ 1, *leu2*Δ 0, *met15*Δ 0, *ura3*Δ 0	In House
BY4742	*MATα* , *his3*Δ 1, *leu2*Δ 0, *lys2*Δ 0, *ura3*Δ 0	In House
yNB39	BY4743;Mata/alpha:hisΔ1/3his3Δ1;Leu2Δ0/leu2Δ0;lys2Δ0/LYS2; MET15/met15Δ0;ura3Δ0/ura3Δ0;OR232w::kanMX4/YOR232w	Euroscarf
yNB59	BY4743;Mata/alpha:hisΔ1/3his3Δ1;Leu2Δ0/leu2Δ0;lys2Δ0/LYS2; MET15/met15Δ0;ura3Δ0/ura3Δ0;OR232w::kanMX4/YOR232w, pTEF –MGE1, 2µ, URA.	This study
yNB65	*Mat* a, *his*Δ1, *leu2*Δ0, *lys2*Δ0, *ura3*Δ0, YOR232w::KANMX4 ,pTEF –MGE1, 2µ, URA	This study
yNB67	BY4741; *Mat* a, *his*Δ1, *leu2*Δ0, *lys2*Δ0, *ura3*Δ0, YOR232w::KANMX4 pTEF- MGE1, 2µ, LEU	This study
yNB68	BY4741; *Mat* a, *his*Δ1, *leu2*Δ0, *lys2*Δ0, *ura3*Δ0, YOR232w::KANMX4, pTEF- H130L MGE1,2µ,LEU	This study
yNB69	BY4741; *Mat* a, *his*Δ1, *leu2*Δ0, *lys2*Δ0, *ura3*Δ0, YOR232w::KANMX4, pTEF- M155L MGE1, 2µ, LEU	This study
yNB70	BY4741; *Mat* a, *his*Δ1, *leu2*Δ0, *lys2*Δ0, *ura3*Δ0, YOR232w::KANMX4, pTEF- H167L MGE1, 2µ, LEU	This study

2.2.19 Yeast media

Standard yeast protocols were used for culturing yeast strains. Wild type yeast strains were grown in YPD that contained 1% yeast extract, 2% peptone and 2% dextrose. Synthetic Dextrose (SD) minimal medium contained 0.73% Yeast Nitrogen Base with amino acids,

0.4% ammonium sulphate and 2% glucose. Yeast transformations were performed by following standard lithium acetate method [171] .

2.2.20 Serial dilution and H_2O_2 resistance assay

Yeast strains with either wild type or mutant(s) were grown overnight in YPD and Sc-Leu medium. 0.5 OD of cells will be serially diluted by 10 folds and 10 µl of each suspension were spotted on either SD plates or SD plates containing 0.5 or 1 mM H_2O_2 concentrations and will be incubated at 30°C for 2-3 days. Also, cultures were grown overnight and they were diluted freshly into Sc-Leu medium in the presence and absence of H_2O_2 (1mM) at 30°C. The growth were monitored for every 2 hours by taking OD_{600}. To derive statistical significance, three independent cultures of wild type and mutant were grown in the presence and absence of H_20_2.

2.2.21 Isolation of yeast mitochondria

Briefly, yeast cells were grown in Sc-Lac pH5.5 media at 30°C. Cells were harvested at 1 or 2 OD_{600nm}. Cultures were centrifuged at 5000 rpm for 5 min and cell pellet washed with autoclaved distilled water. The cells treated with 10 mM DTT in 0.1 M Tris-SO_4, pH 9.4 buffer for 15 min and centrifuged at 5000 rpm for 5 min. Zymolyase treatment was done in 1.2 M Sorbitol /20 mM phosphate buffer pH 7.0 and after getting 50% lysis of cells (lysis monitored at OD_{600}) the resulting spheroplasts were washed with 1.2 M Sorbitol for two or three times and the pellet was collected. The pellet was suspended in SEM buffer (250 mM sucrose,1 mM EDTA,10 mM MOPS,1 mM PMSF, 0.5% BSA pH7.5) and homogenized using dounce homogenizer (15 times). The homogenate was centrifuged at 3500 rpm. The supernatant was collected and centrifuged at 10,000 rpm for 10 min and the pellet was dissolved in SEM buffer and centrifuged at 3500 rpm for 5 min and the pellet was discarded. The supernatant was centrifuged at 10000 rpm for 10 min and the pellet washed 3 times in

SEM buffer. The resultant crude mitochondria was solubilised at the concentration of 1mg/ ml in SEM buffer (without BSA) and kept frozen at -80^{o}C.

2.2.22 In organelle cross linking

Wild-type yeast mitochondria and mutant Mge1(Mge1-M155L) mitochondria were pre incubated with various concentrations of Antimycin A on ice for 20 min in a buffer containing 20 mM Hepes(pH 7.4) and 0.6 M sorbitol. To this reaction disuccinimidylsuberate (DSS, Pierce), a membrane- permeable cross-linker was added at 100 µM final concentration. The reaction was left for 30 min at room temperature and quenched by the addition of 50 mMTris–HCl (pH 7.5). Samples were analyzed by SDS-PAGE and western immunostained with anti-Mge1 and anti-mtHsp70 antibodies.

Samples were also subjected to immunoprecipitation after cross linking. Mitochondria samples were solubilized in lysis buffer (50 mMTris-HClpH 8.0, 150 mM NaCl, 1% NP-40, 0.5% Deoxycholate, 0.1% SDS and protease inhibitors) and incubated on ice for 30 min. Lysates were centrifuged for 15 min at 13,000 rpm at 4ºC. The clear supernatant fractions were incubated with protein A beads for 1 hr at 4ºC to remove non-specific interactions. Pre-cleared lysates were incubated with Mge1 antibody for 5 hr at 4ºC on a rotator. Protein A beads were added to the lysates and further incubated for another 4 hr at 4ºC. The beads were washed four times with mitochondrial lysis buffer. Samples were resolved on SDS–PAGE, western transferred and probed with antibodies specific to mHsp70.

2.2.24 Measurement of ROS

Yeast strains Wild type Mge1 and Mge1-M155L were grown over night in Sc-LEU medium. Cells (10^7 cells/ml) were pre-incubated in YPD medium with 20 µM DCFH-DA at 30^0C for 1h followed by incubating with increasing concentrations of Antimycin A at 30^0C for 1h.

Then the cells were isolated by centrifugation and were washed with phosphate buffer saline. The resulting cell pellet was resuspended in 100 µl of phosphate buffer saline. Fluorescence intensity of the cell suspension containing 10^7 cells was read with fluorescence spectrophotometer (Perkin Elmer,USA) at an excitation wavelength of 480 nm and an emission wavelength at 525 nm [172].

2.2.25 In vitro Transcription and Translation

About 500 ng of Plasmid DNA carrying yeast SU9-DHFR, COX1V and AAC proteins were incubated with 20 µl of TNT T7 master mix (Promega, USA) by addition of 1 µl ^{35}S-Methionine (specific activity-1000 TBq/mmole) at 30 ^{0}C for 90 min. The translated proteins were resolved on 10% SDS PAGE and transferred on to nitro cellulose membrane and translated proteins were detected by using phosphor imaging.

2.2.26 In vitro protein import

Radiolabeled precursor proteins were generated by *in vitro* transcription/translation in the presence of [^{35}S]-methionine using rabbit reticulocyte lysate (Promega). Mitochondria isolated from the strains expressing Mge1 wild type or M155L mutant were treated either with 20µM Antimycin A or 5µM Valinomycin on ice for 15min. The mitochondria samples were incubated with import buffer (fatty acid-free BSA, sucrose, 80 mM KCl, 5 mM MgCl2, 5 mM methionine, 10 mM MOPS/KOH pH7.0, 5 mM ATP pH7.0 and 1 mM DTT) with [^{35}S]-methionine labelled precursor proteins at 30^{0}C for different time points. After the indicated time points, mitochondria were isolated by centrifugation and washed in SEM buffer. The samples were either directly subjected to SDS-PAGE or protease protection analysis in the presence of trypsin for 15 on ice followed by inhibiting the trypsin by soybean trypsin inhibitor and washing the mitochondria samples in SEM buffer. The samples were separated on SDS-PAGE and analyzed by phosphor imaging.

2.2.27 ATPase assay of mHsp70

The ATPase activity of mhsp70 was analyzed by measuring the release of inorganic phosphate from [γ-^{32}P]ATP using the method as described [173].Recombinant mHsp70 (1ug) was incubated with or without 5 ug of wild type or Mge1-M155L mutant in an ATPase assay buffer (50 mM Hepes/KOH pH 7.2, 5 mM $MgCl_2$ and 100 mMKCl) in the presence of 0.05 mM [γ-^{32}P]ATP (3000 Ci/mmol). At different time intervals 25 µl of reaction mixture was taken and mixed with 7 volumes of 1 M perchloric acid and 1 mM sodium phosphate and kept on ice. After addition of 16 volumes of 20 mM ammonium molybdate and isopropyl acetate, the samples were mixed and centrifuged at 15,000 g for 30 seconds in a microfuge to separate organic and inorganic phase.The amount of radioactive inorganic phosphate released as phospho-molybdate complex in organic phase was measured by scintillation counting. Control reactions were performed to eliminate the background non-specific hydrolysis of ATP.

2.3 Results

2.3.1 Cloning, Expression and purification of Human and Yeast Mge1

To characterize the function of Mge1 under oxidative stress we have cloned Mge1 into a pET28 (a^+) vector. Briefly Yeast Mge1 gene was amplified by polymerase chain reaction from yeast genomic DNA using specific primers (NB18 and NB19) and the amplified product was shown in Fig.2.1.A (Left Panel)**.** Further, the amplified product was digested with *EcoR1* and *Xho1* restriction enzymes, gel purified and cloned into pET28 (a^+) vector using the same sites. The cloned gene was confirmed by restriction digestion (**Fig. 2.1A, Right Panel)** and the sequence conformed by automated sequencing (Bioserve, India).

We also cloned Human Mge1 (GRPEL1) gene into a pET28 (a^+) vector. In brief, total cDNA was made from HeLa cells RNA using reverse transcriptase as described in the Methods. From the total cDNA, the human Mge1 was amplified by using human Mge1 ORF specific primers (NB 223 and NB 224) and the amplified product was shown in Fig.2.1.B. Further, we have cloned human Mge1 gene into *BamH1* & *Xho1* digested pET28a vector as described in the Methods. The clone was confirmed by restriction digestion with *BamH1* & *Xho1* enzymes (**Fig.2.1B)** and the sequence was confirmed by automated sequencing (Bioserve, India).

The pET28a vector harbouring human and yeast MGE1, Pet21b vector harbouring mHSP70 (a kind gift from Debkumar Pain, Rutgers University, USA) genes were transformed into *E.coli* Rosetta gammei bacterial strain. Expression of recombinant protein was induced by 1 mM isopropyl-β-D-thiogalactopyranoside to bacterial cultures when they attained an OD_{600nm} equal to 0.6. The expressed recombinant protein was present in soluble form in case of yeast or human Mge1 and in inclusion bodies in case of mHsp70. The soluble and insoluble recombinant proteins were purified on a Ni-NTA affinity column (Clontech) as described in the methods. The purified proteins were shown in **Fig.2.1C**.

The polyclonal antibodies for yeast Mge1 was raised in Newzeland white rabbit as described in methods. The raised antibodies were purified using antigen coupled sepharose beads (GE Health care) as described in the Methods. The purified monospecific antibodies of Mge1 are specific and detected a major band at 27 kDa in total cell lysates and mitochondrial extracts of yeast (**Fig.2.1D)**.

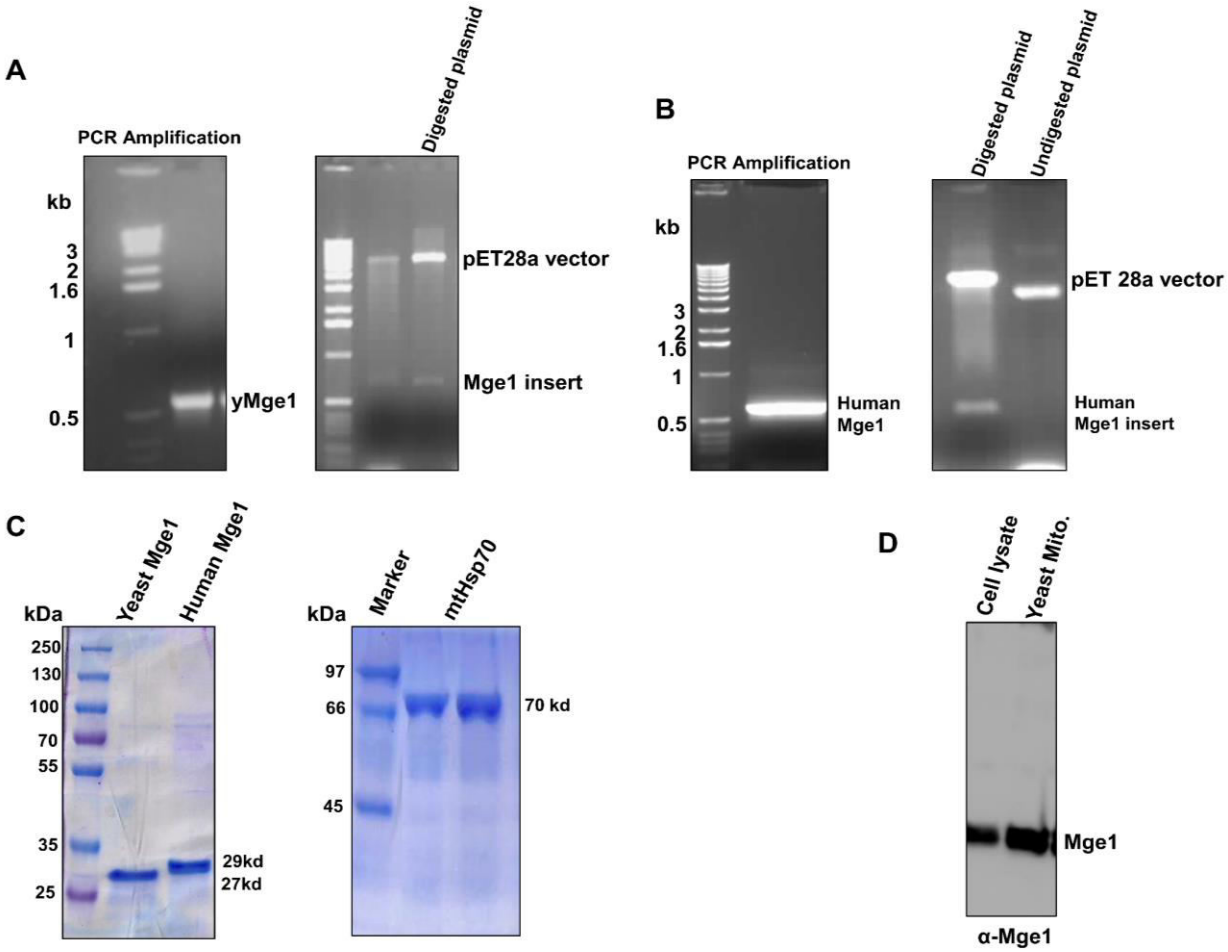

Figure 2.1 Cloning, Expression and Raising of antibodies to Mge1: To characterize the Mge1 *in vitro*, we cloned Mge1 into bacterial expression vector pET28 (a^+). **(A)** 1% Agarose gel electrophoresis analysis of PCR amplified yeast Mge1 gene. Restriction digestion of pET28-yeast Mge1 with *EcoR1&Xho1* enzymes followed by 1% Agarose gel electrophoresis to confirm the presence of amplified insert. **(B)** 1% Agarose gel electrophoresis analysis of PCR amplified Human Mge1 gene. Restriction digestion of pET28 Human Mge1 with *Bamh1 & Xho1* enzymes followed by 1% Agarose gel electrophoresis to confirm the presence of amplified insert. **(C)** Recombinant yeast and human Mge1 and yeast mHsp70 proteins were expressed and purified using Ni-NTA column and analysed by 10% SDS PAGE. **(D)** Polyclonal antibodies were raised against yeast Mge1 in rabbit and purified using CNBr-activated sepharose beads. The cross reactivity was checked by western blot analysis both with total yeast cell lysate and yeast mitochondria.

2.3.2 Oxidative stress reduces Mge1 and mHsp70 complex formation in vitro

It is known that Mge1 acts as thermo sensor. In response to heat shock, the active dimeric form of Mge1 monomerizes and fails to interact with Hsp70 [153]. We are interested to see whether Mge1 is also responds to oxidative stress. It is known that some proteins undergo oxidation when they are exposed to H_2O_2 *in vitro* [174]. To investigate whether Mge1 responds to oxidative stress, we treated purified recombinant Mge1 with increasing concentrations of H_2O_2 followed by cross linking with amine reactive cross-linkerbis(sulfosuccinimidyl) suberate BS^3). The samples were resolved on SDS-PAGE and coomassie stained gels were analysed. Mge1 migrates as a 27 kDa monomer in the absence of a cross-linker. In the presence of BS^3, Mge1 migrates as a ~60 kDa homodimer reflecting the efficiency of the cross-linking agent. However, in the presence of H_2O_2, appearance of monomer increased in a concentration dependant manner despite the presence of cross linker. These results suggest that Mge1 loses its dimer formation ability in the presence of oxidative stress triggered by H_2O_2 (**Fig .2.2A**).

To determine whether the Mge1 response to H_2O_2 is conserved across species, we repeated the experiment using purified human Mge1 (GRPEL1).Consistent to the observation made using yeast Mge1, the dimer form of human Mge1 is also susceptible to H_2O_2 as shown in **Fig.2.2B**. These results suggest that Mge1 loses its dimer formation ability in the presence of oxidative stress triggered by H_2O_2. Because the dimerization of Mge1 was shown to be crucial for its interaction with mHsp70, we evaluated the effect of H_2O_2 on this interaction using recombinant purified yeast Mge1 and mHsp70. We incubated recombinant mHsp70 with Mge1 that was either left untreated or treated with H_2O_2. The reaction mixtures were cross linked, resolved on SDS-PAGE and stained with coomassie blue. A high molecular weight cross linked band was observed at ~130 kDa upon incubation of Mge1 with mHsp70

in the absence of H_2O_2. Interestingly, formation of this complex decreases with prior treatment of Mge1 with increasing concentration of H_2O_2 (**Fig.2.2C**). To confirm the constituents of the 130 kDa complex, western blotting was carried out using antibodies specific for Mge1 (**Fig. 2.2D**) and mHsp70 (**Fig. 2.2E**). Both antibodies detected a similar strong high 130 kDa molecular weight band in the absence of H_2O_2 suggesting that indeed Mge1 and mHsp70 are exists in a high molecular weight complex. To rule out the possible interference of H_2O_2 with BS^3cross-linking efficiency, we used glutathione *S*-transferase (GST), a dimeric protein [175], as a control and cross-linked with BS^3in the presence and absence of H_2O_2. Most of the GST remains as a dimer in the presence of H_2O_2, indicating that $BS^3$is not affected by H_2O_2 (**Fig. 2.2F**). Taken together, our results clearly show that Mge1 is able to modulate its interaction with mHsp70 in a manner that is dependent on the oxidative stress *in vitro*. Mge1 is able to switch from an active dimer to an inactive monomer form by sensing the oxidative stress.

Interestingly, we find recombinant Mge1 co-purify with a small amount of bacterial DnaK protein, the bacterial homolog of eukaryotic mHsp70 (**Fig. 2 A,B** indicated as *). DnaK also forms a high molecular weight complex with Mge1 (Fig.2C, indicated as **) and we find that this interaction is dependent on the Mge1 dimer as pre-treatment of Mge1 with H_2O_2 decreases the amount of the Mge1-DnaK complex (**Fig.2C**) and thus indicating the mechanism may be conserved across evolution.

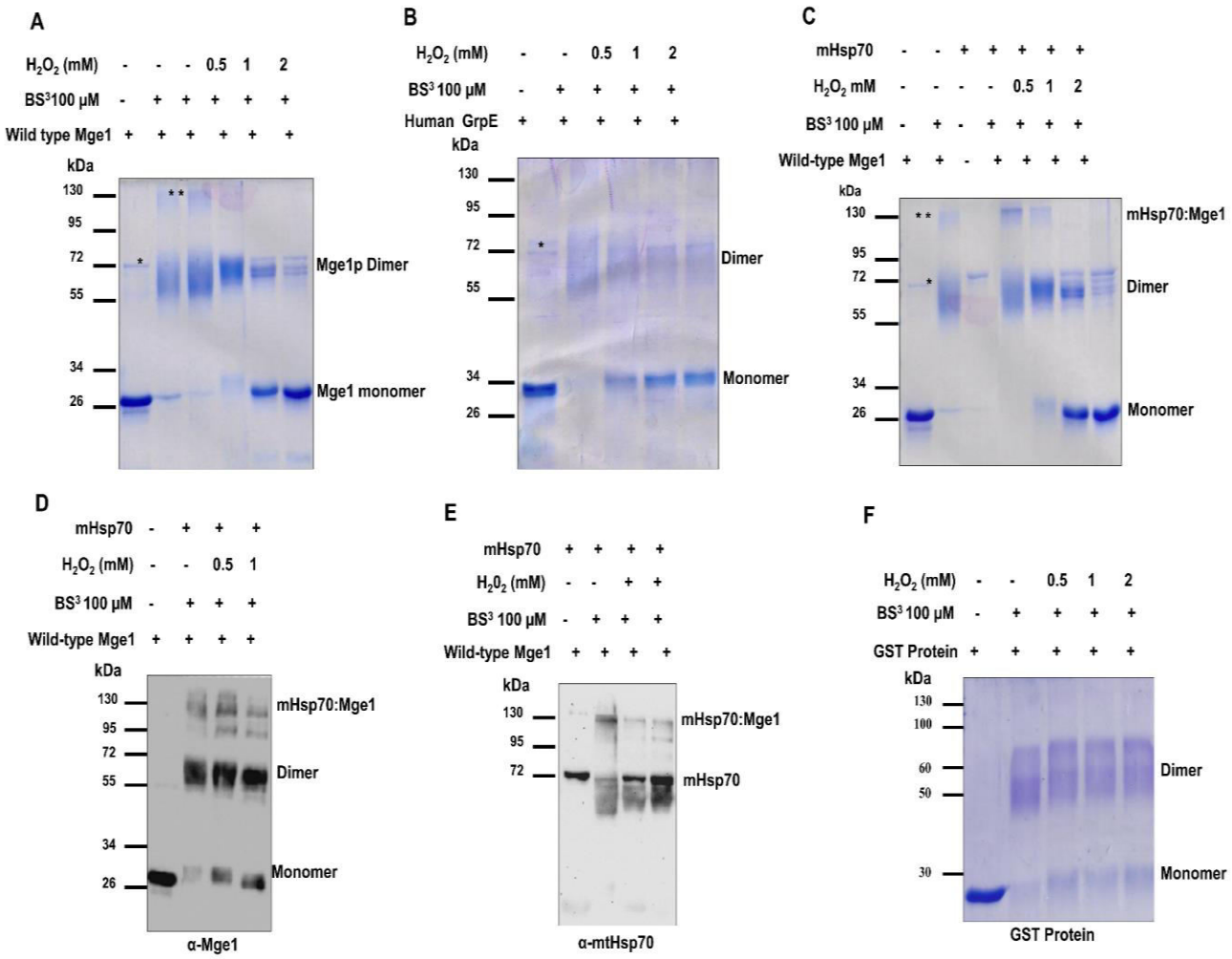

Figure 2.2 H_2O_2 treatment of Mge1 causes the dissociation of dimer and reduces the interaction of Mge1 with mtHsp70: (A) and (B) Cross linking of yeast or human Mge1 (2.5 µg) was carried out in 20 mM sodium phosphate (pH 7.4) buffer in the presence and absence of H_2O_2 for 20 min at room temperature. The samples were either cross linked for 20 minutes with the addition of 100µM BS^3 or left untreated. The cross linking reactions were left for 30min at the room temperature, quenched and adducts were resolved by 10% SDS-PAGE and stained with commassie. Fig.1A is the commassie stained yeast Mge1 cross linked adducts where as Fig.1B represents the human Mge1 cross linked adducts. **(C)** Purified Mge1 was treated with or without increasing concentrations of H_2O_2(0.5 and 1 mM) for 20 min at room temperature. The samples were incubated with purified mHsp70 for 10 minutes followed by cross linking with BS^3 for 20 minutes at room temperature. The reactions were quenched with Tris buffer. The cross linked adducts were separated on SDS-PAGE stained with commassie. **(D)** The cross-linked adducts were separated on SDS–PAGE

and Western transferred and probed with antibodies specific for Mge1 **(E)** or mHsp70 antibodies. **(F)** Purified recombinant GST protein was subjected to increasing concentrations of $H_2O_2$and cross-linked, and cross-linked adducts were separated and stained with Coomassie. Asterisk (*) indicates the copurifiedDnaK with recombinant yeast Mge1; double asterisks(**) indicates the DnaK–Mge1 complex.

2.3.3 Cloning ,Expression and Purification of Mge1 Mutants

Since pre-treatment of Mge1 with H_2O_2 induces conformational change and affects its interaction with mHsp70, we further investigated the amino acid residues in Mge1 that are prone to oxidative modification. Generally, cysteine and metheonine are most susceptible to oxidation followed by tryptophan, histidine and tyrosine [176]. Surprisingly, yeast Mge1 protein is devoid of any cysteine amino acid but contains only one methionine at 155 and three histidines (at position 130,167,184). Further, methionine M155, histidine167 and 184 residues are highly conserved across species (**Fig.2.3A)**. To test whether methionine 155, histidine 130, 167 and 184 amino acid residues undergoes oxidative modification upon exposure to H_2O_2, we mutated methionine 155 to leucine (Mge1-M155L mutant), histidine to leucine at position 130 (Mge1-H130L), 167 (Mge1-H167L) and position 184 (Mge1-H184L) by site directed mutagenesis as described in the Methods. All the proteins were expressed in bacteria and purified to homogeneity (**Fig. 2.3B**).

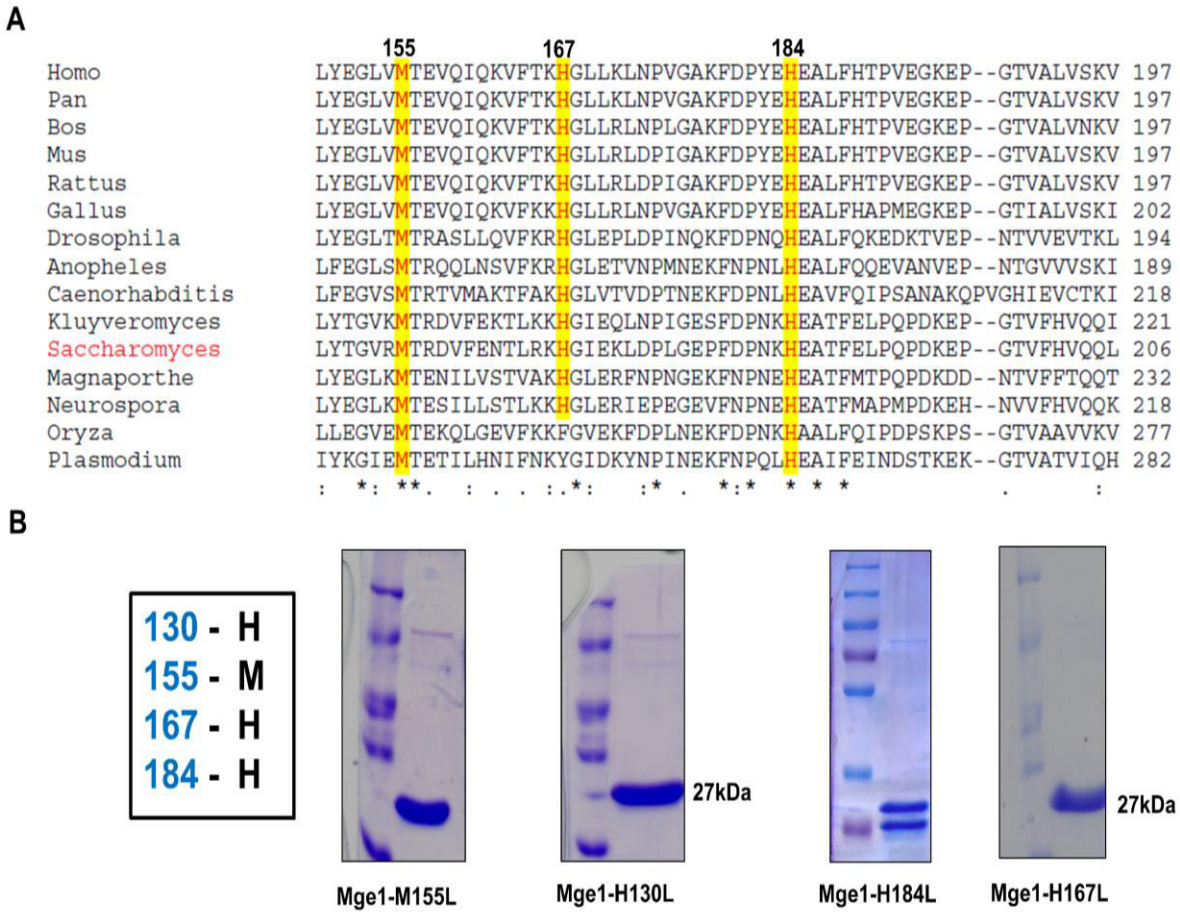

Figure 2.3 Expression and Purification of Mge1 Mutants: (A) A multiple sequence alignment of C-terminal of Mge1 (149-197) across eukaryotic species,yellow-shaded amino acids are point to the conserved oxidative prone amino acids. **(B)** The purified recombinant Mge1 Mutants (Mge1-M155L,Mge1-130L,Mge1-H167L and Mge1H184L) by using Ni-NTA column and analysed by 10% SDS PAGE.

2.3.4 Methionine 155 in Mge1 is prone to oxidative modification in vitro

The purified proteins were treated with increasing concentrations of H_2O_2 and cross linked with BS^3 followed by separating the samples on SDS-PAGE and coomassie stained for further analysis. In the absence of H_2O_2 treatment, Mge1 wild type Mge1-M155L, Mge1-H130L, Mge1-H167L and Mge1-H184L mutants forms a ~60 kDa dimer upon cross linking (**Fig.2.4A**). We find that H_2O_2 treatment causes the dissociation of dimer to monomer in wild type Mge1, Mge1-H130L and Mge1-H184L mutant. However, Mge1-M155L mutant is

resistant to dissociation of dimer in the presence of H_2O_2 when compared to wild type and other mutants (**Fig. 2.4A**). Mge1-H167L mutant is also partially resistance to dissociation of dimeric form to monomer in the presence of H_20_2 (Fig.2C). In addition, Mge1-M155L mutant forms relatively stable complex with mHsp70 when compared to wild type even after pre treatment with H_2O_2 (**Fig.2.4B**). Similar results were obtained when we performed western immunoprecipitation analysis of H_20_2 treated purified wild type and Mge1-M155L mutant in the presence of mHsp70. We have observed reduced co-precipitation of mHsp70 with Mge1 antibody when wild type Mge1 was treated with H_20_2 when compared to untreated or Mge1-M155L treated with H_2O_2 (**Fig.2.4C**). Since the crystal structure of E.coli GrpE is available [169], we would like to see the position of this residue in the 3D structure of the protein. This may also provide some insights into a possible mechanism of inactivation of the protein. We have modelled the structure of yeast Mge1 using I-TASSER [177], [178] server based on E.coli GrpE crystal structure and find that the methionine 155 position is present in the helical region of the protein **(Fig.2.4D)**. The helical region is downstream of the dimerization domain. Interestingly, we find that this residue is present on the outer surface of the helical region and may be available for possible modifications. Like wild type Mge1, Mge1-M155L also co-purify with small amount of DnaK and forms a high molecular weight 130 kDa complex upon cross linking (indicated as **). However, this complex is more susceptible to H_20_2 treatment when compared to Mge1-M155-mHsp70 complex **(Fig.2.4D)**. These results likely suggest the involvement of methionine 155 in oxidative response of Mge1.

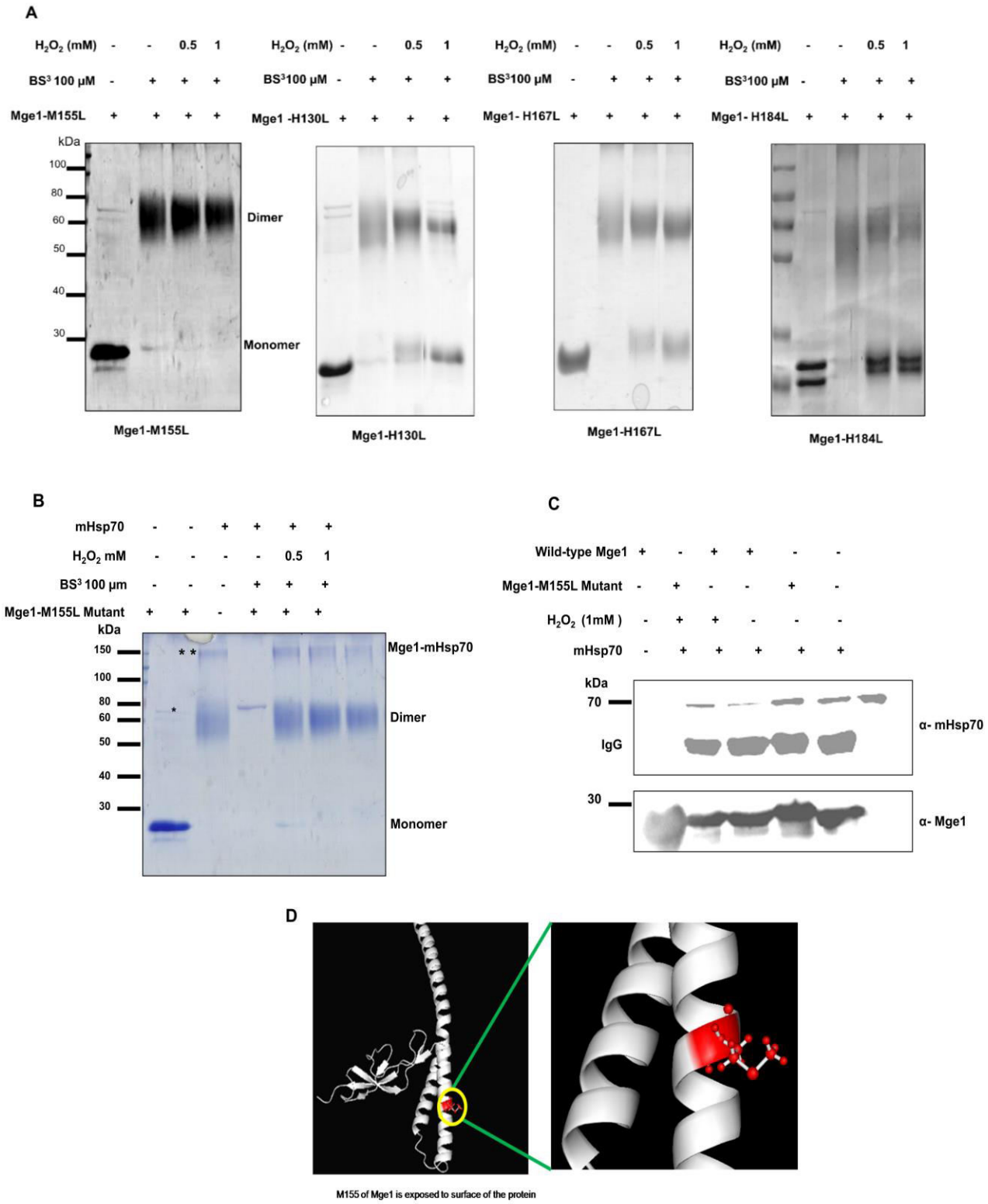

Figure 2.4 Mge1 M155 mutant is resistant to H_20_2 induced oxidative stress: (A) Mge1Mutants (M155L, H130L, H167L and H184L) was pre incubated in 20 mM sodium phosphate (pH 7.5), 150 mM NaCl , 20 mM HEPES in the presence or absence of H_2O_2 for 20 minutes. Then the samples were cross linked with BS^3 final concentration at 100 µM.

Samples were incubated at room temperature for 30min and quenched by Tris–HCl pH 7.5. The samples were resolved by SDS-PAGE and stained with comassie. **(B)** Purified Mge1-M155L was preincubated in 20 mM sodium phosphate (pH 7.4) buffer in the presence or absence of H_2O_2 for 20 min before incubation with mHsp70 for 10 min.Then the samples were cross-linked with BS^3 final concentration at 100 μM. Samples were incubated at room temperature for 30 min and quenched by Tris-HCl buffer. The samples were resolved on SDS–PAGE and Coomassiestained. **(C)** Purified wild type and Mge1-M155L were treated with 1 mM H_2O_2 for 20 min, followed by incubation with mHsp70 for 10 min. Then the samples were immunoprecipitated with anti Mge1 antibodies and probed with antibodies specific for mHsp70 (top) and Mge1 (bottom). This blot is representative of two independent experiments. Asterisk, the copurified DnaK with recombinant yeast Mge1-M155L; double asterisks, the DnaK–Mge1-M155L complex. **(D)** Met 155 of Mge1 protein is exposed towards the surface of protein: Position of the Met 155 was shown using PyMol. Asterisk (*) indicates the copurified DnaK with recombinant yeast Mge1; double asterisks(**) indicates the DnaK–Mge1 complex.

2.3.5 Altered structure of Mge1 with H_2O_2 treatment

Since H_2O_2 induced structural transition of Mge1 from dimer to monomer, we used CD Spectroscopy to analyse structural changes in Mge1 in the presence of H_2O_2 and secondary structural alterations were quantified using CDNN 2.1 software. The CD spectraof WT Mge1 exhibited two negative bands in the ultraviolet region, at 208 and 218 nm. There is a gradual and significant alteration of spectrum in wild type Mge1 treated with increasing concentration of H_2O_2 as shown in (**Fig.2.5A**). Overall, alpha helical, beta and anti-parallel turns in wild type Mge1 are considerably altered with increasing concentration of H_2O_2 (**Table 2.2**). It is evident from the spectrum that the isodichroic point is at 203nm and is not altered with varying concentration of H_2O_2 indicating the presence of a two state conformation.

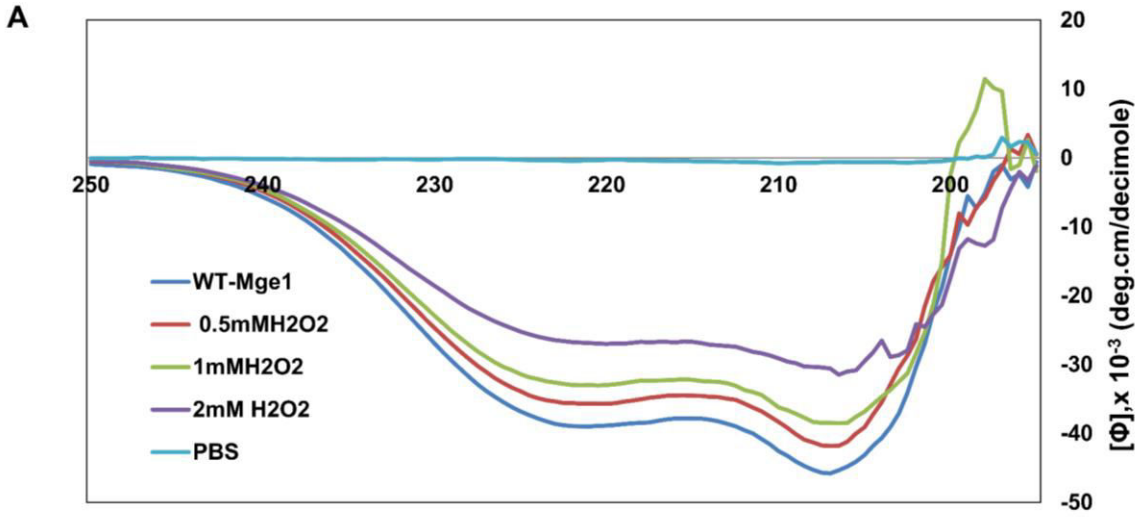

Table 2.2

	Wild-type mge1p	0.5mMH_2O_2	1mMH_2O_2	2mMH_2O_2
	200-260nm	200-260nm	200-260nm	200-260nm
Helix	75.00%	65.90%	63.50%	44.50%
Antiparallel	2.00%	3.20%	3.50%	6.00%
Parallel	2.00%	3.20%	3.60%	6.60%
Beta-Turn	10.00%	12.20%	12.60%	16.20%
Rndm.coil	11.00%	15.50%	16.70%	26.80%

Figure 2.5A Circular dichroism analysis of Mge1 under oxidative stress: Purified and dialyzed Mge1 (40 µM) wild-type samples in phosphate buffer were used for CD spectra analysis at 20°C at a scan rate of 60°C/h in a 2-mm–path-length cuvette. Wild type **(A)** were pretreated with 0.5, 1, or 2 mM H_2O_2 for 15 min before spectral analysis.Secondary structural analysis of H_2O_2-treated recombinant wild-type Mge1 from **Figure A**. **Table 2.2** Secondary structural analysis of H_2O_2-treated recombinant wild-type Mge1 from Figure 2.5A

It also suggests that loss of helical stability is possibly due to partial unfolding of Mge1 protein. In case of Mge1-M155L mutant, the shape of the spectrum is similar to that of wild type in the absence of H_2O_2 (**Fig.2.5B**). However, treatment of Mge1-M155L mutant with increasing concentrations of H_2O_2 does not alter the alpha helical and beta sheet structures appreciably (**Table 2.3**). These results show that M155L mutation stabilizes the Mge1 structure and protects it from H_2O_2 induced oxidative stress. This is consistent with our

earlier observations of a stable Mge1-M155L-mHsp70 complex in the presence of H_2O_2 *in vitro.*

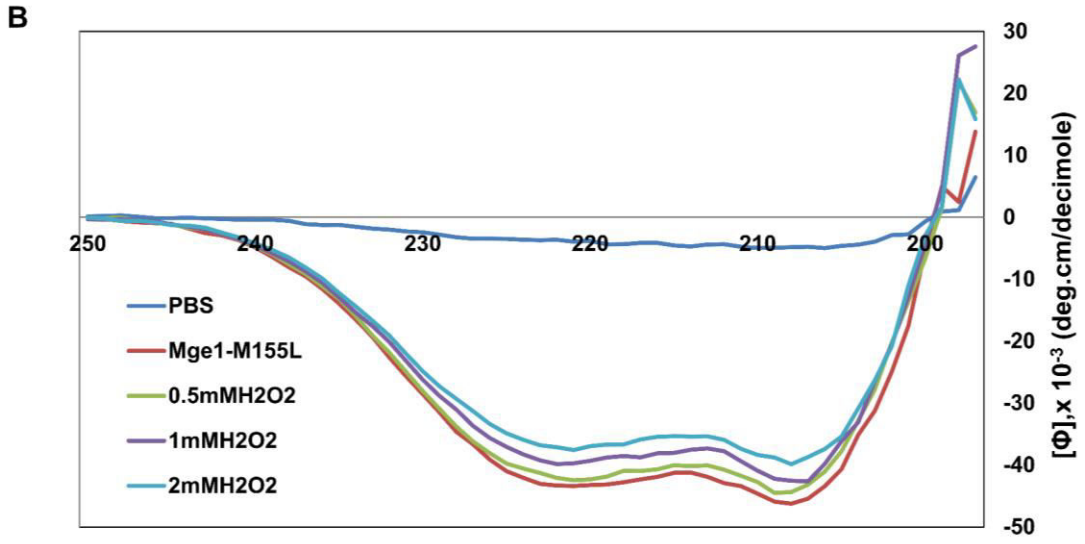

Table 2.3

	Mge1- M155L	0.5mMH_2O_2	1mMH_2O_2	2mMH_2O_2
	200-260nm	200-260nm	200-260nm	200-260nm
Helix	72.00%	70.20%	67.50%	64.40%
Antiparallel	2.50%	2.70%	3.00%	3.50%
Parallel	2.40%	2.60%	3.00%	3.50%
Beta-Turn	11.10%	11.50%	12.00%	12.50%
Rndm.coil	12.00%	13.00%	14.50%	16.10%

Figure 2.5B Circular dichroism analysis of Mge1 under oxidative stress: Purified and dialyzed Mge1-M155L (40 µM) mutant samples in phosphate buffer were used for CD spectra analysis at 20°C at a scan rate of 60°C/h in a 2-mm–path-length cuvette. Mutant Mge1 **(B)** were pretreated with 0.5, 1, or 2 mM H_2O_2 for 15 min before spectral analysis. Secondary structural analysis of H_2O_2-treated recombinant Mge1-M155L mutant from **Figure B. Table 2.3** Secondary structural analysis of H_2O_2-treated recombinant Mge1-M155L mutant from Figure 2.5B.

2.3.6 Mge1 acts as an oxidative sensor in vivo

To understand the *in vivo* significance of Mge1 in oxidative stress, we cloned the full length Mge1 and its mutants in pTEF-LEU vector by using *BamH1* and *Xho1* sites as shown in

(**Fig.2.6A**). We also generated chromosomal MGE1 deleted haploid yeast strains harbouring and expressing MGE1 wild type or MGE1 mutants under high copy plasmid. Mge1-H130L mutant was included as a control for any non-specific activity of the Mge1-M155L mutant. We compared the phenotype of wild type MGE1 strain with MGE1 mutants on SC-Leu plates supplemented with 0.5 mM or 1.0 mM H_2O_2 (**Fig.2.6B**). Exponentially growing yeast cells expressing either wild type Mge1 or Mge1 mutants were serially diluted and spotted on SC-Leu plates with increasing concentration of H_2O_2. We find that both wild type Mge1 and Mge1-M155L mutant have comparable growth on SC-Leu. However, Mge1-H130L mutant has poor growth. Wild type Mge1 is sensitive to H_2O_2 as its growth is retarded even at 0.5 mM H_2O_2. Most importantly, we find that Mge1-M155L mutant has considerable growth in the presence of both 0.5 mM and 1mM H_2O_2 when compared to wild type. The slow growth of Mge1-H130L mutant is further exacerbated in the presence of H_2O_2. To confirm the results obtained on plates, we grew the above strains in liquid SC-Leu medium with or without 1mM H_2O_2. All the strains display similar growth profile in SC-Leu medium (**Fig.2.6C**). However, consistent with our previous results on SC-Leu plates with H_2O_2, Mge1-M155L mutant is relatively more resistant to H_2O_2 while both wild type and Mge1-H130L mutant are inhibited by H_2O_2. A single point mutation in Mge1 protein at M155L is able to rescue poor growth of wild type yeast in the presence of H_2O_2. These results further show that Mge1 plays a significant role in oxidative stress response and methionine 155 is crucial for this activity.

To exclude the possibility of altered protein expression in Mge1-M155L mutant is responsible for the resistance to oxidative stress, we evaluated the steady state levels of mitochondrial proteins in wild type and Mge1-M155L mutant by using antibodies specific for porin, Tim44, mHsp70, Tim22, CCPO, Aconitase, Tim23 and Tom40 (**Fig.2.6D**). As shown in (**Fig.2.6D)**, there is no change in steady state levels of mitochondrial proteins in Mge1-M155L mutant when compared to wild type.

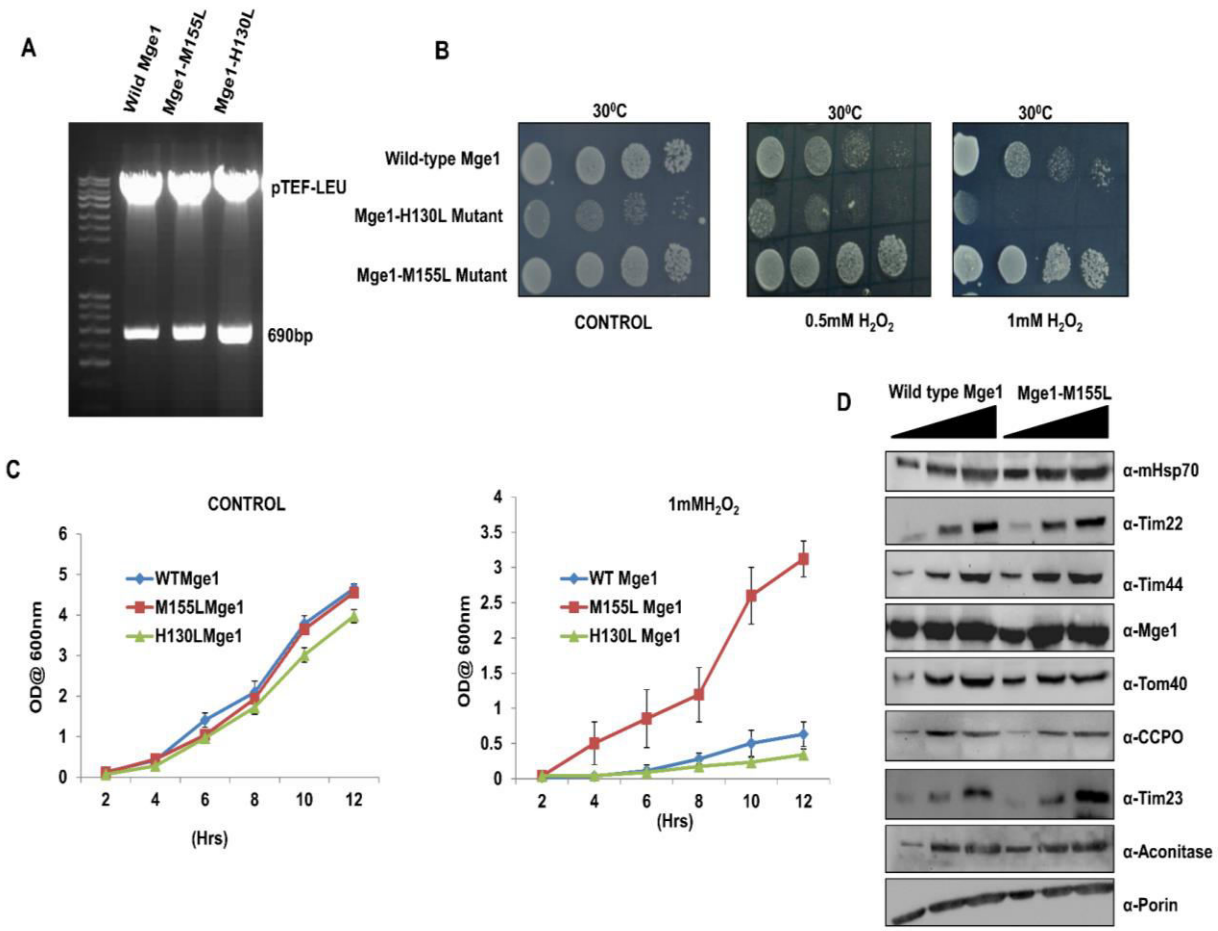

Figure 2.6 Sensitivity of wild-type and mutant Mge1-M155L strains to H_2O_2:

To characterize the Mge1 *in vivo*. **(A)** we cloned Mge1and its mutants into yeast expression vector pTEF-LEU. 1% Agarose gel electrophoresis analysis of PCR amplified yeast Mge1gene. Restriction digestion of pTEF-yeast Mge1 with *EcoR1&Xho1* enzymes followed by 1% Agarose gel electrophoresis to confirm the presence of amplified insert. **(B)** Yeast strains yNB71, yNB72, and yNB73 carrying wild-type MGE1 and MGE1-H130L and MGE1-M155L, respectively, were grown overnight in Sc-Leu medium. Then one OD of cells was serially diluted by 10-fold, and 10 µl of each suspension was spotted on either SD plates or SD plates containing 0.5 or 1 mM H_2O_2 concentration as indicated in the figure and incubated at 30°C for 3 days. **(C)** Overnight-grown wild-type or mutant cell lines were freshly diluted into SC-Leu medium in the presence and absence of H_2O_2 (1 mM) at 30°C. The growth was monitored every 2 hours by taking OD_{600}. To derive statistical significance, three independent cultures of wild type and mutant were grown in the presence and absence of H_2O_2. **(D)**The indicated amounts of mitochondria isolated from either wild-type Mge1 or Mge1-M155L mutant were analyzed by SDS–PAGE and immunostaining with antibodies against specific mitochondrial proteins.

To address if the resistance of Mge1 M155L mutant to H_2O_2 is due to stable interaction of mHsp70-Mge1 complex under oxidative stress *in vivo*, we used Antimycin A, an electron transport chain complex III inhibitor which is known to generate ROS in yeast [179]. Generation of ROS by Antimycin A was measured by fluorescence emission at 520 nm by DCFDA as described in the Methods section. Antimycin A induces similar amount ROS in all yeast strains that were tested (**Fig.2.7A**). To study the *in vivo* response of Mge1 to ROS, mitochondria were isolated from wild type and Mge1-M155L mutant and were incubated with increasing concentrations of Antimycin A followed by cross linking with DSS, a membrane permeable cross linker (Pierce, USA) [180], [181]. The cross linked products were resolved on SDS-PAGE, western blotted and probed with Mge1 antibody to look at the Mge1 dimer and other interacting protein complexes in the presence and absence of Antimycin A (**Fig.2.7B**). In the absence of AntimycinA but in the presence of cross linker, three high molecular weight complexes and one ~130 kDa complex containing Mge1 were present in both wild type and Mge1-M155L mutant (**Fig.2.7 B&C**). The 60 kDa complex is likely to be Mge1 dimer and the high molecular weight complexes are likely to contain mHsp70 and Mge1[153] or Mge1 interacting complexes. However, the formations of high molecular weight complexes are considerably reduced with Antimycin A treatment in wild type but not in Mge1-M155L mutant mitochondria (**Fig.2.7C**). Correspondingly, there is an increase in Mge1 monomer and dimer formation in wild type but not in mutant mitochondria (**Fig.2.7C**).

To determine whether Mge1 containing high molecular weight complexes indeed contain mHsp70, wild type and mutant mitochondria samples were treated with Antimycin A (10 and 20 µM) and cross-linked with DSS. Later, mitochondrial samples were solubilized, immunoprecipitated with antibodies specific for Mge1 (**Fig.2.7D**) and probed with mHsp70 antibodies. We were able to detect mHsp70 (**Fig.2.7E**) in Mge1 mediated immunoprecipitated samples of wild type mitochondria in the absence of cross linker. In the

presence of cross linker, mHsp70 was observed in a high molecular weight complexes (**Fig.2.7D&E**) The amount of Mge1-mHsp70 complexes immunoprecipitated with Mge1 antibodies is consistently reduced by 50-60% in the presence of 20 µM of Antimycin A in wild type mitochondria despite equal amount of IgG in all fractions (**Fig.2.7D&E**).There is no substantial decrease in Mge1-mHsp70 complexes in Mge1-M155L mutant mitochondria samples compared to wild type (**Fig.2.7E**). Our observations are consistent with our *in vitro* findings that Mge1 interaction with mHsp70 diminishes with oxidative stress and that M155L within Mge1 is important for imparting this sensitivity.

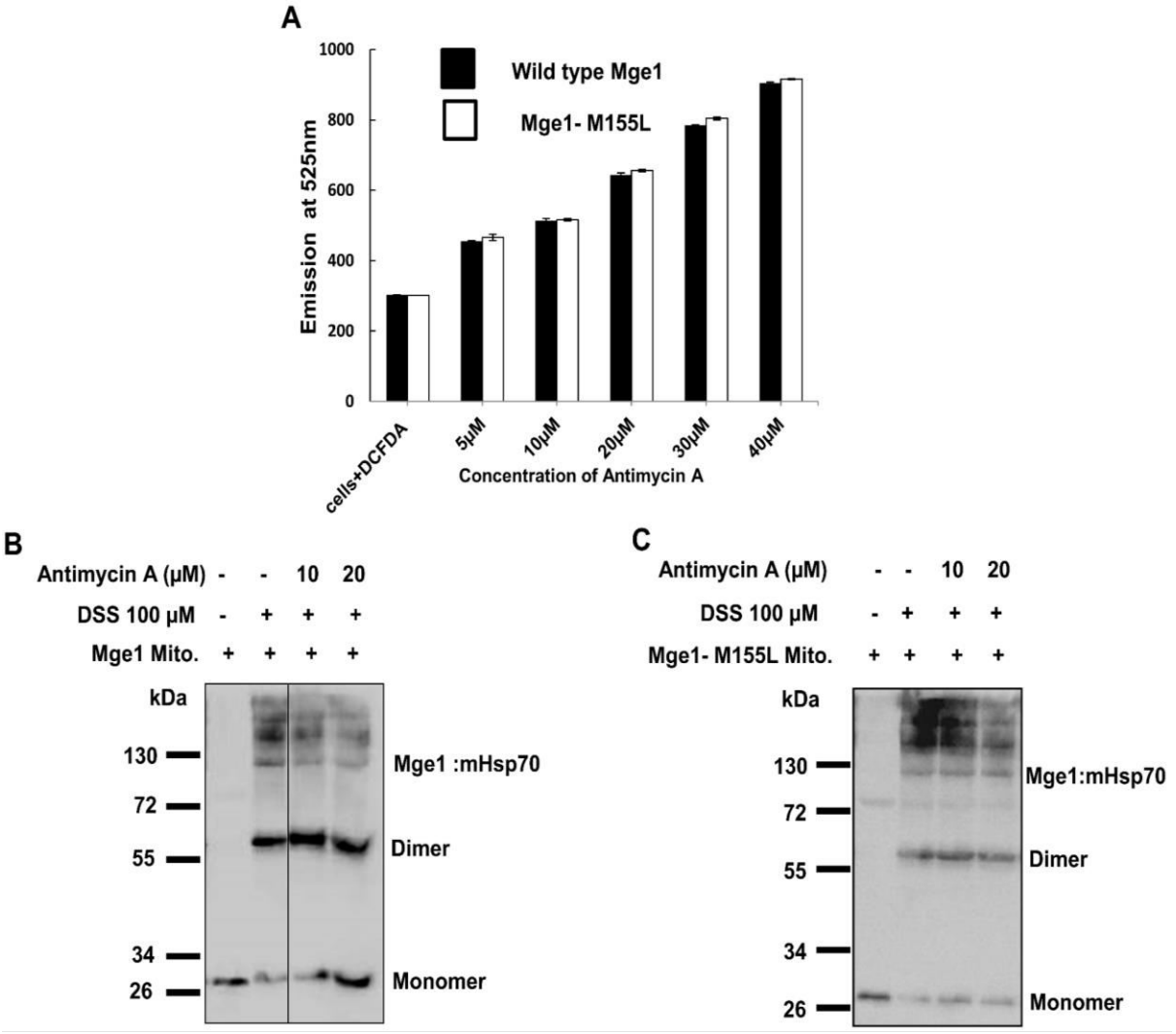

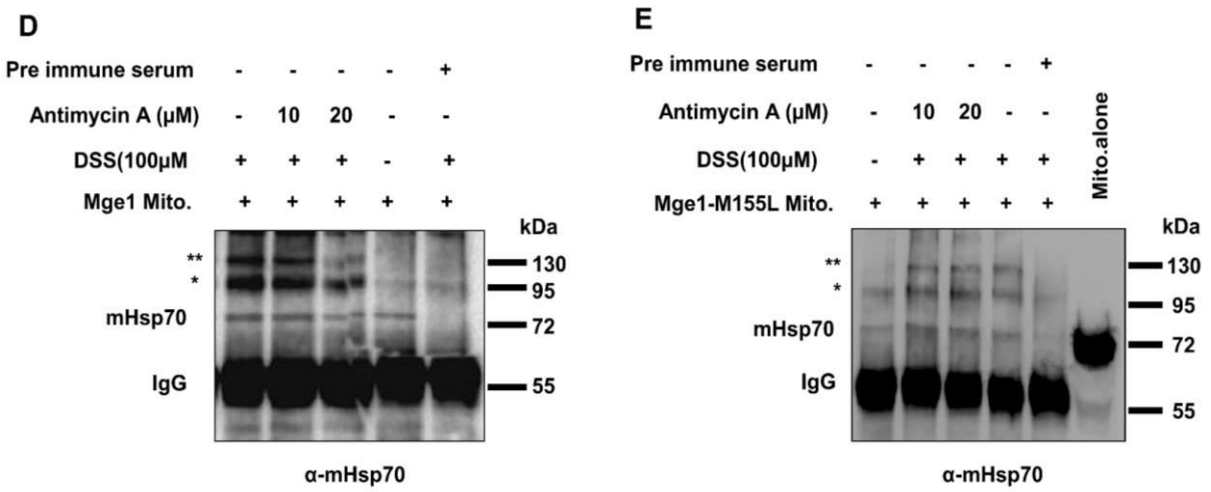

Figure 2.7 Effect of oxidative stress on the oligomeric state and interaction of Mge1 with mHsp70 in mitochondria: (A) ROS measurement was carried out as described in *Materials and Methods*; the fluorescence signal derived from wild type and Mge1-M55L mutant in the absence or presence of increasing concentrations of antimycin A is shown. **(B&C)** Mitochondria were isolated from wild-type (B) or Mge1-M155L mutant (C),Mitochondria were treated without or with antimycin A and subjected to cross-linking with membrane-permeable cross-linker DSS. Samples were incubated at room temperature for 30 min, and the reaction was quenched by addition of Tris-HCl (pH 7.5) buffer. Samples were separated on SDS–PAGE, Western transferred, and probed with antibodies specific for Mge1. **(D&E)** Wild-type Mge1 (D) and Mge1-M155L mutant (E) mitochondria were treated with or without antimycin A and subjected to cross-linking with the membrane-permeable cross-linker DSS. Samples were incubated at room temperature for 30 min, and the reaction was quenched by addition of Tris-HCl (pH 7.5) buffer. The samples were subjected to immunoprecipitation with Mge1 antibodies and immunodecorated with mHsp70 antibodies. Preimmune serum was used as a control (D&E). We loaded 20 μg of mitochondria (E) to identify the mobility of mHsp70.

2.3.7 Mge1-M155L mutant rescues protein import defect during oxidative stress

Based on our observations so far, we hypothesized that the dissociation of Mge1 from Hsp70 in presence of oxidative stress should impact protein import. We utilized the well established *in vitro* import assay to determine the effect of antimycin on protein import. We used ^{35}S methionine labeled matrix targeting cytochrome oxidase subunit IV (CoxIV), Su9-DHFR and

an inner membrane targeting ATP/ADP carrier (AAC) for import assays. The import of CoxIV and Su9-DHFR is monitored by processing of N terminal mitochondrial presequence by mitochondrial processing peptidase and the protection of mature form from an externally added protease. Import of AAC is monitored by its resistance to protease. We performed kinetics of import of CoxIV, Su9-DHFR and AAC in mitochondrial fractions isolated from wild type and M155L mutant. As shown (**Fig.2.8A**), CoxIV and Su9-DHFR are effectively processed and the mature form is protected from the externally added protease in wild type and M155L mutant mitochondria (**Fig.2.8A**). However, imported CoxIV and Su9-DHFR are poorly protected from protease treatment at early time points in wild type mitochondria that were pre-treated with antimycin. However, CoxIV and Su9-DHFR are protected at early time points in antimycin treated M155L mutant sample and is comparable to that observed in untreated samples at all time points (**Fig.2.8A**). Interestingly, the processing of CoxIV and Su9-DHFR does not decrease with antimycin treatment both in wild type and M155L mutant. We did not observe any decrease in the import of inner membrane protein AAC either in wild type or M155L mutant in the absence or presence of antimycin at all kinetic time points (**Fig.2.8A**). The effect observed with antimycin is not due to alteration in the membrane potential as we see normal processing of precursor proteins. Further, the processing of precursor protein requires membrane potential as the addition of valinomycin inhibits the processing of preprotein and protection from protease treatment in wild type and mutant mitochondria (**Fig.2.8A**). We conclude that ROS decreases the mHsp70 import cycle and M155L mutation suppresses the defect caused by the alteration of the Hsp70-Mge1 interaction.

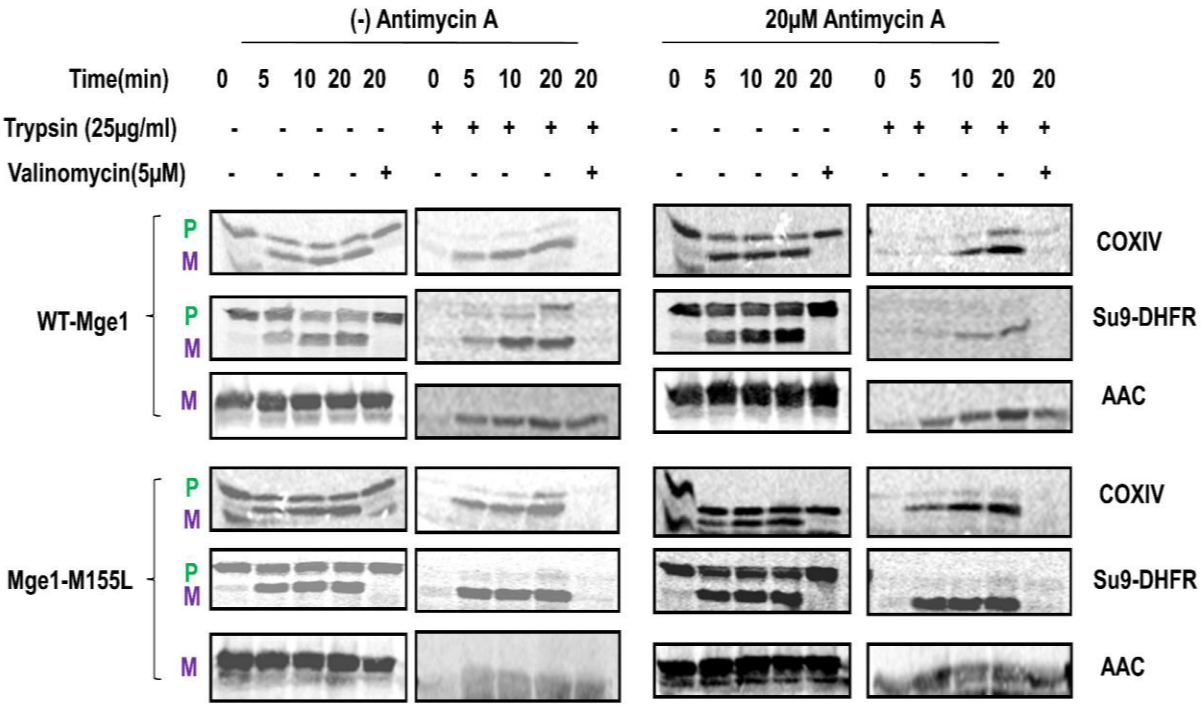

Figure 2.8 Effect of oxidative stress on protein import: (A) Mitochondria isolated from wild type or mutants were either pretreated with 20 μM antimycin A for 20 min or left on ice before import. Mitochondria were treated with valinomycin (5 μM) for 10 min on ice. Reticulocyte lysate–synthesized, ^{35}S-labeled mitochondrial precursor proteins (CoxIV,Su9-DHFR and AAC) were imported with or without antimycin A into pretreated wild-type Mge1 and Mge1-M155L mutant mitochondria for different time points. The samples were incubated with (right) and without (left) 25 μg/ml trypsin and analyzed by SDS–PAGE, followed by digital autoradiography as mentioned in *Materials and Methods*. This is a representative figure of two independent experiments. (**M-**mature; the mature form of an imported protein; **P** -pre; the precursor form of a mitochondrial-destined protein)

2.3.8 Mge1-M155L mutant rescues ATPase activity of Hsp70 during oxidative stress

To further analyze the role of oxidative stress on interaction of Mge1 with mHsp70 function, we utilized the steady state ATPase activity of Hsp70 in the presence of Mge1. Mge1 assists in release of ADP for ATP on Hsp70 and thereby accelerates the ATP hydrolysis. The ATPase activity of mHsp70 was measured *in vitro* as described in the Methods. Recombinant mHsp70 alone shows low level of ATPase activity (**Fig.2.9A**). Addition of wild

type or Mge1-M155L mutant stimulates the ATPase activity of mHsp70 by three fold. However, treatment of wild type Mge1 mutant with H_20_2 prior to incubation with mHsp70 reduces the ATPase activity of mHsp70 significantly when compared to Mge1-M155L mutant. Our results suggest that oxidative stress decreases the interaction of Mge1 with mHsp70 and thereby modulates its function.

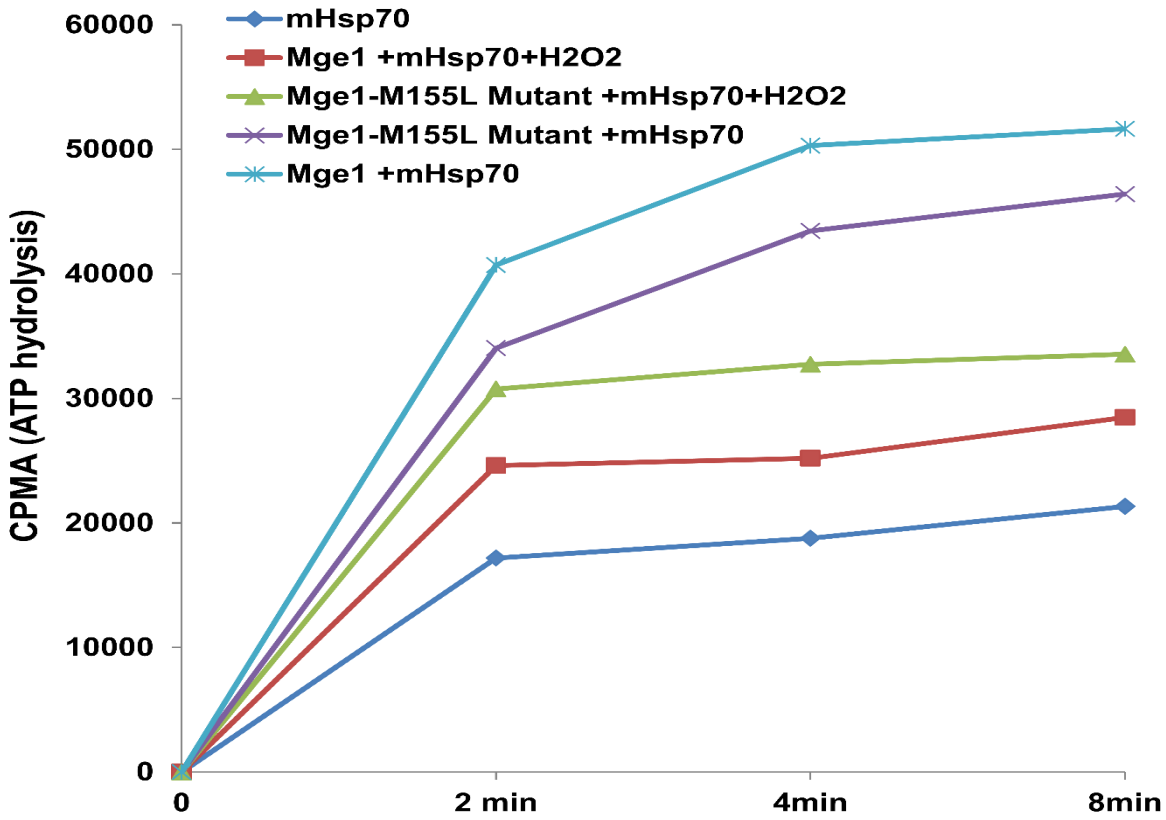

Figure 2.9 Effect of oxidative stress on ATPase activity of mHsp70: (A) Purified Mge1 and Mge1-M155L mutant were treated with or without 1mM H_2O_2 for 20 min in 20 mM HEPES/KOH, pH 7.2, buffer. Then the proteins were incubated with recombinant Hsp70 in ATPase assay buffer, and we analyzed the release of labeled Pi at different time points as indicated in *Materials and Methods*.

2.4 Discussion

We have shown for the first time that Mge1, a co-chaperone of mHsp70, can act as an oxidative sensor both *in vitro* and *in vivo*. Mge1 acts as a switch for sensing oxidative stress

within the cell by changing its conformation from an active dimer to an inactive monomer. This conformational change in Mge1 is translated into a reduced interaction of Mge1 with mHsp70 thereby affecting the function of mHsp70 that is required for the vectorial transport of proteins across the mitochondrial cell membranes. Based on our results we speculate that during oxidative stress, mHsp70. ADP remains associated with precursor protein that is being translocated across the inner membrane of mitochondria. Our studies show that there is reduced interaction of Mge1 with mHsp70 during oxidative stress and this may reflect in decreased ADP to ATP exchange on mHsp70. As a result, mitochondria may be stalling the transport of proteins into the mitochondrial matrix to prevent accumulation of unfolded proteins in the mitochondria.

Mitochondria electron transport chain is the major source of ROS generation within a cell. High level of ROS leads to alteration in the structure of proteins, lipids and DNA [157], [160]. Further, oxidative stress in the form of H_2O_2 reduces the activity of several mitochondrial proteins like Aconitase, alphaketoglutarate dehydrogenase and succinate dehydrogenase in mammalian cells [161]. In addition, accumulation of oxidized proteins in the mitochondria has been correlated to ageing [182]. Several evidences suggest that the role of mitochondrial mediated oxidative stress in progression of several neurological disorders [183], [184]. However, very little is known about the mechanistic insights of mitochondria generated ROS in regulating mitochondrial metabolism and biogenesis. One of the key regulators in mitochondrial biogenesis is translocation of nuclear encoded proteins into various compartments of mitochondria. It has been shown that redox conditions influence the import of pre-proteins in higher eukaryotes. Pre-treatment of mammalian mitochondria with paraquat, an oxidizing agent causes the production of ROS at the level of complex I [185] and causes reduction in the import of pre-ornithine transcarbamylase (pOTC) in intact cells as well as *in vitro.* Oxidative stress also leads to a decrease in the processing of pre-protein

superoxide dismutase in Sf9 cells [186], [187]. The mechanism behind the reduced protein import into mitochondria in mammalian cells and in Sf9 cells is not known.

Yeast Mge1 is a homolog of *E. coli* GrpE [165]. Similar to the nucleotide exchange activity of Mge1, the N-terminal helical region of GrpE is also involved in the exchange of nucleotides on DnaK.The unfolding of the N-terminal region of GrpE retards the release of ADP from DnaK [188], [189]. Heat stress is known to decrease the interaction of Mge1 with mHsp70 in eukaryotes [189]. This reduced interaction causes a decrease in mHsp70 activity as the exchange of ATP for ADP is inhibited.

The present study was stemmed from the observation that Mge1 acts as thermo sensor during heat stress and undergoes conformational changes that results in reduced ATPase cycle of mHsp70. Based on the observation that pro-oxidant conditions also reduce the import of pre proteins, we evaluated whether Mge1 has any relevance in protein import during oxidative stress. It is probable that alteration in Mge1 structure may be one of the reasons for alteration in the import of pre-proteins during oxidative conditions. Using, yeast as a model system we show that generation of ROS in mitochondria by the addition of Antimycin A destabilizes the Mge1-mHsp70 complex formation (**Fig.2.7**). Mge1 is also required for Ssq, a second mHsp70 localized in mitochondria that is required for import and assembly of Fe-S proteins [190]. Intriguingly, delta ssq cells are sensitive to growth on H_2O_2 plates. Although over-expression of Ssc (mHsp70) in delta ssq cells suppresses some of the defects caused by ssq deletion, it does not rescue the slow growth on H_2O_2 plates [191]. This effect may be due to alteration in the structure of Mge1 and reduced interactions with mHsp70 and Ssq under these conditions. Further, we observed 3-4 high molecular weight complexes when we performed in organelle cross linking and probed with (**Fig.2.7 D&E**) Mge1 but we could not pull down these complexes may be due to epitope specificity (**Fig.2.7D&E**). These additional

complexes that we observed in organelle cross linking likely to be Ssq-Mge1 containing complexes or other Mge1 containing complexes.

Amino acids methionine, cysteine, tryptophan, histidine and tyrosine are prone to modifications during oxidative stress [176]. In the presence of oxidative stress these amino acids modifies as large polar sulfoxide groups that increases the affinity for hydrogen bonding leading to destabilization of the proteins. It is assumed that methionine serves as a ROS scavenger in the cell to protect the cellular structure and integrity [192] . Interestingly, yeast Mge1 protein is devoid of any cysteine amino acids and contains only one methionine. Mutating the lone methionine to leucine does show effect on Mge1 regulation during oxidative stress both *in vitro* and *in vivo* (**Fig.2.4**).

In summary, we have provided clear evidence that Mge1 responds to oxidative stress and its activity depends on the metabolic and redox environment of the matrix. Our results also suggest that Mge1 plays a key role in regulating mitochondrial Hsp70 chaperone system and thereby mitochondrial metabolism during oxidative stress. This mechanism of Mge1 action during oxidative stress appears to be conserved across evolution from yeast to humans. It is likely that there are other stresses besides heat and oxidative stress that might elicit the same response from Mge1.

Chapter 3

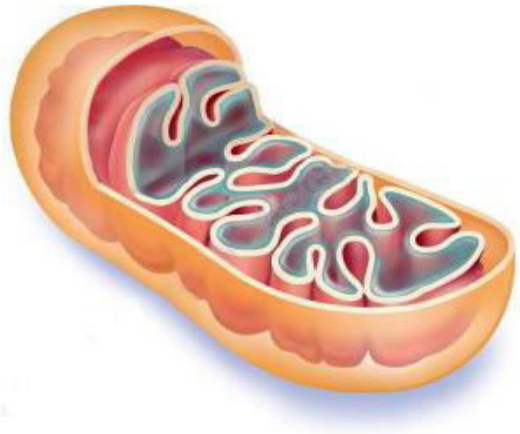

Influence of Thermal stress on the structure & functional properties of Mge1, a mitochondrial component of protein import motor

3.1 Introduction

Hsp70 class of proteins are evolutionally conserved ATP dependent molecular chaparones. These proteins are involved in protein folding, prevention of protein aggregation, stress response and remodelling of protein complexes. These chaparones are also associated with protein translocation machineries in different cellular compartments like ER, chloroplasts and mitochondria [193], [194]. In yeast mitochondria, three kinds of Hsp70 family of chaparones (Ssc1, Ssq and Ecm10) are involved in regulation of mitochondria proteostasis (healthy proteome) and protein translocation.Out of these three Hsp70s, Ssc-1 is the major molecular chaparone complex, comprises *SSc-1*, Mge1 and Mdj1 proteins, involved in protection of partially folded proteins, translocation of proteins and survival under stress conditions [195], [196]. The other mitochondrial Hsp70 homologues like Ssq chaperone system is involved in the biogenesis of Fe-S cluster containing proteins.whereas the least characterized Ecm10 chaparone system seems to be involved in protein translocation.

Hsp70s comprises a nucleotide binding N-terminal domain and substrate binding C-terminal domain. These domains are connected through a disordered loop [197]. The binding and hydrolysis of ATP results in conformation change in Hsp70 that modulates its affinity for substrate. In ATP bound state, the affinity of Hsp70 towards substrate is low with fast on/off kinetics due to formation of tense state (T state) whereas in ADP bound state, the affinity of Hsp70 towards substrate is high with slow on/off kinetics due to formation of relaxed state (R state) [151]. Hsp70 has low intrinscic ATPase activity and slow ADP dissociation kinetics and hence it depends on cochaparones for stimulation of ATPase activity and recycling of ATP for ADP.

Chaparones play an important role in many pathological diseases that are associated with aggregated proteins such as Alzheimer's, Parkinson's and Huntington's. Molecular

chaparones prevent the thermal denaturation of proteins. During thermal stress, chaperones recognize the exposed hydrophobic peptide segments of proteins and thereby prevent irreversible formation of protein aggregates. Although, individual components involved in Hsp70 chaperone cycle has been well studied but communication in between these components is still to be explored in detail. In general, thermal stress, *i.e*. a transient increase in temperature induces the expression of chaperones and co-chaperones [198] . In addition to over expression, temperature dependent structural modulation or alteration in chaperones have been observed [151]. GrpE an evolutionally conserved nucletodie exchange factor of DnaK (Hsp70) has been identified as a thermal sensor [152]. In response to thermal stress the active dimeric GrpE becomes monomer and fails to interact with Dnak. GrpE represents a functionally conserved NEF family with representative candidates in archea, eubacteria and eukaryotic related organelles such as chloroplasts and mitochondria. Mge1, a yeast mitochondrial homolog of *E.coli* GrpE has also been shown to undergo a reversible structural alteration during thermal stress [153]. The long N-terminal helix appears to be important for thermal sensor property as mutation of arginine at position 40 to cysteine in GrpE causes stabilization of dimer due to formation of cysteine-cysteine disulfide bond in between monomers[151]. The stabilized pair of long N-terminal helices abolishes the thermal transition in GrpE and stabilizes the interaction with DnaK. This stable interaction at non-permissive temperature increases the aggregation of proteins due to reduced recycling of DnaK [199]. It was hypothesised that temperature dependent unwinding of long pair helices followed by destabilization of beta sheet domain in E.coli GrpE. A recent report (12) has also shown that orientation of a long pair helix of *GK* GrpE affects the both ATP/ADP exchange rate and affinity towards Hsp70.

E.coli and *Thermus thermophiles*(Th) GrpE share 25.9% sequence homology whereas yeast Mge1 and E.coli GrpE share about 32.6% sequence homology. Despite the low level of

sequence identity, CD spectra of both Mge1 and Th GrpE suggest that they have similar secondary structure. Further, GrpE is the only member in GrpE/Dnaj/DnaK chaperones complex that undergo thermal transition and affect the ratio between low affinity ATP bound and high affinity ADP bound state of DnaK. Although all GrpE homologues have similar function and secondary structure, they are different in their structural stability and structural transition during thermal stress. The temperature dependent structural transition in E.coli and yeast Mge1 is attributed to the unfolding of long N-terminal helices followed by destabilization of beta sheet. However, in Thermophiles, melting of the beta sheet domain at transition temperature induces the unwinding of N-terminal helices during thermal stress. Further, crystal structures of E.coli and thermophilus reveals that the N-terminal 33 aminoacids are disordered in case of Ecoli GrpE whereas coiled-coil domain is observed as in case of Thermus GrpE[152], [200].

In our previous chapter, we have shown that yeast Mge1 acts as an oxidative sensor and Mge1-M155L mutant resistant to oxidative stress [201]. In this chapter, while characterising several Mge1 mutants that we are generated, the mutant His167 to Leucine, which is located at junction between N-terminal helical bundle and beta sheet structures shows the thermal stability. His167 is located in the short turn region connecting the terminal helix and the first strand of the beta sheet region. Incidentally His167 is followed by Gly168, a residue that imparts conformational flexibility. The beta sheet region has been shown to interact with DnaK. Thus Histidine to leucine mutation introduces a conformational flexibility to the Mge1 at this region.

Thermal denaturation and refolding studies suggest that Mge1-H167L is indeed more stable when compared to wild type. Mge1-H167L mutant acquires thermal stability and thermal tolerance under non-permissive conditions. Molecular dynamics simulation studies with 3D modelled structure of Mge1-H167L mutant show that formation of coiled-coil N-terminal

alpha helices which resemble like Thermus thermophiles GrpE. Interestingly, Thermus thermophiles GrpE have leucine residue at the corresponding site. The hydrophobic residue leucine at 167th position instead of Histidine in Mge1 provides more flexibility in the local region. This is due to loss of hydrogen bond with surrounding amino acids in particular Thr 163. This study suggests that flexible Mge1-H167L mutant may have rapid ATP/ADP exchange kinetics on Hsp70 and facilitate the folding of proteins mediated by Hsp70 chaperone system thereby protects the cell under thermal stress.

3.2 Materials and methods

3.2.1 Structure Modeling of Mge1

The template structure for building the 3D model of Mge1 was obtained using BLAST searches [202] against Protein Data Bank [203]. The homodimer model was built using MODELLER [204] that builds the protein structures by the satisfaction of spatial restraints. This method is incorporated in the Discovery studio (D.S.) 2.5 suite of software. The reliability of stereochemical geometry of the protein was tested using PROCHECK [205]. The template and model structures were superimposed using MAPSCI [206] to estimate the extent of similarity that is estimated by the root mean square deviation (RMSD) of Cα atoms of both proteins.

In both A and B chains of Mge1, single amino acid mutation His167Leu was incorporated using "protein modeling" protocol, "build mutation" module in D.S. 2.5 and the structures were optimized. The MD simulations of both native and His167Leu mutant proteins were performed using the GROMACS 4.5.5 package with the GROMOS96 43a1 force fields [207]. The complexes were subjected to MD simulations for 50 nano seconds (ns) at isothermal-isobaric conditions in a periodic triclinic box (15.56nm x 9.362nm x 8.0nm) using explicit solvent- SPC/E model water molecules with an edge length of approximately 9 Å.

Both native and mutant Mge1 proteins have -2 charges which were neutralized by adding of 2 Na^+ ions.The local minimum of the system was found using the steepest-descent algorithm for 5000 steps and 1000 pico seconds (ps) position restrained dynamics to distribute water molecules throughout the system. Finally we performed MD simulations of the whole system for 50 ns, using 0.002 ps time step. The Particle Mesh Ewald (PME) summation method [208], [209] was employed for the calculation of the electrostatics, with a real space cut-off of 10 Å, PME order of 6 and a relative tolerance between long- and short- range energies of 10^{-6}. Short range interactions were evaluated using a neighbor list of 10 Å updated every 10 steps, and the Lennard-Jones (LJ) interactions and the real space electrostatic interactions were truncated at 9 Å. The V-rescale thermostat [210] was used to maintain the temperature; the Parrinello-Rahman algorithm was employed to maintain the pressure at 1 atm and LINCS algorithm [211] was applied to fix all bonds.

The trajectory file obtained from MD simulations was analyzed. The RMSD of certain atoms in a molecule with respect to a reference structure can be calculated with the program g_rms of GROMACS by least-square fitting the structure to the reference structure. Further we also analyzed the RMSF of protein Cα atoms using r_rmsf to understand the dynamic flexibility in various regions of the structure. Similarly PE and KE of the structures were also analyzed using g_energy.

3.2.2 In vitro cross linking of recombinant proteins

Cross linking of purified recombinant yeast wild type and Mge1-M167L mutant (H167L) was performed with bis (sulfosuccinimidyl) suberate (BS^3; Pierce) at room temperature in 20 mM sodium phosphate (pH 7.4), 150 mM NaCl, 20mM HEPES and 50 mM Borate. 2.5 µg of purified proteins were pre-incubated at different temperatures (25°C, 37°C, 42°C) for 20 min and BS^3 was added to a final concentration of 0.1 mM. The reaction was left for 30 min at the

indicated temperature and quenched by the addition of 40 mM Tris–HCl (pH 7.5). Samples were analyzed by SDS-PAGE.

3.2.3 Yeast media

Standard yeast protocols were used for culturing yeast strains. Wild type yeast strains were grown in YPD that contained 1% yeast extract, 2% peptone and 2% dextrose. Synthetic Dextrose (SD) minimal medium contained 0.73% Yeast Nitrogen Base with amino acids, 0.4% ammonium sulphate and 2% glucose. For mitochondria isolation semi synthetic lactose medium contained 2% lactose with yeast extract, ammonium chloride, calcium chloride, magnesium chloride, potassium phosphate and glucose was used as described.Yeast cells were grown at 30^{o}C. Yeast transformations were performed by following standard lithium acetate method [171].

3.2.4 CD Spectroscopy analysis

Circular dichroism (CD) spectra at far-ultraviolet region (190-250nm) were recorded using circular dichroic spectrometer (Jasco J-810 japan) at different temperatures i.e. from 25^{0}C to 70^{0}C with 2 mm path length quartz cell, response time 50 nm/s speed. Three scans of each spectrum were averaged and baselines of buffer alone were subtracted. The protein concentrations of both WT and mutant were 100 µg/ ml (5µm). Denaturation curves were obtained by collecting data at ellipticity at 222 nm at scan rate 60 deg/hour. The data were analysed by plotting temperature against ellipticity at 222 nm and Tm calculated by fitting data into two state equation .

3.2.5 In-organelle cross linking and immunoprecipitation

Mitochondria were isolated from yeast as describe [212]. Mitochondria isolated from WT and Mge1-H167L were pre-incubated at different temperature (25°C and 42°C) for 15min in 20

mM Hepes buffer pH7.4 followed by addition of a membrane permeable cross-linker, disuccinimidyl suberate (DSS, Pierce) at 100 µM final concentration.The reaction was further incubated for 30 min at room temperature and quenched by addition of 40 mM Tris–HCl (pH 7.5). Samples were either analyzed directly by SDS-PAGE or subjected to immunoprecipitation.

Mitochondria samples were solubilized in lysis buffer (50 mM Tris-HCl pH 8.0, 150 mM NaCl, 1% NP-40,0.5% Deoxycholate, 0.1% SDS and protease inhibitors) and incubated on ice for 30 min. Lysates were centrifuged for 15 min at 13,000 rpm at 4ºC. The clear supernatant fractions were incubated with protein A beads for 1hr at 4ºC to remove non-specific interactions. Pre-cleared lysates were incubated with Mge1 antibody for 4 hr at 4ºC on a rotator. Protein A beads were added to the lysates and further incubated for another 4hr at 4ºC. The beads were washed four times with mitochondrial lysis buffer. Samples were resolved on SDS–PAGE, western transferred and probed with antibodies specific to mHsp70.

3.2.6 Protein aggregation assay

For each protein aggregation assay, 100 µg of mitochondria was suspended in aggregation assay buffer (250 mM Sucrose, 10 mM MOPS, 80 mM KCl, 5 mM MgCl2, 3 mM ATP and 4 mM NADH) and incubated at different temperature (25°C,37°C, 42°C) for 20 mins [213]. Then mitochondria samples were centrifuged at 10000 rpm for 10 mins and the pellet was solubilized in lysis buffer (0.5% Trition X 100, 200 mM KCl, 30 mM Tris-HCl pH 7.5, 5 mM EDTA) with protease inhibitor cocktail (PIC). The solubilized mitochondria were centrifuged at 25000 rpm for 30 min. The supernatant fraction (soluble fraction) was collected and the pellet (aggregated fraction) was re-suspended in lysis buffer. 10% Total, 20 % of supernatant fraction and total pellet fraction were separated on SDS-PAGE .

3.3 Results

Mge1, a nucleotide exchange factor for mtHsp70 highly is conserved in its secondary structure from extremophiles like Thermus thermophiles to mesophiles like Homo sapiens. Sequence alignment shows that yeast Mge1 shares 34% identity with E.coli GrpE. Previous functional studies and crystallography studies suggest that beta sheet of protein helps in nucleotide exchange activity. This domain unfolds after unfolding of N-terminal domain at first transition temperature of GrpE thereby it affects the nucleotide exchange activity during thermal unfolding.

3.3.1 Mge1 H167L mutant is resistant to thermal stress

We expressed and purified the recombinant wild type and Mge1-H167L mutant proteins from bacterial cells as described in the methods. The purified proteins are shown in **Fig.3.1A**. A gradual increase in temparature causes the unfolding of a protein due to conformational change in its structure. Thermal induced unfolding gives valuable information about the stability of the protein. To assess the thermal induced unfolding, we recorded a series of CD spectra of wild type and Mge1-H167L mutant in a wider temperature range **Fig.3.1B&C** shows the comparison of wild type and Mge1-H167L mutant CD spectra collected from 20^{o}C to 70^{o}C. The mean residual eliplicity at 222 nm was calculated for wild type and mutant as a function of increasing temperature and plotted **Fig.3.1 B & C**. It is evident from the spectrum that the isodichroic point is at 203 nm and is not altered with increasing temperature, indicating the presence of single state cooperative transition from the folded dimeric state to the unfolded monomer. The spectrum obtained at lower temperature (20 to 30^{O}C) mainly represents the folded structure as most of the secondary structure is retained in both wild type and Mge1-H167L mutant . Increase in the temperature from 35-70^{o}C causes the substantial loss in secondary structure of wild type when compared to Mge1-H167L mutant. Mean

residual eliplicity curves indicate that wild type Mge1 has a clear cooperative thermal transition with midpoint at 42°C. In contrast to WT, Mge1 H167L mutant shows increased stability with midpoint shifted to 46°C **Fig.3.1.D**. CD studies shows that Mge1 H167L mutant is stable when compared to wild type.

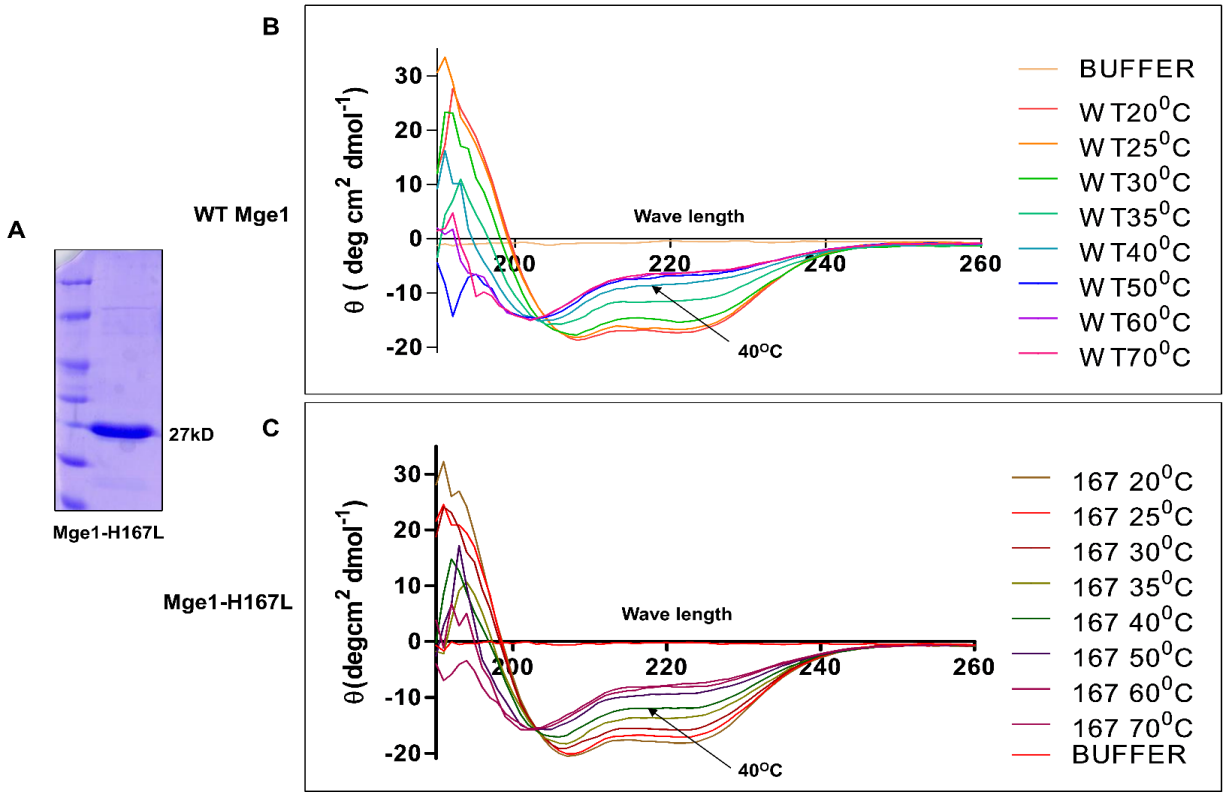

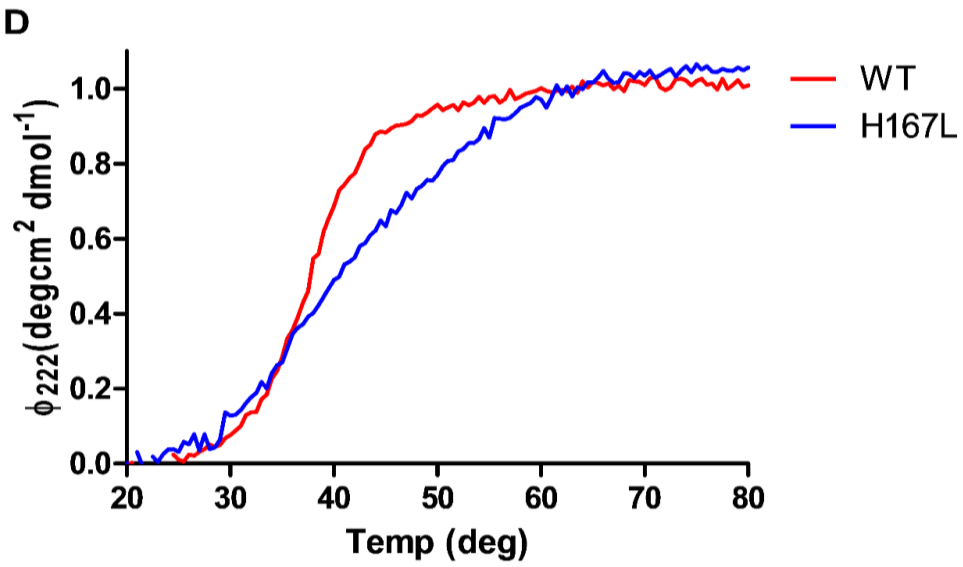

Figure 3.1 Thermal unfolding of Mge1: **(A)**The purified recombinant Mge1 Mutant (Mge1-H167L) by using Ni-NTA column and analysed by 12% SDS PAGE. **(B)&(C)** Circular dichroism spectra of 20 μM WTMge1 and Mge1-H167L in phosphate buffer, pH 7.2,were recorded at the indicated temperatures when the signal at 222 nm. The spectra at 20-30°C are identical to the spectrum of wild-type Mge1,but at 40^{O}C changes in circular dichroism were monitored at 222 nm. **(D)** Differential scanning calorimetry of WT Mge1 and Mge1-H167L were scanned from 20 to 80°C.

Like Ecoli GrpE [169], Mge1 exists as a dimer in solution. To investigate the oligomeric state of thermal stress on Mge1, we incubated purified recombinant protein at 25, 37 ,42 degress for one hour followed by cross linking with BS^3 cross linker. The samples were resolved on SDS-PAGE and commassie stained gels were analyzed . In the absence of a cross linking reagent, Mge1 migrates as molecular mass of 27 kDa monomer. However, in the presence of soluble cross linker BS^3, Mge1 migrates as a ~60 kDa homodimer. However, the appearance of monomer is increased when the cross linking of Mge1 was performed at 37^{o}C. The dimeric Mge1 is completely dissociated into monomer when the cross linking was performed at 42^{o}C **Fig.3.2A**. These results suggest that thermal stress causes the disordering of secondary structure followed by dissociation of dimeric Mge1. We investigated Mge1-H167L mutant response towards thermal induced dimer dissociation. We incubated Mge1-H167L mutant at different temperatures prior to cross linking with BS^3 cross linker and separated on SDS-PAGE and commassie stained . Mge1-H167L mutant also forms ~60 kDa homo dimer upon cross linking. However, Mge1 mutant is partially resistance to thermal induced dissociation of dimer into monomer either at 37 or 42^{o}C. These results suggest that involvement of histidine 167 residue in structural stability of Mge1 during thermal stress **Fig.3.2A** .

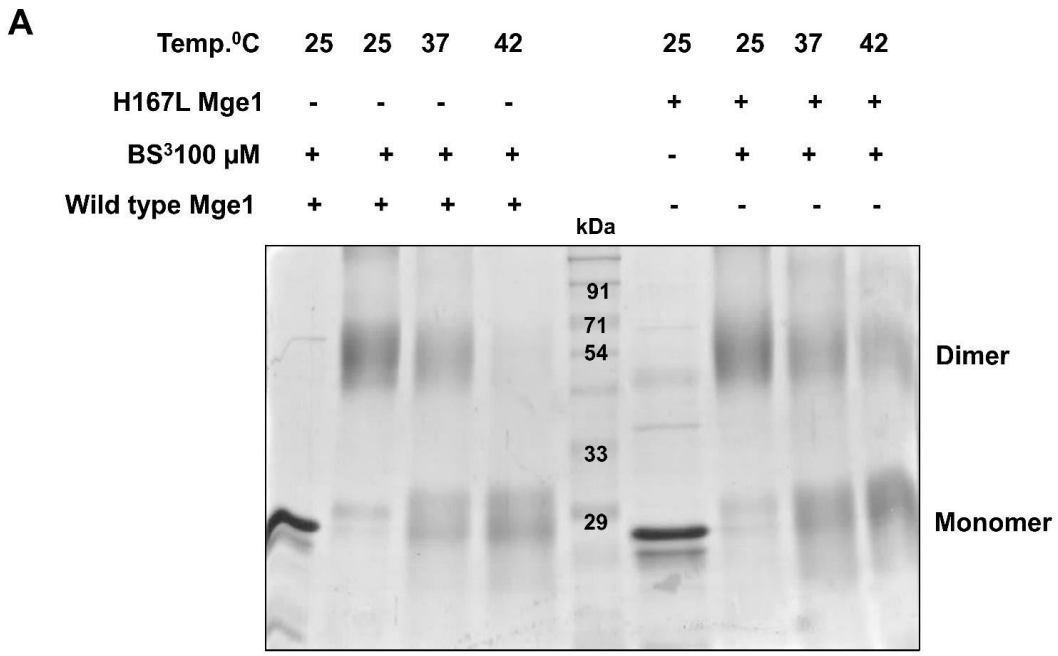

Figure 3.2 Denaturation of Mge1p involves dimer dissociation: (A) Cross linking of WT Mge1and Mge1-H167L (2.5 µg) was carried out in 20 mM sodium phosphate (pH 7.4) buffer in different temperatures (25,37,42^{O}C) for 20 min.The samples were either cross linked for 20 minutes with the addition of 100 µM BS^3 or left untreated. The cross linking reactions were left for 30min at the room temperature, quenched and adducts were resolved by 10%SDS-PAGE and stained with commassie.

3.3.2 Mge1 H167L protects cells from stress mediated protein aggregation

Most of the proteins have a finite tendency to misfold or unfold during stress conditions and form protein aggregates. Thermal stress can induce aggregation of proteins in mitochondria. So far, the evidence has implicated Mge1 with a role of an thermal sensor, a modulator of Hsp70 and a regulator of mitochondrial protein import and protein folding in the thermal stress response pathway. We wished to examine the role of Mge1-H167L mutant in prevention of aggregation of proteins during thermal stress. Mitochondria were isolated from both wild type and Mge1-H167L mutant were treated at different temperatures (25^{0}C,37^{0}C and 42^{0}C) for 20 minutes in presence of energy before centrifuging the samples. The supernatant and pellet fractions were resolved on SDS-PAGE. As shown from the **Fig.3.3A**,

mitochondria isolated from the strain expressing wt Mge1 are more prone to aggregation when compared to the mitochondria isolated from the strain expressing Mge1-H167L mutant.These results suggest that Mge1-H167L mutant is partially resistant to thermal induced aggregation of proteins.

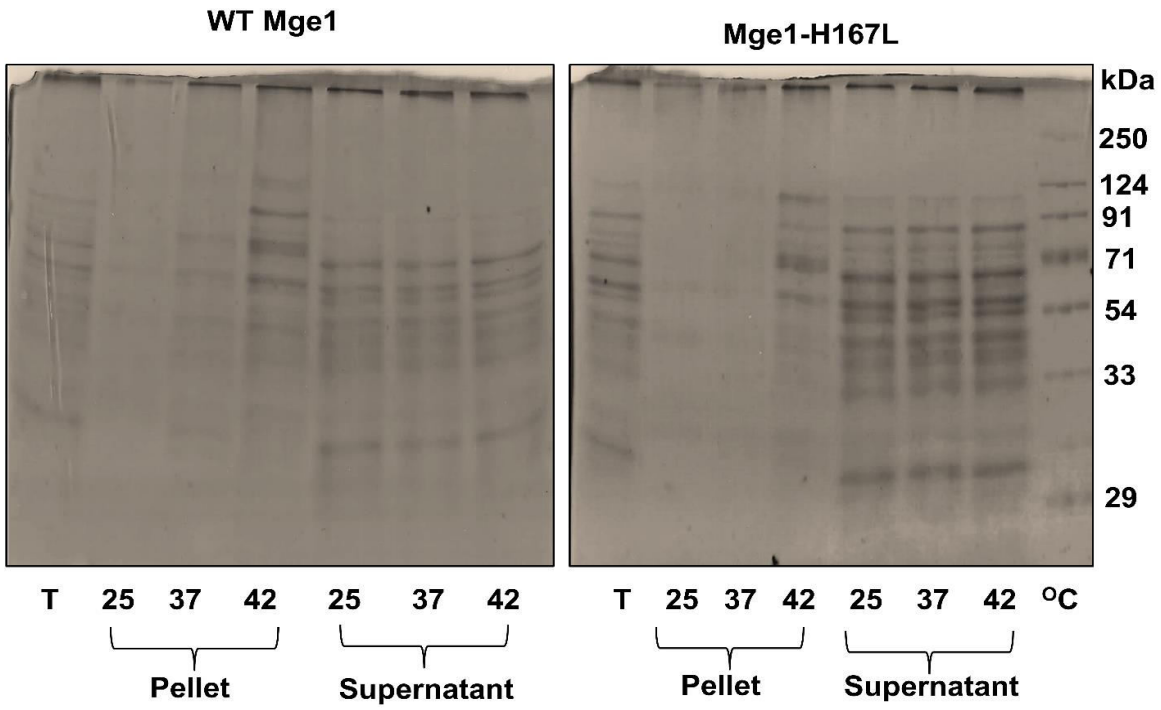

Figure 3.3 Mge1-167L strain is partially resistant to thermal induced protein aggregation: (**A**) Mitochondria isolated from either WT Mge1 or Mge1-H167L strains were incubated at different temperature as indicated in the figure and aggregated proteins were separated by centrifugation. The soluble and insoluble proteins were separated on SDS-PAGE and coomassie stained. Aggregated proteins are shown by an arrow. T, indicates the total protein fraction. 20% soluble protein fraction, 10% total protein and 100% pellet protein fraction was used for analysis on SDS-PAGE.

To understand the *in vivo* significance of Mge1 in thermal stress, we generated chromosomal MGE1 deleted haploid yeast strains harbouring and expressing MGE1 wild type or MGE1 mutant yNB70 (H167L MGE1) under high copy plasmid. We compared the phenotype of parent strain (BY4741) wild type MGE1 strain with mutant MGE1 strain on YPD plates.

Exponentially growing yeast cells expressing either wild type Mge1 or Mge1 mutant were serially diluted along with parent strain and spotted on YPD plates and incubated at different temperatures (25^0C,42^0C). We find that parent and strain over-expressing Mge1 or Mge1-H167L mutant have comparable growth on YPD plates at 25 degress. However, both parent and strain expressing wild type Mge1 show diminished growth at 42 degrees As shown **Fig.3.4A**. Most importantly, we find that Mge1-H167L mutant has considerable growth at higher temperature. These results show that Mge1-H167L mutant show significant role in the thermal stress response and histidine 167 seems to be playing a role in thermal induced denaturation.

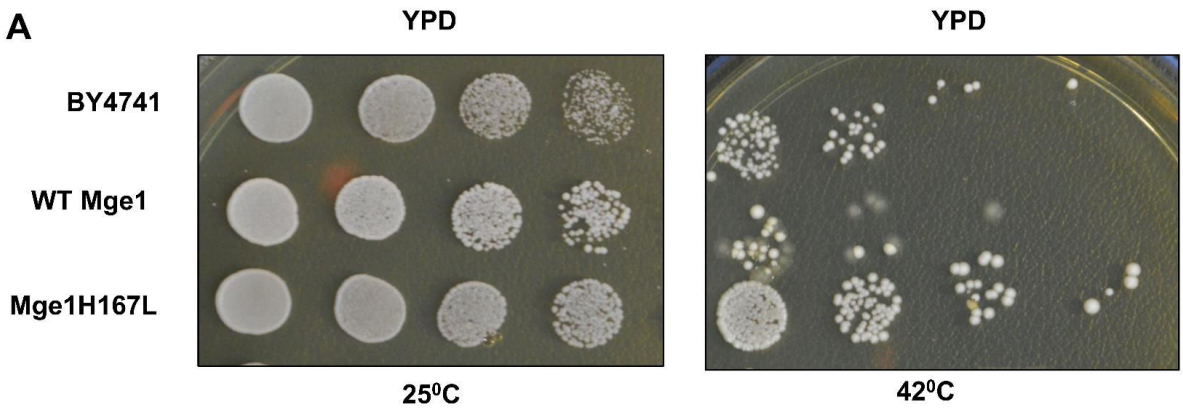

Figure 3.4 Sensitivity of wild-type and mutant Mge1-H167L strains to Thermal stress: (**A**)Yeast strains yNB67 and yNB70 carrying wild-type MGE1 and MGE1-H167L respectively, were grown overnight in YPD medium. Then one OD of cells was serially diluted by 10-fold, and 10 µl of each suspension was spotted on YPD plates pre incubated with different temperatures (25^OC and 42^OC) as indicated in the figure and incubated at 30°C for 2 days.

To investigate the *in vivo* response of Mge1 to thermal stress, mitochondria were isolated from wild type and Mge1-H167L mutant and were incubated with indicate temperatures (25^0C,42^0C) followed by cross linking with DSS, a membrane permeable cross linker (Pierce, USA). Later, mitochondrial samples were solubilized, immunoprecipitated with antibodies

specific for Mge1 and probed with mHsp70 antibodies as indicated in the methods. We were able to detect mHsp70 in Mge1 immunoprecipitated samples of wild type mitochondria in the absence of cross linker. In the presence of cross linker most of mHsp70 is detected as 130 kDa complex which probably comprises a dimeric Mge1-Hsp70 complex. However, most of this complex is dissociated at higher temperature. Similar results were found when we carried out immunoprecipitation of Mge1 H167L mutant mitochondria with Mge1 antibody and probed with Hsp70. Although, Mge1 H167L mutant is structurally stable at non-permissive temperature (**Fig.3.5 A**), it fails to immunoprecipitate more amount of Hsp70. These results suggest that a dynamic and flexible interaction in between Mge1 H167L mutant and Hsp70 may facilitate the fast ATP for ADP exchange kinetics results in efficient ATPase cycle of Hsp70 chaparone system.

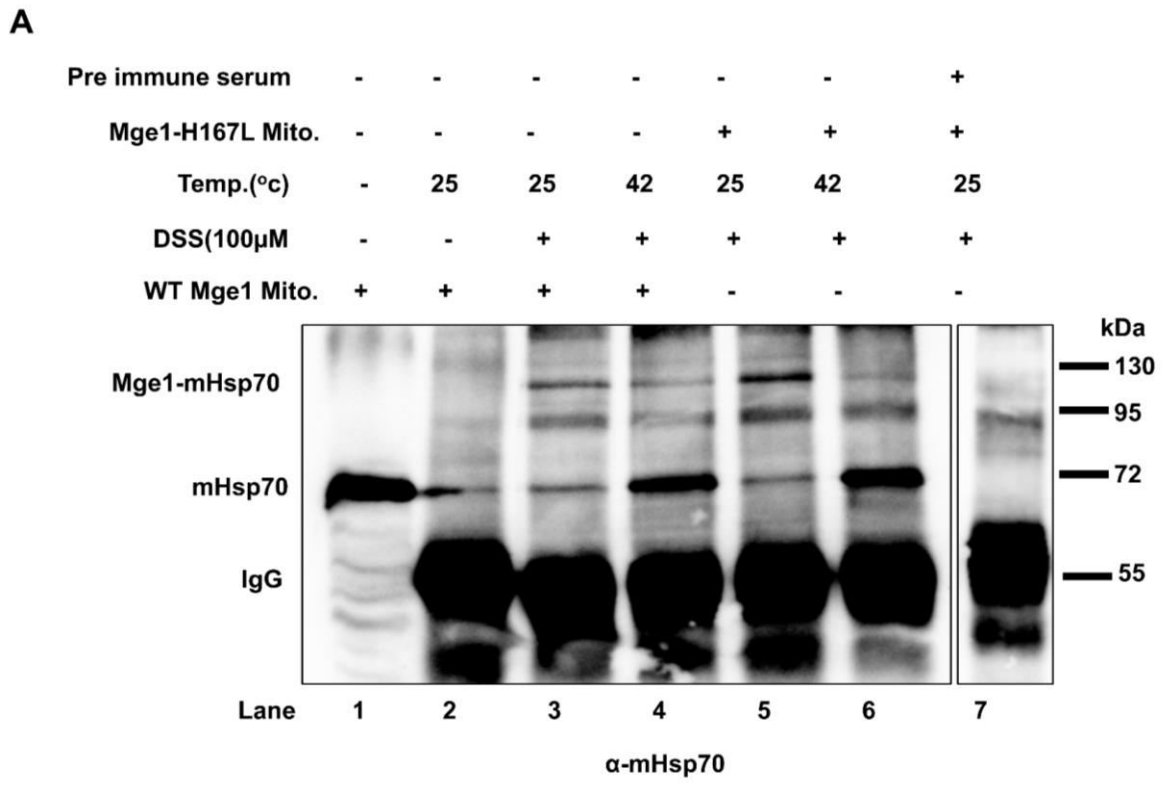

Figure 3.5 Effect of Thermal stress on the oligomeric state and interaction of Mge1 with mHsp70: (**A**)Wild-type Mge1 and Mge1-H167L mutant mitochondria were incubated at different temperatures (25^{O}C and 42^{O}C) and subjected to cross-linking (lanes3-7) with the membrane-permeable cross-linker DSS. Samples were incubated at room temperature for 30

min, and the reaction was quenched by addition of Tris-HCl (pH 7.5) buffer. The samples were subjected to immunoprecipitation with Mge1 antibodies and immunodecorated with mHsp70 antibodies. Preimmune serum was used as a control (lane7). 20 µg of mitochondrial extract was loaded (lane 1) to identify the mobility of mHsp70**.**

3.3.4 Molecular simulation studies

To understand the molecular basis for enhanced thermal stability of mutated Mge1, we employed computational methods, modeled the 3D structure of Mge1, mutated a single amino acid residue (His167Leu) in both chains of the homodimer and carried out molecular dynamics (MD) simulations of the native and mutant proteins.

The Mge1 from Yeast has been modelled based on the crystal structure of E.coli and a full-length *Geobacillus kaustophilus HTA426* $GrpE_{Gka}$ homodimer in complex with DNAK. The pair wise sequence alignment between Mge1 and *E. coli* Grpe2 (PDB_ID: 1DKG)[169] used as a guide for homology model is shown in **Fig.3.6A**. In the modeled Mge1 (60 amino acid onwards), each monomer comprises an N-terminal long helix, central region that contributes two helices to the formation of a four helical bundle in the dimer and a C-terminal beta-sheet region. In the previously reported crystal structures, DNAK is shown to interact with this beta-sheet region. The model and template structures superimposed using MAPSCI had a root mean square deviation (RMSD) of 0.36 Å. The superimposition shown in **Fig.3.6B** indicated that both template and model structures are highly similar. The stereochemical quality of the model structure was validated using PROCHECK that showed that more than 90% were within the allowed region of the Ramachandran plot.In the template structure (PDB_ID: 1DKG), the aromatic side chain of Phe137 (equivalent of His167 in Mge1) of A chain is in van der waals distance with Phe 91 of the B chain. Likewise, the Phe137 in B chain is in contact with Phe91 of A chain. As a result, there are extended hydrophobic contacts mediated by CH-Pi interactions. In the Mge1 model structure, we observed that this

spatial arrangement of histidine (His167) and phenylalanine (Phe117) in both chains is retained and this contributes to the stability of the homodimer as shown in **Fig.3.6C**. Further, in the Mge1 model, the ND1of imidazole ring of His167 forms a hydrogen bond with the main chain carbonyl oxygen of Thr163 in both chains, which is one of the factors responsible for the rigidity of the local conformation.

In the Mge1 His167 Leu substitution mutant, the hydrophobic residue leucine retains the extended non-bonding interactions between the two chains as shown in **Fig.3.6D**, and therefore maintain structural rigidity. By mutating to leucine, an amino acid of similar carbon chain length, the hydrogen bond with Thr163 would be lost making the local region more flexible. Incidentally we later observed in the $GrpE_{Tth}$ from a higher temperature organism, His at the corresponding site is replaced with leucine [214] as can be seen in Fig.3.6A. The trajectories of the 50 ns MD simulations for both native and mutant proteins were analysed. The root mean square fluctuation (RMSF) (**Fig.3.7A**) indicated that major fluctuations are observed in the N-terminal helices (60 to 77 amino acids by 8-11.5 Å) and the long loop connecting the helices involved in the chain reversal (133-143 amino acids by ~7Å) for the formation of four helical bundle. These large fluctuations were seen in both native and His167Leu homodimers. Comparison of various GrpE's has shown greater flexibility in the N-terminal regions in all the structures determined so far [215].

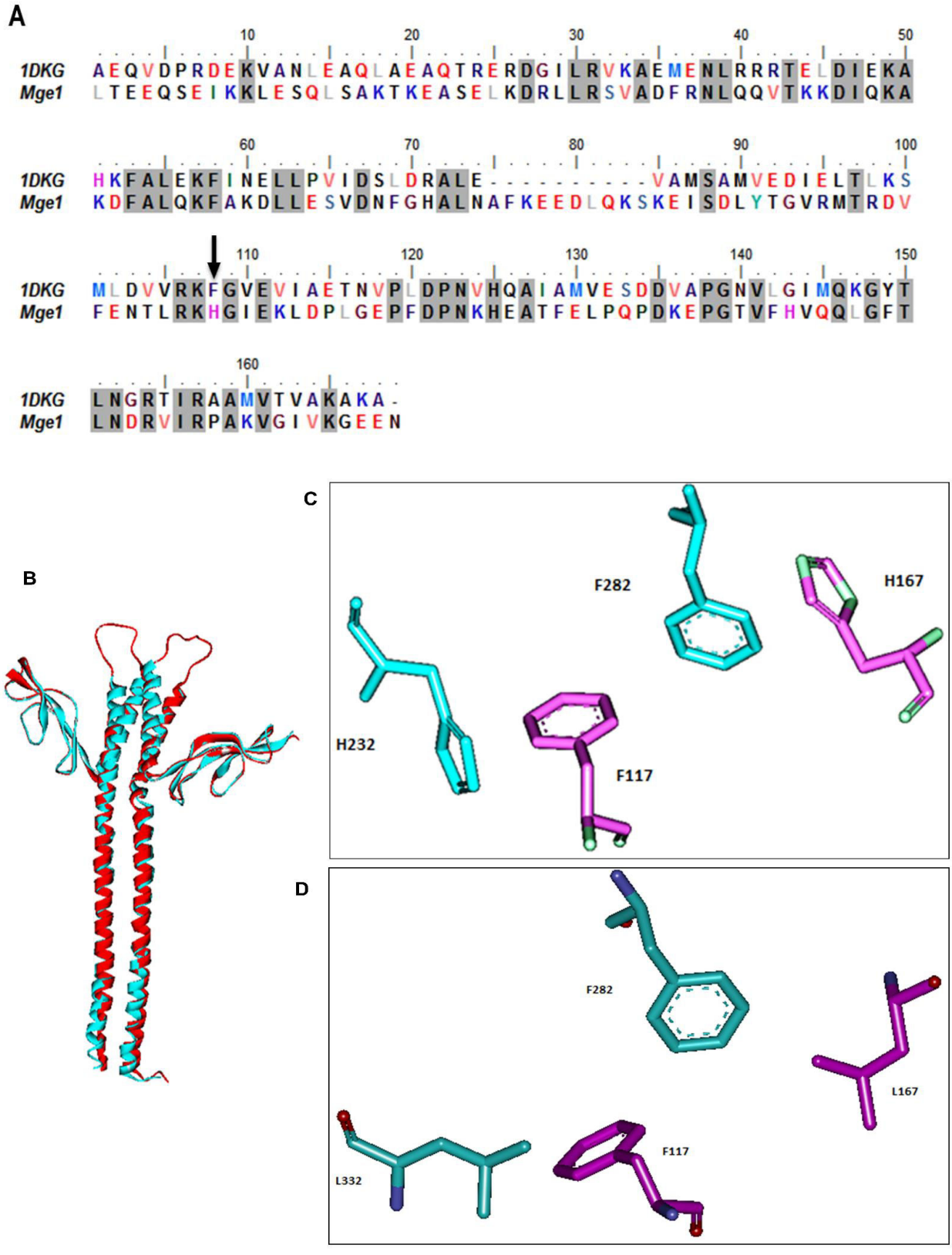

Figure 3.6 Spatial arrangment of Mge1 aminoacid residues: (**A**) Sequence alignment of $GrpE_{Eco}$ PDB_ID: 1DKG and Mge1.(**B**) Individual and superimposed conformations of the PDB_ID:1DKG template (E.coli GrpE) (blue) and Mge1 model (red). (**C**) Spatial

Arrangement of His and Phe in the native Mge1 (pink: A chain, cyan: B chain). (**D**) Spatial Arrangement of Leu and Phe in the mutant Mge1 (pink: A chain, cyan: B chain).

The kinetic energy (**Fig.3.7A**) and potential energy plots (**Fig.3.7B**) show that the structures are stable over the duration of MD simulations in both native and mutant Mge1 proteins. From the RMSF plots (**Fig.3.7C**) we observed that in both chains, the N- terminal long helices have high fluctuations. The first 17 amino acid residues N- terminal helical region has fluctuations of the order 8 Å, 11.5Å in native and mutant proteins respectively. In both chains of the native protein, the rest of the N-terminal helical region has less fluctuations (less than 4 Å) and the corresponding region in mutant protein is nearly 7.5 Å. The loop region (133 –143 amino acids residues) of chain A has similar fluctuations in both native and mutant proteins. This loop in B chain of native protein has (2.5Å) fluctuations while that of the mutant has greater fluctuations. In both native and mutant proteins the four helical bundle region have less fluctuations indicating that this regions forms the protein core that is structurally rigid. Intriguingly, a nearly 10 amino acid region connecting 2^{nd} and 3^{rd} beta- strands in the beta-sheet region of the native protein has higher fluctuations in the A chain compared to the similar region in B chain while in the mutant protein, B chain has higher fluctuations compared to the A chain. Further, the beta-sheet region in A chain of native protein has higher fluctuations compared to the mutant, while in the B chain, the mutant protein has higher fluctuations compared to the native.

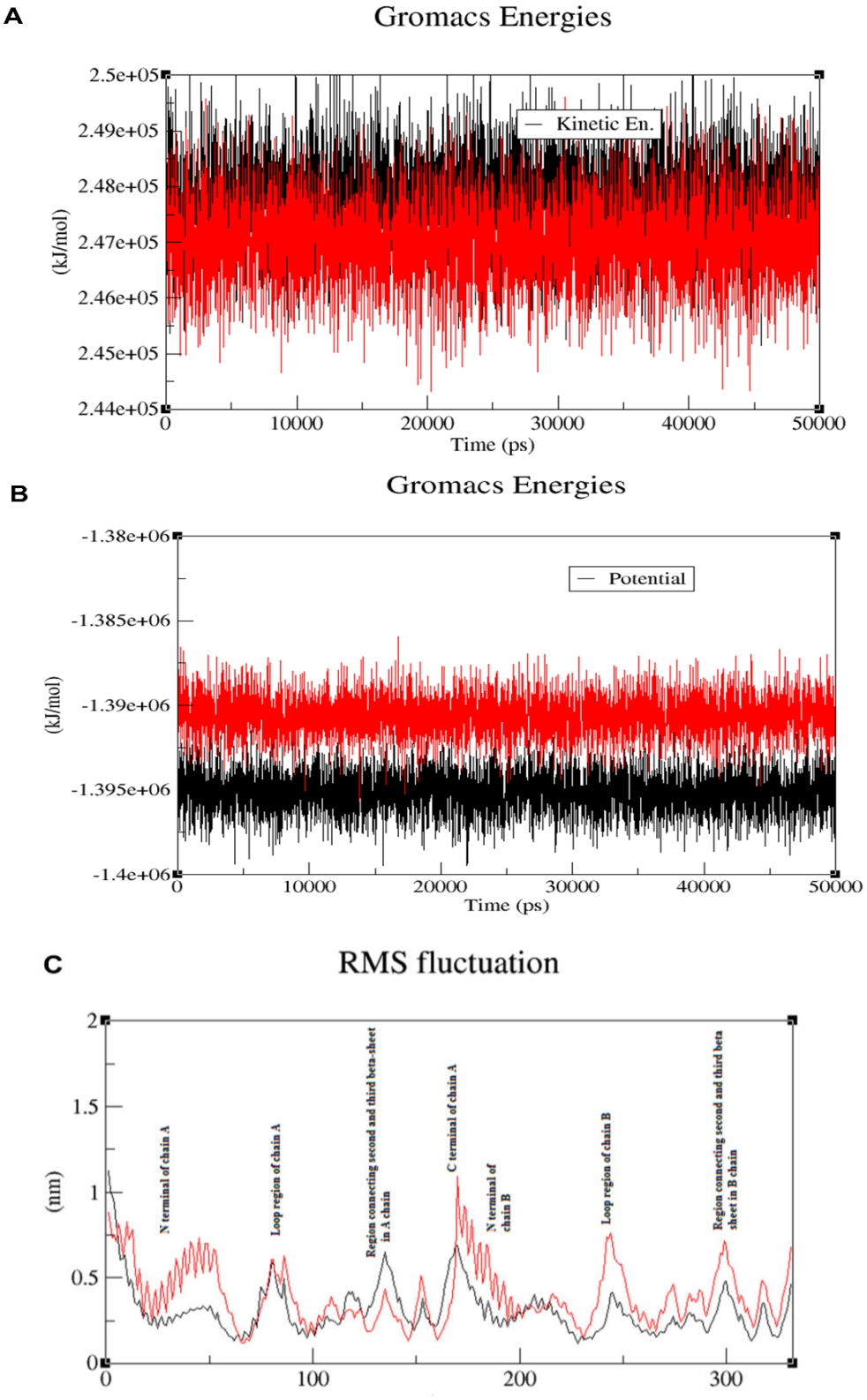

Figure 3.7 Molecular dynamics simulations of Mge1:(A) Kinetic energy plot of WT (black) and H167L mutant (red) of Mge1. (B) Potential energy plot of WT (black) and H167 mutant (red) of Mge1.(C) The root mean square fluctuation (RMSF) plots of WT (black) and H167L mutant (red) of Mge1.

Collectively, these results suggest that intrinsic flexibility observed in Mge1 mutant is almost similar to that of T.Thermophilus GrpE when compared to wild type Mge1 and E.coli GrpE. Thus mutation in Mge1 confers a selective advantage in acquiring stability during thermal unfolding. Further Mge H167L mutant can exert a positive effect on Hsp70 through rapid ATP/ADP exchange kinetics thereby facilitated the folding of proteins mediated by Hsp70 during thermal folding.

3.4 Discussion

Molecular chaperones are required for survival and adaptation to heat shock. Both cytosolic chaperone Hsp104 and mitochondrial chaperones like Hsp70 and Hsp78 are required to survive at non permissive temperature in yeast [216]–[218]. Mitochondrial Hsp70 is close analogue of DnaK chaperone in E coli. Hsp70 chaparone system consists of Mdj1 and Mge1 as co-chaperones that regulates the chaperone cycle. The cycle includes nucleotide dependent binding and release of peptides essential for protein import, refolding of denatured proteins and prevention of aggregated proteins. Optimal tuned binding and release of client peptides by Hsp70 are controlled by Mdj1 under normal physiological conditions. During heat shock temperatures, Mt Hsp70 seems to be more important in preventing aggregation of proteins through enhanced sequestration of misfolded polypeptide segments. Mge1 exists as homodimer that binds to Hsp70 in the ratio of 2:1. It functions as a nucleotide exchange factor of Hsp70 by promoting dissociation of ADP and binding of ATP. We have shown earlier that Mge1 acts as an oxidative sensor and Mge1-M155L mutant resistant to oxidative stress [201]. It is known that Mge1 also acts as a thermal sensor[153]. It has been shown that either yeast Mge1 or Mge1 homologue Ecoli GrpE responds to higher temperature shift by dissociation of dimer form to monomer. The monomeric form of Mge1 has less ability to bind Hsp70/DnaK and thereby prevents the exchange of ATP for ADP on Hsp70. Reduction

in nucleotide exchange activity helps in T-R conformational shift in Hsp70 results in a higher fraction of substrates are being sequestered by high affinity Hsp70. However the molecular mechanism for structural transition during thermal unfolding of Mge1 is not known.

The co-crystal structure of E.coli N-terminal 33 amino acids truncated GrpE with ATPase domain of DnaK was solved [219]. The GrpE forms an asymmetric homodimer with unusual quaternary structure. The dimer comprises two long N-terminal alpha helices of each monomer (tail) followed by two short alpha helices at the end results in formation of four-helix bundle at the dimer interface. Two COOH-terminal end of four helix bundle projects two small beta sheet domains of total 6 short beta sheets that are present in C-terminus. The short 60 amino acids compact beta sheet domain at C-terminal does not contribute to the dimer interface.

The ATPase domain of Hsp70 consists of two large and total of four sub-domains: Sub-domain 1A and IIA are present at the base whereas sub-domains 1B and IIB are present at the side of nucleotide binding pocket. Although GrpE is not near to the nucleotide binding site of DnaK, the two faces of proximal beta sheet of GrpE is in prominent contact with 1B and IIB sub-domains of DnaK. Glu^{28} of DnaK and Arg^{183} of GrpE is involved in intermolecular hydrogen bond. The proximal GrpE Phe^{86} is involved in proper positioning of Arg^{183} of Mge1.

It has been shown that formation of four helix bundle but not the long N-terminal alpha helical tail is important for the stability of dimer as GrpE (1-138 and 88-197) constructs without tail domain are able to form dimer. However, the long N-terminal helix appears to be important for thermal sensor property as substitution of cysteine at position 40 instead of arginine stabilizes the dimer due to formation of cysteine-cysteine disulfide bond in between monomers. Further, the long N-terminal alpha helices in dimer do not form canonical coil-

coil structure and are in parallel to each other along length of helix axis. The structure of $GrpE_{Tth}$ from *Thermus thermophilus* was solved by Nakamura et al.2010 and the crystal structure of a full-length *Geobacillus kaustophilus HTA426* $GrpE_{Gka}$ homodimer in complex with DNAK was resolved[215]. By comparing the structures of GrpE from *E. coli* and *T. thermophilus*[214] reveals some similarities and important dissimilarities in their topology. It was assumed that GrpE can be present in two topologies, topology A forms in $GrpE_{Eco}$ and topology B forms in $GrpE_{Tth}$ [214]. The main difference between these two topologies is the connectivity of the two helices in a monomer that are a part of the four helical bundle. Subsequently, it has been shown that $GrpE_{Gka}$ also has the topology A [215] that is in agreement with $GrpE_{Eco}$. Intesrestingly, Thermophile GrpE structure reveals that the formation of canonical coiled-coil domain with 33 amino acids of N-terminus tail domain. In addition, the temperature dependent structural transition in E.coli and yeast Mge1 is attributed to the unfolding of long N-terminal helices followed by destabilization of beta sheet whereas in Thermophiles, melting of the beta sheet domain at permissive transition temperature induces the unwinding of N-terminal helices during thermal stress. These studies indicate the importance, four helical bundle, N-terminal helices and beta sheet in structural stability during thermal transition.

In this study we find that substitution of histidine at 167^{th} position with leucine which is located at junction between N-terminal helical bundle and beta sheet structures show thermal stability and partially prevents the protein aggregation. Thermal denaturation and refolding studies suggest that Mge1-H167L is indeed more stable when compared to wild type. Mge1-H167L mutant as it acquires thermal stability and thermal tolerance under non-permissive conditions.Molecular dynamics simulation studies with 3D modelled structure of Mge1-H167L mutant show that formation of coiled-coil N-terminal alpha helices which resemble like Thermus thermophiles GrpE. Further, Thermus thermophiles GrpE have leucine residue

at the corresponding site. His167 is located in the short turn region connecting the terminal helix and the first strand of the beta sheet region. Incidentally His167 is followed by Gly168, a residue that imparts conformational flexibility. This Histidine to leucine mutation probably introduces a conformational flexibility to the Mge1 at this region. The hydrophobic residue leucine at 167th position instead of Histidine in Mge1 provides more flexibility in the local region. This is due to loss of hydrogen bond with surrounding amino acids in particular Thr 163.

It was interesting to observe the differences between $GrpE_{Eco}$, $GrpE_{Tth}$ and $GrpE_{Gka}$ [215]. Clearly, the $GrpE_{Tth}$ had greater N-terminal helical fluctuations compared to the other two proteins indicating the intrinsic flexibility of protein from thermophilic organism as observed by us in the His167 Leu Mge1 mutant though at a lower scale because of a single point mutation.

This flexibility in Mge1 mutant partially mimics the structure of thermophile GrpE by melting beta sheet at transition temperature and prevents the unwinding of alpha helices. Our study suggest that the connection between beta sheet and long N-terminal helices in acquiring the thermal stability. Further this flexibility in Mge1 may facilitate the dynamic interaction with Hsp70 thereby shift the equilibrium towards R conformation for sequestration of misfolded proteins during thermal stress.

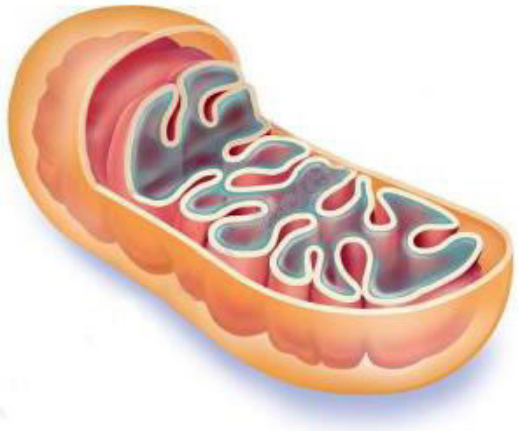

BIBLIOGRAPHY

[1] K. Henze and W. Martin, “Evolutionary biology: essence of mitochondria.,” *Nature*, vol. 426, no. 6963, pp. 127–8, Nov. 2003.

[2] E. Cadenas, A. Boveris, C. I. Ragan, and A. O. Stoppani, “Production of superoxide radicals and hydrogen peroxide by NADH-ubiquinone reductase and ubiquinol-cytochrome c reductase from beef-heart mitochondria.,” *Arch. Biochem. Biophys.*, vol. 180, no. 2, pp. 248–57, Apr. 1977.

[3] B. Landolfi, S. Curci, L. Debellis, T. Pozzan, and A. M. Hofer, “Ca2+ homeostasis in the agonist-sensitive internal store: functional interactions between mitochondria and the ER measured In situ in intact cells.,” *J. Cell Biol.*, vol. 142, no. 5, pp. 1235–43, Sep. 1998.

[4] P. Mitchell and J. Moyle, “Estimation of membrane potential and pH difference across the cristae membrane of rat liver mitochondria.,” *Eur. J. Biochem.*, vol. 7, no. 4, pp. 471–84, Feb. 1969.

[5] D. D. Newmeyer, D. M. Farschon, and J. C. Reed, “Cell-free apoptosis in Xenopus egg extracts: inhibition by Bcl-2 and requirement for an organelle fraction enriched in mitochondria.,” *Cell*, vol. 79, no. 2, pp. 353–64, Oct. 1994.

[6] T. G. Frey and C. A. Mannella, “The internal structure of mitochondria.,” *Trends Biochem. Sci.*, vol. 25, no. 7, pp. 319–24, Jul. 2000.

[7] M. Colombini, “A candidate for the permeability pathway of the outer mitochondrial membrane.,” *Nature*, vol. 279, no. 5714, pp. 643–5, Jun. 1979.

[8] K. Mihara, G. Blobel, and R. Sato, “In vitro synthesis and integration into mitochondria of porin, a major protein of the outer mitochondrial membrane of Saccharomyces cerevisiae.,” *Proc. Natl. Acad. Sci. U. S. A.*, vol. 79, no. 23, pp. 7102–6, Dec. 1982.

[9] M. G. Vander Heiden, N. S. Chandel, X. X. Li, P. T. Schumacker, M. Colombini, and C. B. Thompson, “Outer mitochondrial membrane permeability can regulate coupled respiration and cell survival.,” *Proc. Natl. Acad. Sci. U. S. A.*, vol. 97, no. 9, pp. 4666–71, Apr. 2000.

[10] W. Voos, H. Martin, T. Krimmer, and N. Pfanner, “Mechanisms of protein translocation into mitochondria.,” *Biochim. Biophys. Acta*, vol. 1422, no. 3, pp. 235–54, Nov. 1999.

[11] M. Schleyer and W. Neupert, “Transport of proteins into mitochondria: translocational intermediates spanning contact sites between outer and inner membranes.,” *Cell*, vol. 43, no. 1, pp. 339–50, Nov. 1985.

[12] P. Mitchell and J. Moyle, “Chemiosmotic hypothesis of oxidative phosphorylation.,” *Nature*, vol. 213, no. 5072, pp. 137–9, Jan. 1967.

[13] W. T. Daems and E. Wisse, “Shape and attachment of the cristae mitochondriales in mouse hepatic cell mitochondria.,” *J. Ultrastruct. Res.*, vol. 16, no. 1, pp. 123–40, Sep. 1966.

[14] C. M. Koehler, E. Jarosch, K. Tokatlidis, K. Schmid, R. J. Schweyen, and G. Schatz, “Import of mitochondrial carriers mediated by essential proteins of the intermembrane space.,” *Science*, vol. 279, no. 5349, pp. 369–73, Jan. 1998.

[15] C. D. Moyes and D. A. Hood, “Origins and consequences of mitochondrial variation in vertebrate muscle.,” *Annu. Rev. Physiol.*, vol. 65, pp. 177–201, Jan. 2003.

[16] M. Takahashi and D. A. Hood, “Chronic stimulation-induced changes in mitochondria and performance in rat skeletal muscle.,” *J. Appl. Physiol.*, vol. 74, no. 2, pp. 934–41, Feb. 1993.

[17] G. Paradies and F. M. Ruggiero, “Age-related changes in the activity of the pyruvate carrier and in the lipid composition in rat-heart mitochondria.,” *Biochim. Biophys. Acta*, vol. 1016, no. 2, pp. 207–12, Apr. 1990.

[18] G. Paradies, G. Petrosillo, and F. M. Ruggiero, “Cardiolipin-dependent decrease of cytochrome c oxidase activity in heart mitochondria from hypothyroid rats.,” *Biochim. Biophys. Acta*, vol. 1319, no. 1, pp. 5–8, Mar. 1997.

[19] E. D. Robin and R. Wong, “Mitochondrial DNA molecules and virtual number of mitochondria per cell in mammalian cells.,” *J. Cell. Physiol.*, vol. 136, no. 3, pp. 507–13, Sep. 1988.

[20] D. Bogenhagen and D. A. Clayton, “Mouse L cell mitochondrial DNA molecules are selected randomly for replication throughout the cell cycle.,” *Cell*, vol. 11, no. 4, pp. 719–27, Aug. 1977.

[21] C. T. Moraes, “What regulates mitochondrial DNA copy number in animal cells?,” *Trends Genet.*, vol. 17, no. 4, pp. 199–205, Apr. 2001.

[22] G. Attardi and G. Schatz, “Biogenesis of mitochondria.,” *Annu. Rev. Cell Biol.*, vol. 4, pp. 289–333, Jan. 1988.

[23] R. O. Poyton and J. E. McEwen, “Crosstalk between nuclear and mitochondrial genomes.,” *Annu. Rev. Biochem.*, vol. 65, pp. 563–607, Jan. 1996.

[24] D. J. Schnell and D. N. Hebert, “Protein translocons: multifunctional mediators of protein translocation across membranes.,” *Cell*, vol. 112, no. 4, pp. 491–505, Feb. 2003.

[25] W. Wickner and R. Schekman, “Protein translocation across biological membranes.,” *Science*, vol. 310, no. 5753, pp. 1452–6, Dec. 2005.

[26] W. Neupert and J. M. Herrmann, “Translocation of proteins into mitochondria.,” *Annu. Rev. Biochem.*, vol. 76, pp. 723–49, Jan. 2007.

[27] A. Sickmann, J. Reinders, Y. Wagner, C. Joppich, R. Zahedi, H. E. Meyer, B. Schönfisch, I. Perschil, A. Chacinska, B. Guiard, P. Rehling, N. Pfanner, and C. Meisinger, "The proteome of Saccharomyces cerevisiae mitochondria.," *Proc. Natl. Acad. Sci. U. S. A.*, vol. 100, no. 23, pp. 13207–12, Nov. 2003.

[28] S. W. Taylor, E. Fahy, and S. S. Ghosh, "Global organellar proteomics.," *Trends Biotechnol.*, vol. 21, no. 2, pp. 82–8, Feb. 2003.

[29] J. M. Herrmann, S. Longen, D. Weckbecker, and M. Depuydt, "Biogenesis of mitochondrial proteins.," *Adv. Exp. Med. Biol.*, vol. 748, pp. 41–64, Jan. 2012.

[30] N. Bolender, A. Sickmann, R. Wagner, C. Meisinger, and N. Pfanner, "Multiple pathways for sorting mitochondrial precursor proteins.," *EMBO Rep.*, vol. 9, no. 1, pp. 42–9, Jan. 2008.

[31] A. Chacinska, C. M. Koehler, D. Milenkovic, T. Lithgow, and N. Pfanner, "Importing mitochondrial proteins: machineries and mechanisms.," *Cell*, vol. 138, no. 4, pp. 628–44, Aug. 2009.

[32] F. Perocchi, L. J. Jensen, J. Gagneur, U. Ahting, C. von Mering, P. Bork, H. Prokisch, and L. M. Steinmetz, "Assessing systems properties of yeast mitochondria through an interaction map of the organelle.," *PLoS Genet.*, vol. 2, no. 10, p. e170, Oct. 2006.

[33] D. J. Pagliarini, S. E. Calvo, B. Chang, S. A. Sheth, S. B. Vafai, S.-E. Ong, G. A. Walford, C. Sugiana, A. Boneh, W. K. Chen, D. E. Hill, M. Vidal, J. G. Evans, D. R. Thorburn, S. A. Carr, and V. K. Mootha, "A mitochondrial protein compendium elucidates complex I disease biology.," *Cell*, vol. 134, no. 1, pp. 112–23, Jul. 2008.

[34] S. Karniely, N. Regev-Rudzki, and O. Pines, "The presequence of fumarase is exposed to the cytosol during import into mitochondria.," *J. Mol. Biol.*, vol. 358, no. 2, pp. 396–405, Apr. 2006.

[35] P. Marc, A. Margeot, F. Devaux, C. Blugeon, M. Corral-Debrinski, and C. Jacq, "Genome-wide analysis of mRNAs targeted to yeast mitochondria.," *EMBO Rep.*, vol. 3, no. 2, pp. 159–64, Feb. 2002.

[36] N. Regev-Rudzki, S. Karniely, N. N. Ben-Haim, and O. Pines, "Yeast aconitase in two locations and two metabolic pathways: seeing small amounts is believing.," *Mol. Biol. Cell*, vol. 16, no. 9, pp. 4163–71, Sep. 2005.

[37] K. Mihara and T. Omura, "Cytoplasmic chaperones in precursor targeting to mitochondria: the role of MSF and hsp 70.," *Trends Cell Biol.*, vol. 6, no. 3, pp. 104–8, Mar. 1996.

[38] J. C. Young, N. J. Hoogenraad, and F. U. Hartl, "Molecular chaperones Hsp90 and Hsp70 deliver preproteins to the mitochondrial import receptor Tom70.," *Cell*, vol. 112, no. 1, pp. 41–50, Jan. 2003.

[39] F.-N. Vögtle, S. Wortelkamp, R. P. Zahedi, D. Becker, C. Leidhold, K. Gevaert, J. Kellermann, W. Voos, A. Sickmann, N. Pfanner, and C. Meisinger, "Global analysis

of the mitochondrial N-proteome identifies a processing peptidase critical for protein stability.," *Cell*, vol. 139, no. 2, pp. 428–39, Oct. 2009.

[40] S. Kutik, D. Stojanovski, L. Becker, T. Becker, M. Meinecke, V. Krüger, C. Prinz, C. Meisinger, B. Guiard, R. Wagner, N. Pfanner, and N. Wiedemann, "Dissecting membrane insertion of mitochondrial beta-barrel proteins.," *Cell*, vol. 132, no. 6, pp. 1011–24, Mar. 2008.

[41] P. Rehling, K. Model, K. Brandner, P. Kovermann, A. Sickmann, H. E. Meyer, W. Kühlbrandt, R. Wagner, K. N. Truscott, and N. Pfanner, "Protein insertion into the mitochondrial inner membrane by a twin-pore translocase.," *Science*, vol. 299, no. 5613, pp. 1747–51, Mar. 2003.

[42] K. Model, C. Meisinger, and W. Kühlbrandt, "Cryo-electron microscopy structure of a yeast mitochondrial preprotein translocase.," *J. Mol. Biol.*, vol. 383, no. 5, pp. 1049–57, Nov. 2008.

[43] Y. Abe, T. Shodai, T. Muto, K. Mihara, H. Torii, S. Nishikawa, T. Endo, and D. Kohda, "Structural basis of presequence recognition by the mitochondrial protein import receptor Tom20.," *Cell*, vol. 100, no. 5, pp. 551–60, Mar. 2000.

[44] J. Dudek, P. Rehling, and M. van der Laan, "Mitochondrial protein import: common principles and physiological networks.," *Biochim. Biophys. Acta*, vol. 1833, no. 2, pp. 274–85, Feb. 2013.

[45] T. Becker, L. Böttinger, and N. Pfanner, "Mitochondrial protein import: from transport pathways to an integrated network.," *Trends Biochem. Sci.*, vol. 37, no. 3, pp. 85–91, Mar. 2012.

[46] N. Wiedemann, N. Pfanner, and P. Rehling, "Import of precursor proteins into isolated yeast mitochondria.," *Methods Mol. Biol.*, vol. 313, pp. 373–83, Jan. 2006.

[47] J. M. Herrmann, F. Kauff, and H. E. Neuhaus, "Thiol oxidation in bacteria, mitochondria and chloroplasts: common principles but three unrelated machineries?," *Biochim. Biophys. Acta*, vol. 1793, no. 1, pp. 71–7, Jan. 2009.

[48] S. Kutik, D. A. Stroud, N. Wiedemann, and N. Pfanner, "Evolution of mitochondrial protein biogenesis.," *Biochim. Biophys. Acta*, vol. 1790, no. 6, pp. 409–15, Jun. 2009.

[49] J. M. Herrmann and J. Riemer, "Mitochondrial disulfide relay: redox-regulated protein import into the intermembrane space.," *J. Biol. Chem.*, vol. 287, no. 7, pp. 4426–33, Feb. 2012.

[50] D. Mokranjac, M. Sichting, D. Popov-Celeketić, K. Mapa, L. Gevorkyan-Airapetov, K. Zohary, K. Hell, A. Azem, and W. Neupert, "Role of Tim50 in the transfer of precursor proteins from the outer to the inner membrane of mitochondria.," *Mol. Biol. Cell*, vol. 20, no. 5, pp. 1400–7, Mar. 2009.

[51] Y. Tamura, Y. Harada, T. Shiota, K. Yamano, K. Watanabe, M. Yokota, H. Yamamoto, H. Sesaki, and T. Endo, "Tim23-Tim50 pair coordinates functions of

translocators and motor proteins in mitochondrial protein import.," *J. Cell Biol.*, vol. 184, no. 1, pp. 129–41, Jan. 2009.

[52] M. Meinecke, R. Wagner, P. Kovermann, B. Guiard, D. U. Mick, D. P. Hutu, W. Voos, K. N. Truscott, A. Chacinska, N. Pfanner, and P. Rehling, "Tim50 maintains the permeability barrier of the mitochondrial inner membrane.," *Science*, vol. 312, no. 5779, pp. 1523–6, Jun. 2006.

[53] N. N. Alder, R. E. Jensen, and A. E. Johnson, "Fluorescence mapping of mitochondrial TIM23 complex reveals a water-facing, substrate-interacting helix surface.," *Cell*, vol. 134, no. 3, pp. 439–50, Aug. 2008.

[54] A. Chacinska, M. Lind, A. E. Frazier, J. Dudek, C. Meisinger, A. Geissler, A. Sickmann, H. E. Meyer, K. N. Truscott, B. Guiard, N. Pfanner, and P. Rehling, "Mitochondrial presequence translocase: switching between TOM tethering and motor recruitment involves Tim21 and Tim17.," *Cell*, vol. 120, no. 6, pp. 817–29, Mar. 2005.

[55] S. Martinez-Caballero, S. M. Grigoriev, J. M. Herrmann, M. L. Campo, and K. W. Kinnally, "Tim17p regulates the twin pore structure and voltage gating of the mitochondrial protein import complex TIM23.," *J. Biol. Chem.*, vol. 282, no. 6, pp. 3584–93, Feb. 2007.

[56] M. van der Laan, N. Wiedemann, D. U. Mick, B. Guiard, P. Rehling, and N. Pfanner, "A role for Tim21 in membrane-potential-dependent preprotein sorting in mitochondria.," *Curr. Biol.*, vol. 16, no. 22, pp. 2271–6, Nov. 2006.

[57] N. Wiedemann, M. van der Laan, D. P. Hutu, P. Rehling, and N. Pfanner, "Sorting switch of mitochondrial presequence translocase involves coupling of motor module to respiratory chain.," *J. Cell Biol.*, vol. 179, no. 6, pp. 1115–22, Dec. 2007.

[58] M. K. Dienhart and R. A. Stuart, "The yeast Aac2 protein exists in physical association with the cytochrome bc1-COX supercomplex and the TIM23 machinery.," *Mol. Biol. Cell*, vol. 19, no. 9, pp. 3934–43, Sep. 2008.

[59] K. Shariff, S. Ghosal, and A. Matouschek, "The force exerted by the membrane potential during protein import into the mitochondrial matrix.," *Biophys. J.*, vol. 86, no. 6, pp. 3647–52, Jun. 2004.

[60] M. van der Laan, M. Meinecke, J. Dudek, D. P. Hutu, M. Lind, I. Perschil, B. Guiard, R. Wagner, N. Pfanner, and P. Rehling, "Motor-free mitochondrial presequence translocase drives membrane integration of preproteins.," *Nat. Cell Biol.*, vol. 9, no. 10, pp. 1152–9, Oct. 2007.

[61] D. Mokranjac, D. Popov-Celeketić, K. Hell, and W. Neupert, "Role of Tim21 in mitochondrial translocation contact sites.," *J. Biol. Chem.*, vol. 280, no. 25, pp. 23437–40, Jun. 2005.

[62] T. Shiota, H. Mabuchi, S. Tanaka-Yamano, K. Yamano, and T. Endo, "In vivo protein-interaction mapping of a mitochondrial translocator protein Tom22 at work.," *Proc. Natl. Acad. Sci. U. S. A.*, vol. 108, no. 37, pp. 15179–83, Sep. 2011.

[63] A. Geissler, A. Chacinska, K. N. Truscott, N. Wiedemann, K. Brandner, A. Sickmann, H. E. Meyer, C. Meisinger, N. Pfanner, and P. Rehling, "The mitochondrial presequence translocase: an essential role of Tim50 in directing preproteins to the import channel.," *Cell*, vol. 111, no. 4, pp. 507–18, Nov. 2002.

[64] H. Yamamoto, M. Esaki, T. Kanamori, Y. Tamura, S. ichi Nishikawa, and T. Endo, "Tim50 is a subunit of the TIM23 complex that links protein translocation across the outer and inner mitochondrial membranes.," *Cell*, vol. 111, no. 4, pp. 519–28, Nov. 2002.

[65] L. de la Cruz, R. Bajaj, S. Becker, and M. Zweckstetter, "The intermembrane space domain of Tim23 is intrinsically disordered with a distinct binding region for presequences.," *Protein Sci.*, vol. 19, no. 11, pp. 2045–54, Nov. 2010.

[66] O. Lytovchenko, J. Melin, C. Schulz, M. Kilisch, D. P. Hutu, and P. Rehling, "Signal recognition initiates reorganization of the presequence translocase during protein import.," *EMBO J.*, vol. 32, no. 6, pp. 886–98, Mar. 2013.

[67] J. Martin, K. Mahlke, and N. Pfanner, "Role of an energized inner membrane in mitochondrial protein import. Delta psi drives the movement of presequences.," *J. Biol. Chem.*, vol. 266, no. 27, pp. 18051–7, Sep. 1991.

[68] X. Qian, M. Gebert, J. Höpker, M. Yan, J. Li, N. Wiedemann, M. van der Laan, N. Pfanner, and B. Sha, "Structural basis for the function of Tim50 in the mitochondrial presequence translocase.," *J. Mol. Biol.*, vol. 411, no. 3, pp. 513–9, Aug. 2011.

[69] A. P. van Loon, A. W. Brändli, and G. Schatz, "The presequences of two imported mitochondrial proteins contain information for intracellular and intramitochondrial sorting.," *Cell*, vol. 44, no. 5, pp. 801–12, Mar. 1986.

[70] S. M. Glaser and M. G. Cumsky, "A synthetic presequence reversibly inhibits protein import into yeast mitochondria.," *J. Biol. Chem.*, vol. 265, no. 15, pp. 8808–16, May 1990.

[71] B. S. Glick, A. Brandt, K. Cunningham, S. Müller, R. L. Hallberg, and G. Schatz, "Cytochromes c1 and b2 are sorted to the intermembrane space of yeast mitochondria by a stop-transfer mechanism.," *Cell*, vol. 69, no. 5, pp. 809–22, May 1992.

[72] A. Gruhler, I. Arnold, T. Seytter, B. Guiard, E. Schwarz, W. Neupert, and R. A. Stuart, "N-terminal hydrophobic sorting signals of preproteins confer mitochondrial hsp70 independence for import into mitochondria.," *J. Biol. Chem.*, vol. 272, no. 28, pp. 17410–5, Jul. 1997.

[73] A. Chacinska, M. van der Laan, C. S. Mehnert, B. Guiard, D. U. Mick, D. P. Hutu, K. N. Truscott, N. Wiedemann, C. Meisinger, N. Pfanner, and P. Rehling, "Distinct forms of mitochondrial TOM-TIM supercomplexes define signal-dependent states of preprotein sorting.," *Mol. Cell. Biol.*, vol. 30, no. 1, pp. 307–18, Jan. 2010.

[74] D. Popov-Čeleketić, K. Waegemann, K. Mapa, W. Neupert, and D. Mokranjac, "Role of the import motor in insertion of transmembrane segments by the mitochondrial TIM23 complex.," *EMBO Rep.*, vol. 12, no. 6, pp. 542–8, Jun. 2011.

[75] M. P. Mayer, "Timing the catch.," *Nat. Struct. Mol. Biol.*, vol. 11, no. 1, pp. 6–8, Jan. 2004.

[76] K. E. Matlack, B. Misselwitz, K. Plath, and T. A. Rapoport, "BiP acts as a molecular ratchet during posttranslational transport of prepro-alpha factor across the ER membrane.," *Cell*, vol. 97, no. 5, pp. 553–64, May 1999.

[77] Ú. Flores-Pérez and P. Jarvis, "Molecular chaperone involvement in chloroplast protein import.," *Biochim. Biophys. Acta*, vol. 1833, no. 2, pp. 332–40, Feb. 2013.

[78] F. U. Hartl and M. Hayer-Hartl, "Molecular chaperones in the cytosol: from nascent chain to folded protein.," *Science*, vol. 295, no. 5561, pp. 1852–8, Mar. 2002.

[79] T. Langer, C. Lu, H. Echols, J. Flanagan, M. K. Hayer, and F. U. Hartl, "Successive action of DnaK, DnaJ and GroEL along the pathway of chaperone-mediated protein folding.," *Nature*, vol. 356, no. 6371, pp. 683–9, Apr. 1992.

[80] X. Zhu, X. Zhao, W. F. Burkholder, A. Gragerov, C. M. Ogata, M. E. Gottesman, and W. A. Hendrickson, "Structural analysis of substrate binding by the molecular chaperone DnaK.," *Science*, vol. 272, no. 5268, pp. 1606–14, Jun. 1996.

[81] R. Russell, R. Jordan, and R. McMacken, "Kinetic characterization of the ATPase cycle of the DnaK molecular chaperone.," *Biochemistry*, vol. 37, no. 2, pp. 596–607, Jan. 1998.

[82] M. K. Greene, K. Maskos, and S. J. Landry, "Role of the J-domain in the cooperation of Hsp40 with Hsp70.," *Proc. Natl. Acad. Sci. U. S. A.*, vol. 95, no. 11, pp. 6108–13, May 1998.

[83] J. Jiang, E. G. Maes, A. B. Taylor, L. Wang, A. P. Hinck, E. M. Lafer, and R. Sousa, "Structural basis of J cochaperone binding and regulation of Hsp70.," *Mol. Cell*, vol. 28, no. 3, pp. 422–33, Nov. 2007.

[84] J. F. Swain, G. Dinler, R. Sivendran, D. L. Montgomery, M. Stotz, and L. M. Gierasch, "Hsp70 chaperone ligands control domain association via an allosteric mechanism mediated by the interdomain linker.," *Mol. Cell*, vol. 26, no. 1, pp. 27–39, Apr. 2007.

[85] K. Mapa, M. Sikor, V. Kudryavtsev, K. Waegemann, S. Kalinin, C. A. M. Seidel, W. Neupert, D. C. Lamb, and D. Mokranjac, "The conformational dynamics of the mitochondrial Hsp70 chaperone.," *Mol. Cell*, vol. 38, no. 1, pp. 89–100, Apr. 2010.

[86] M. Sikor, K. Mapa, L. V. von Voithenberg, D. Mokranjac, and D. C. Lamb, "Real-time observation of the conformational dynamics of mitochondrial Hsp70 by spFRET.," *EMBO J.*, vol. 32, no. 11, pp. 1639–49, May 2013.

[87] L. Burri, K. Vascotto, S. Fredersdorf, R. Tiedt, M. N. Hall, and T. Lithgow, “Zim17, a novel zinc finger protein essential for protein import into mitochondria.,” *J. Biol. Chem.*, vol. 279, no. 48, pp. 50243–9, Nov. 2004.

[88] M. Sichting, D. Mokranjac, A. Azem, W. Neupert, and K. Hell, “Maintenance of structure and function of mitochondrial Hsp70 chaperones requires the chaperone Hep1.,” *EMBO J.*, vol. 24, no. 5, pp. 1046–56, Mar. 2005.

[89] H. Yamamoto, T. Momose, Y.-I. Yatsukawa, C. Ohshima, D. Ishikawa, T. Sato, Y. Tamura, Y. Ohwa, and T. Endo, “Identification of a novel member of yeast mitochondrial Hsp70-associated motor and chaperone proteins that facilitates protein translocation across the inner membrane.,” *FEBS Lett.*, vol. 579, no. 2, pp. 507–11, Jan. 2005.

[90] H. Fraga, E. Papaleo, S. Vega, A. Velazquez-Campoy, and S. Ventura, “Zinc induced folding is essential for TIM15 activity as an mtHsp70 chaperone.,” *Biochim. Biophys. Acta*, vol. 1830, no. 1, pp. 2139–49, Jan. 2013.

[91] M. Blamowska, W. Neupert, and K. Hell, “Biogenesis of the mitochondrial Hsp70 chaperone.,” *J. Cell Biol.*, vol. 199, no. 1, pp. 125–35, Oct. 2012.

[92] M. Blamowska, M. Sichting, K. Mapa, D. Mokranjac, W. Neupert, and K. Hell, “ATPase domain and interdomain linker play a key role in aggregation of mitochondrial Hsp70 chaperone Ssc1.,” *J. Biol. Chem.*, vol. 285, no. 7, pp. 4423–31, Feb. 2010.

[93] F. Gärtner, W. Voos, A. Querol, B. R. Miller, E. A. Craig, M. G. Cumsky, and N. Pfanner, “Mitochondrial import of subunit Va of cytochrome c oxidase characterized with yeast mutants.,” *J. Biol. Chem.*, vol. 270, no. 8, pp. 3788–95, Feb. 1995.

[94] M. van der Laan, A. Chacinska, M. Lind, I. Perschil, A. Sickmann, H. E. Meyer, B. Guiard, C. Meisinger, N. Pfanner, and P. Rehling, “Pam17 is required for architecture and translocation activity of the mitochondrial protein import motor.,” *Mol. Cell. Biol.*, vol. 25, no. 17, pp. 7449–58, Sep. 2005.

[95] D. Schiller, “Pam17 and Tim44 act sequentially in protein import into the mitochondrial matrix.,” *Int. J. Biochem. Cell Biol.*, vol. 41, no. 11, pp. 2343–9, Nov. 2009.

[96] D. P. Hutu, B. Guiard, A. Chacinska, D. Becker, N. Pfanner, P. Rehling, and M. van der Laan, “Mitochondrial protein import motor: differential role of Tim44 in the recruitment of Pam17 and J-complex to the presequence translocase.,” *Mol. Biol. Cell*, vol. 19, no. 6, pp. 2642–9, Jun. 2008.

[97] D. Popov-Celeketić, K. Mapa, W. Neupert, and D. Mokranjac, “Active remodelling of the TIM23 complex during translocation of preproteins into mitochondria.,” *EMBO J.*, vol. 27, no. 10, pp. 1469–80, May 2008.

[98] M. Marom, D. Dayan, K. Demishtein-Zohary, D. Mokranjac, W. Neupert, and A. Azem, “Direct interaction of mitochondrial targeting presequences with purified

components of the TIM23 protein complex.," *J. Biol. Chem.*, vol. 286, no. 51, pp. 43809–15, Dec. 2011.

[99] N. Handa, S. Kishishita, S. Morita, R. Akasaka, Z. Jin, J. Chrzas, L. Chen, Z.-J. Liu, B.-C. Wang, S. Sugano, A. Tanaka, T. Terada, M. Shirouzu, and S. Yokoyama, "Structure of the human Tim44 C-terminal domain in complex with pentaethylene glycol: ligand-bound form.," *Acta Crystallogr. D. Biol. Crystallogr.*, vol. 63, no. Pt 12, pp. 1225–34, Dec. 2007.

[100] M. Marom, R. Safonov, S. Amram, Y. Avneon, E. Nachliel, M. Gutman, K. Zohary, A. Azem, and Y. Tsfadia, "Interaction of the Tim44 C-terminal domain with negatively charged phospholipids.," *Biochemistry*, vol. 48, no. 47, pp. 11185–95, Dec. 2009.

[101] J. Berthold, M. F. Bauer, H. C. Schneider, C. Klaus, K. Dietmeier, W. Neupert, and M. Brunner, "The MIM complex mediates preprotein translocation across the mitochondrial inner membrane and couples it to the mt-Hsp70/ATP driving system.," *Cell*, vol. 81, no. 7, pp. 1085–93, Jun. 1995.

[102] M. Schlame, "Cardiolipin remodeling and the function of tafazzin.," *Biochim. Biophys. Acta*, vol. 1831, no. 3, pp. 582–8, Mar. 2013.

[103] N. G. Kronidou, W. Oppliger, L. Bolliger, K. Hannavy, B. S. Glick, G. Schatz, and M. Horst, "Dynamic interaction between Isp45 and mitochondrial hsp70 in the protein import system of the yeast mitochondrial inner membrane.," *Proc. Natl. Acad. Sci. U. S. A.*, vol. 91, no. 26, pp. 12818–22, Dec. 1994.

[104] H. C. Schneider, J. Berthold, M. F. Bauer, K. Dietmeier, B. Guiard, M. Brunner, and W. Neupert, "Mitochondrial Hsp70/MIM44 complex facilitates protein import.," *Nature*, vol. 371, no. 6500, pp. 768–74, Oct. 1994.

[105] K. N. Truscott, W. Voos, A. E. Frazier, M. Lind, Y. Li, A. Geissler, J. Dudek, H. Müller, A. Sickmann, H. E. Meyer, C. Meisinger, B. Guiard, P. Rehling, and N. Pfanner, "A J-protein is an essential subunit of the presequence translocase-associated protein import motor of mitochondria.," *J. Cell Biol.*, vol. 163, no. 4, pp. 707–13, Nov. 2003.

[106] Y. Li, J. Dudek, B. Guiard, N. Pfanner, P. Rehling, and W. Voos, "The presequence translocase-associated protein import motor of mitochondria. Pam16 functions in an antagonistic manner to Pam18.," *J. Biol. Chem.*, vol. 279, no. 36, pp. 38047–54, Sep. 2004.

[107] D. Mokranjac, A. Berg, A. Adam, W. Neupert, and K. Hell, "Association of the Tim14.Tim16 subcomplex with the TIM23 translocase is crucial for function of the mitochondrial protein import motor.," *J. Biol. Chem.*, vol. 282, no. 25, pp. 18037–45, Jun. 2007.

[108] P. R. D'Silva, B. Schilke, M. Hayashi, and E. A. Craig, "Interaction of the J-protein heterodimer Pam18/Pam16 of the mitochondrial import motor with the translocon of the inner membrane.," *Mol. Biol. Cell*, vol. 19, no. 1, pp. 424–32, Jan. 2008.

[109] A. E. Frazier, J. Dudek, B. Guiard, W. Voos, Y. Li, M. Lind, C. Meisinger, A. Geissler, A. Sickmann, H. E. Meyer, V. Bilanchone, M. G. Cumsky, K. N. Truscott, N. Pfanner, and P. Rehling, "Pam16 has an essential role in the mitochondrial protein import motor.," *Nat. Struct. Mol. Biol.*, vol. 11, no. 3, pp. 226–33, Mar. 2004.

[110] C. Kozany, D. Mokranjac, M. Sichting, W. Neupert, and K. Hell, "The J domain-related cochaperone Tim16 is a constituent of the mitochondrial TIM23 preprotein translocase.," *Nat. Struct. Mol. Biol.*, vol. 11, no. 3, pp. 234–41, Mar. 2004.

[111] B. A. Schilke, M. Hayashi, and E. A. Craig, "Genetic analysis of complex interactions among components of the mitochondrial import motor and translocon in Saccharomyces cerevisiae.," *Genetics*, vol. 190, no. 4, pp. 1341–53, Apr. 2012.

[112] J. E. Pais, B. Schilke, and E. A. Craig, "Reevaluation of the role of the Pam18:Pam16 interaction in translocation of proteins by the mitochondrial Hsp70-based import motor.," *Mol. Biol. Cell*, vol. 22, no. 24, pp. 4740–9, Dec. 2011.

[113] S. M. Simon, C. S. Peskin, and G. F. Oster, "What drives the translocation of proteins?," *Proc. Natl. Acad. Sci. U. S. A.*, vol. 89, no. 9, pp. 3770–4, May 1992.

[114] N. Pfanner and M. Meijer, "Protein sorting. Pulling in the proteins.," *Curr. Biol.*, vol. 5, no. 2, pp. 132–5, Feb. 1995.

[115] B. S. Glick, "Can Hsp70 proteins act as force-generating motors?," *Cell*, vol. 80, no. 1, pp. 11–4, Jan. 1995.

[116] B. Gaume, C. Klaus, C. Ungermann, B. Guiard, W. Neupert, and M. Brunner, "Unfolding of preproteins upon import into mitochondria.," *EMBO J.*, vol. 17, no. 22, pp. 6497–507, Nov. 1998.

[117] H. C. Schneider, B. Westermann, W. Neupert, and M. Brunner, "The nucleotide exchange factor MGE exerts a key function in the ATP-dependent cycle of mt-Hsp70-Tim44 interaction driving mitochondrial protein import.," *EMBO J.*, vol. 15, no. 21, pp. 5796–803, Nov. 1996.

[118] K. Okamoto, A. Brinker, S. A. Paschen, I. Moarefi, M. Hayer-Hartl, W. Neupert, and M. Brunner, "The protein import motor of mitochondria: a targeted molecular ratchet driving unfolding and translocation.," *EMBO J.*, vol. 21, no. 14, pp. 3659–71, Jul. 2002.

[119] Q. Liu, P. D'Silva, W. Walter, J. Marszalek, and E. A. Craig, "Regulated cycling of mitochondrial Hsp70 at the protein import channel.," *Science*, vol. 300, no. 5616, pp. 139–41, Apr. 2003.

[120] K. Yamano, M. Kuroyanagi-Hasegawa, M. Esaki, M. Yokota, and T. Endo, "Step-size analyses of the mitochondrial Hsp70 import motor reveal the Brownian ratchet in operation.," *J. Biol. Chem.*, vol. 283, no. 40, pp. 27325–32, Oct. 2008.

[121] P. De Los Rios, A. Ben-Zvi, O. Slutsky, A. Azem, and P. Goloubinoff, "Hsp70 chaperones accelerate protein translocation and the unfolding of stable protein

aggregates by entropic pulling.," *Proc. Natl. Acad. Sci. U. S. A.*, vol. 103, no. 16, pp. 6166–71, Apr. 2006.

[122] P. D. D'Silva, B. Schilke, W. Walter, A. Andrew, and E. A. Craig, "J protein cochaperone of the mitochondrial inner membrane required for protein import into the mitochondrial matrix.," *Proc. Natl. Acad. Sci. U. S. A.*, vol. 100, no. 24, pp. 13839–44, Nov. 2003.

[123] D. Mokranjac, S. A. Paschen, C. Kozany, H. Prokisch, S. C. Hoppins, F. E. Nargang, W. Neupert, and K. Hell, "Tim50, a novel component of the TIM23 preprotein translocase of mitochondria.," *EMBO J.*, vol. 22, no. 4, pp. 816–25, Feb. 2003.

[124] F. Moro, C. Sirrenberg, H. C. Schneider, W. Neupert, and M. Brunner, "The TIM17.23 preprotein translocase of mitochondria: composition and function in protein transport into the matrix.," *EMBO J.*, vol. 18, no. 13, pp. 3667–75, Jul. 1999.

[125] S. Laloraya, B. D. Gambill, and E. A. Craig, "A role for a eukaryotic GrpE-related protein, Mge1p, in protein translocation.," *Proc. Natl. Acad. Sci. U. S. A.*, vol. 91, no. 14, pp. 6481–5, Jul. 1994.

[126] B. Miao, J. E. Davis, and E. A. Craig, "Mge1 functions as a nucleotide release factor for Ssc1, a mitochondrial Hsp70 of Saccharomyces cerevisiae.," *J. Mol. Biol.*, vol. 265, no. 5, pp. 541–52, Feb. 1997.

[127] I. Milisav, F. Moro, W. Neupert, and M. Brunner, "Modular structure of the TIM23 preprotein translocase of mitochondria.," *J. Biol. Chem.*, vol. 276, no. 28, pp. 25856–61, Jul. 2001.

[128] M. T. Ryan, W. Voos, and N. Pfanner, "Assaying protein import into mitochondria.," *Methods Cell Biol.*, vol. 65, pp. 189–215, Jan. 2001.

[129] D. Harman, "Free radical theory of aging.," *Mutat. Res.*, vol. 275, no. 3–6, pp. 257–66, Sep. 1992.

[130] M. P. Murphy, "How mitochondria produce reactive oxygen species.," *Biochem. J.*, vol. 417, no. 1, pp. 1–13, Jan. 2009.

[131] M. Ott, V. Gogvadze, S. Orrenius, and B. Zhivotovsky, "Mitochondria, oxidative stress and cell death.," *Apoptosis*, vol. 12, no. 5, pp. 913–22, May 2007.

[132] J. F. Turrens and A. Boveris, "Generation of superoxide anion by the NADH dehydrogenase of bovine heart mitochondria.," *Biochem. J.*, vol. 191, no. 2, pp. 421–7, Nov. 1980.

[133] R. S. Balaban, S. Nemoto, and T. Finkel, "Mitochondria, oxidants, and aging.," *Cell*, vol. 120, no. 4, pp. 483–95, Feb. 2005.

[134] L. Zhang, L. Yu, and C. A. Yu, "Generation of superoxide anion by succinate-cytochrome c reductase from bovine heart mitochondria.," *J. Biol. Chem.*, vol. 273, no. 51, pp. 33972–6, Dec. 1998.

[135] J. Hirst, J. Carroll, I. M. Fearnley, R. J. Shannon, and J. E. Walker, “The nuclear encoded subunits of complex I from bovine heart mitochondria.,” *Biochim. Biophys. Acta*, vol. 1604, no. 3, pp. 135–50, Jul. 2003.

[136] L. A. Sazanov, “Respiratory complex I: mechanistic and structural insights provided by the crystal structure of the hydrophilic domain.,” *Biochemistry*, vol. 46, no. 9, pp. 2275–88, Mar. 2007.

[137] P. C. Hinkle, R. A. Butow, E. Racker, and B. Chance, “Partial resolution of the enzymes catalyzing oxidative phosphorylation. XV. Reverse electron transfer in the flavin-cytochrome beta region of the respiratory chain of beef heart submitochondrial particles.,” *J. Biol. Chem.*, vol. 242, no. 22, pp. 5169–73, Nov. 1967.

[138] S. Iwata, J. W. Lee, K. Okada, J. K. Lee, M. Iwata, B. Rasmussen, T. A. Link, S. Ramaswamy, and B. K. Jap, “Complete structure of the 11-subunit bovine mitochondrial cytochrome bc1 complex.,” *Science*, vol. 281, no. 5373, pp. 64–71, Jul. 1998.

[139] J. F. Turrens, A. Alexandre, and A. L. Lehninger, “Ubisemiquinone is the electron donor for superoxide formation by complex III of heart mitochondria.,” *Arch. Biochem. Biophys.*, vol. 237, no. 2, pp. 408–14, Mar. 1985.

[140] Y. Liu, G. Fiskum, and D. Schubert, “Generation of reactive oxygen species by the mitochondrial electron transport chain.,” *J. Neurochem.*, vol. 80, no. 5, pp. 780–7, Mar. 2002.

[141] I. V Grigolava, M. I. Ksenzenko, A. A. Konstantinob, A. N. Tikhonov, and T. M. Kerimov, “[Tiron as a spin-trap for superoxide radicals produced by the respiratory chain of submitochondrial particles].,” *Biokhimiia (Moscow, Russ.*, vol. 45, no. 1, pp. 75–82, Jan. 1980.

[142] F. L. Muller, Y. Liu, and H. Van Remmen, “Complex III releases superoxide to both sides of the inner mitochondrial membrane.,” *J. Biol. Chem.*, vol. 279, no. 47, pp. 49064–73, Nov. 2004.

[143] I. G. Kirkinezos and C. T. Moraes, “Reactive oxygen species and mitochondrial diseases.,” *Semin. Cell Dev. Biol.*, vol. 12, no. 6, pp. 449–57, Dec. 2001.

[144] W. Vogt, “Oxidation of methionyl residues in proteins: tools, targets, and reversal.,” *Free Radic. Biol. Med.*, vol. 18, no. 1, pp. 93–105, Jan. 1995.

[145] A. Azem, W. Oppliger, A. Lustig, P. Jenö, B. Feifel, G. Schatz, and M. Horst, “The mitochondrial hsp70 chaperone system. Effect of adenine nucleotides, peptide substrate, and mGrpE on the oligomeric state of mhsp70.,” *J. Biol. Chem.*, vol. 272, no. 33, pp. 20901–6, Aug. 1997.

[146] D. Schiller, Y. C. Cheng, Q. Liu, W. Walter, and E. A. Craig, “Residues of Tim44 involved in both association with the translocon of the inner mitochondrial membrane and regulation of mitochondrial Hsp70 tethering.,” *Mol. Cell. Biol.*, vol. 28, no. 13, pp. 4424–33, Jul. 2008.

[147] A. Matouschek, N. Pfanner, and W. Voos, “Protein unfolding by mitochondria. The Hsp70 import motor.,” *EMBO Rep.*, vol. 1, no. 5, pp. 404–10, Nov. 2000.

[148] O. Deloche and C. Georgopoulos, “Purification and biochemical properties of Saccharomyces cerevisiae’s Mge1p, the mitochondrial cochaperone of Ssc1p.,” *J. Biol. Chem.*, vol. 271, no. 39, pp. 23960–6, Sep. 1996.

[149] S. Sakuragi, Q. Liu, and E. Craig, “Interaction between the nucleotide exchange factor Mge1 and the mitochondrial Hsp70 Ssc1.,” *J. Biol. Chem.*, vol. 274, no. 16, pp. 11275–82, Apr. 1999.

[150] J. P. Grimshaw, I. Jelesarov, H. J. Schönfeld, and P. Christen, “Reversible thermal transition in GrpE, the nucleotide exchange factor of the DnaK heat-shock system.,” *J. Biol. Chem.*, vol. 276, no. 9, pp. 6098–104, Mar. 2001.

[151] J. P. A. Grimshaw, I. Jelesarov, R. K. Siegenthaler, and P. Christen, “Thermosensor action of GrpE. The DnaK chaperone system at heat shock temperatures.,” *J. Biol. Chem.*, vol. 278, no. 21, pp. 19048–53, May 2003.

[152] Y. Groemping and J. Reinstein, “Folding properties of the nucleotide exchange factor GrpE from Thermus thermophilus: GrpE is a thermosensor that mediates heat shock response.,” *J. Mol. Biol.*, vol. 314, no. 1, pp. 167–78, Nov. 2001.

[153] F. Moro and A. Muga, “Thermal adaptation of the yeast mitochondrial Hsp70 system is regulated by the reversible unfolding of its nucleotide exchange factor.,” *J. Mol. Biol.*, vol. 358, no. 5, pp. 1367–77, May 2006.

[154] S. Laloraya, P. J. Dekker, W. Voos, E. A. Craig, and N. Pfanner, “Mitochondrial GrpE modulates the function of matrix Hsp70 in translocation and maturation of preproteins.,” *Mol. Cell. Biol.*, vol. 15, no. 12, pp. 7098–105, Dec. 1995.

[155] B. Westermann, C. Prip-Buus, W. Neupert, and E. Schwarz, “The role of the GrpE homologue, Mge1p, in mediating protein import and protein folding in mitochondria.,” *EMBO J.*, vol. 14, no. 14, pp. 3452–60, Jul. 1995.

[156] R. Dutkiewicz, J. Marszalek, B. Schilke, E. A. Craig, R. Lill, and U. Mühlenhoff, “The Hsp70 chaperone Ssq1p is dispensable for iron-sulfur cluster formation on the scaffold protein Isu1p.,” *J. Biol. Chem.*, vol. 281, no. 12, pp. 7801–8, Mar. 2006.

[157] C. Mammucari and R. Rizzuto, “Signaling pathways in mitochondrial dysfunction and aging.,” *Mech. Ageing Dev.*, vol. 131, no. 7–8, pp. 536–43, Jan. .

[158] D. A. Drechsel and M. Patel, “Differential contribution of the mitochondrial respiratory chain complexes to reactive oxygen species production by redox cycling agents implicated in parkinsonism.,” *Toxicol. Sci.*, vol. 112, no. 2, pp. 427–34, Dec. 2009.

[159] B. Szczesny, T. K. Hazra, J. Papaconstantinou, S. Mitra, and I. Boldogh, “Age-dependent deficiency in import of mitochondrial DNA glycosylases required for repair

of oxidatively damaged bases.," *Proc. Natl. Acad. Sci. U. S. A.*, vol. 100, no. 19, pp. 10670–5, Sep. 2003.

[160] G. Wright, K. Terada, M. Yano, I. Sergeev, and M. Mori, "Oxidative stress inhibits the mitochondrial import of preproteins and leads to their degradation.," *Exp. Cell Res.*, vol. 263, no. 1, pp. 107–17, Feb. 2001.

[161] A.-L. Bulteau, M. Ikeda-Saito, and L. I. Szweda, "Redox-dependent modulation of aconitase activity in intact mitochondria.," *Biochemistry*, vol. 42, no. 50, pp. 14846–55, Dec. 2003.

[162] A. P. D. Demasi, G. A. G. Pereira, and L. E. S. Netto, "Yeast oxidative stress response. Influences of cytosolic thioredoxin peroxidase I and of the mitochondrial functional state.," *FEBS J.*, vol. 273, no. 4, pp. 805–16, Feb. 2006.

[163] H. Saito and H. Uchida, "Initiation of the DNA replication of bacteriophage lambda in Escherichia coli K12.," *J. Mol. Biol.*, vol. 113, no. 1, pp. 1–25, Jun. 1977.

[164] L. Bolliger, O. Deloche, B. S. Glick, C. Georgopoulos, P. Jenö, N. Kronidou, M. Horst, N. Morishima, and G. Schatz, "A mitochondrial homolog of bacterial GrpE interacts with mitochondrial hsp70 and is essential for viability.," *EMBO J.*, vol. 13, no. 8, pp. 1998–2006, Apr. 1994.

[165] W. Voos, B. D. Gambill, S. Laloraya, D. Ang, E. A. Craig, and N. Pfanner, "Mitochondrial GrpE is present in a complex with hsp70 and preproteins in transit across membranes.," *Mol. Cell. Biol.*, vol. 14, no. 10, pp. 6627–34, Oct. 1994.

[166] M. Horst, W. Oppliger, S. Rospert, H. J. Schönfeld, G. Schatz, and A. Azem, "Sequential action of two hsp70 complexes during protein import into mitochondria.," *EMBO J.*, vol. 16, no. 8, pp. 1842–9, Apr. 1997.

[167] Y. Kubo, T. Tsunehiro, S. Nishikawa, M. Nakai, E. Ikeda, A. Toh-e, N. Morishima, T. Shibata, and T. Endo, "Two distinct mechanisms operate in the reactivation of heat-denatured proteins by the mitochondrial Hsp70/Mdj1p/Yge1p chaperone system.," *J. Mol. Biol.*, vol. 286, no. 2, pp. 447–64, Feb. 1999.

[168] S. Schmidt, A. Strub, K. Röttgers, N. Zufall, and W. Voos, "The two mitochondrial heat shock proteins 70, Ssc1 and Ssq1, compete for the cochaperone Mge1.," *J. Mol. Biol.*, vol. 313, no. 1, pp. 13–26, Oct. 2001.

[169] C. J. Harrison, M. Hayer-Hartl, M. Di Liberto, F. Hartl, and J. Kuriyan, "Crystal structure of the nucleotide exchange factor GrpE bound to the ATPase domain of the molecular chaperone DnaK.," *Science*, vol. 276, no. 5311, pp. 431–5, Apr. 1997.

[170] U. K. LAEMMLI, "Cleavage of Structural Proteins during the Assembly of the Head of Bacteriophage T4," *Nature*, vol. 227, no. 5259, pp. 680–685, Aug. 1970.

[171] R. D. Gietz and R. A. Woods, "Yeast transformation by the LiAc/SS Carrier DNA/PEG method.," *Methods Mol. Biol.*, vol. 313, pp. 107–20, Jan. 2006.

[172] J. H. Ryu, Y. Lee, S. K. Han, and H. Y. Kim, “The role of hydrogen peroxide produced by polychlorinated biphenyls in PMR1-deficient yeast cells.,” *J. Biochem.*, vol. 134, no. 1, pp. 137–42, Jul. 2003.

[173] P. V Viitanen, T. H. Lubben, J. Reed, P. Goloubinoff, D. P. O’Keefe, and G. H. Lorimer, “Chaperonin-facilitated refolding of ribulosebisphosphate carboxylase and ATP hydrolysis by chaperonin 60 (groEL) are K+ dependent.,” *Biochemistry*, vol. 29, no. 24, pp. 5665–71, Jun. 1990.

[174] L. Men and Y. Wang, “The oxidation of yeast alcohol dehydrogenase-1 by hydrogen peroxide in vitro.,” *J. Proteome Res.*, vol. 6, no. 1, pp. 216–25, Jan. 2007.

[175] D. A. Fancy and T. Kodadek, “Chemistry for the analysis of protein-protein interactions: rapid and efficient cross-linking triggered by long wavelength light.,” *Proc. Natl. Acad. Sci. U. S. A.*, vol. 96, no. 11, pp. 6020–4, May 1999.

[176] Y. H. Kim, A. H. Berry, D. S. Spencer, and W. E. Stites, “Comparing the effect on protein stability of methionine oxidation versus mutagenesis: steps toward engineering oxidative resistance in proteins.,” *Protein Eng.*, vol. 14, no. 5, pp. 343–7, May 2001.

[177] A. Roy, A. Kucukural, and Y. Zhang, “I-TASSER: a unified platform for automated protein structure and function prediction.,” *Nat. Protoc.*, vol. 5, no. 4, pp. 725–38, Apr. 2010.

[178] Y. Zhang, “I-TASSER server for protein 3D structure prediction.,” *BMC Bioinformatics*, vol. 9, p. 40, Jan. 2008.

[179] E. H. Smith, R. Janknecht, and L. J. Maher, “Succinate inhibition of alpha-ketoglutarate-dependent enzymes in a yeast model of paraganglioma.,” *Hum. Mol. Genet.*, vol. 16, no. 24, pp. 3136–48, Dec. 2007.

[180] D. Mokranjac, M. Sichting, W. Neupert, and K. Hell, “Tim14, a novel key component of the import motor of the TIM23 protein translocase of mitochondria.,” *EMBO J.*, vol. 22, no. 19, pp. 4945–56, Oct. 2003.

[181] S. P. Curran, D. Leuenberger, E. Schmidt, and C. M. Koehler, “The role of the Tim8p-Tim13p complex in a conserved import pathway for mitochondrial polytopic inner membrane proteins.,” *J. Cell Biol.*, vol. 158, no. 6, pp. 1017–27, Sep. 2002.

[182] C. Schöneich, “Reactive oxygen species and biological aging: a mechanistic approach.,” *Exp. Gerontol.*, vol. 34, no. 1, pp. 19–34, Jan. 1999.

[183] M. T. Lin and M. F. Beal, “Mitochondrial dysfunction and oxidative stress in neurodegenerative diseases.,” *Nature*, vol. 443, no. 7113, pp. 787–95, Oct. 2006.

[184] A. Zuin, N. Gabrielli, I. A. Calvo, S. García-Santamarina, K.-L. Hoe, D. U. Kim, H.-O. Park, J. Hayles, J. Ayté, and E. Hidalgo, “Mitochondrial dysfunction increases oxidative stress and decreases chronological life span in fission yeast.,” *PLoS One*, vol. 3, no. 7, p. e2842, Jan. 2008.

[185] H. M. Cochemé and M. P. Murphy, “Complex I is the major site of mitochondrial superoxide production by paraquat.,” *J. Biol. Chem.*, vol. 283, no. 4, pp. 1786–98, Jan. 2008.

[186] G. Wright, V. Reichenbecher, T. Green, G. L. Wright, and S. Wang, “Paraquat inhibits the processing of human manganese-dependent superoxide dismutase by SF-9 insect cell mitochondria.,” *Exp. Cell Res.*, vol. 234, no. 1, pp. 78–84, Jul. 1997.

[187] G. Wright and V. Reichenbecher, “The effects of superoxide and the peripheral benzodiazepine receptor ligands on the mitochondrial processing of manganese-dependent superoxide dismutase.,” *Exp. Cell Res.*, vol. 246, no. 2, pp. 443–50, Feb. 1999.

[188] B. Wu, A. Wawrzynow, M. Zylicz, and C. Georgopoulos, “Structure-function analysis of the Escherichia coli GrpE heat shock protein.,” *EMBO J.*, vol. 15, no. 18, pp. 4806–16, Sep. 1996.

[189] F. Moro, S. G. Taneva, A. Velázquez-Campoy, and A. Muga, “GrpE N-terminal domain contributes to the interaction with Dnak and modulates the dynamics of the chaperone substrate binding domain.,” *J. Mol. Biol.*, vol. 374, no. 4, pp. 1054–64, Dec. 2007.

[190] S. A. Knight, N. B. Sepuri, D. Pain, and A. Dancis, “Mt-Hsp70 homolog, Ssc2p, required for maturation of yeast frataxin and mitochondrial iron homeostasis.,” *J. Biol. Chem.*, vol. 273, no. 29, pp. 18389–93, Jul. 1998.

[191] C. Voisine, B. Schilke, M. Ohlson, H. Beinert, J. Marszalek, and E. A. Craig, “Role of the mitochondrial Hsp70s, Ssc1 and Ssq1, in the maturation of Yfh1.,” *Mol. Cell. Biol.*, vol. 20, no. 10, pp. 3677–84, May 2000.

[192] R. L. Levine, B. S. Berlett, J. Moskovitz, L. Mosoni, and E. R. Stadtman, “Methionine residues may protect proteins from critical oxidative damage.,” *Mech. Ageing Dev.*, vol. 107, no. 3, pp. 323–32, Mar. 1999.

[193] S. A. Rensing and U. G. Maier, “Phylogenetic analysis of the stress-70 protein family.,” *J. Mol. Evol.*, vol. 39, no. 1, pp. 80–6, Jul. 1994.

[194] D. A. Parsell and S. Lindquist, “The function of heat-shock proteins in stress tolerance: degradation and reactivation of damaged proteins.,” *Annu. Rev. Genet.*, vol. 27, pp. 437–96, Jan. 1993.

[195] J. C. Bardwell and E. A. Craig, “Major heat shock gene of Drosophila and the Escherichia coli heat-inducible dnaK gene are homologous.,” *Proc. Natl. Acad. Sci. U. S. A.*, vol. 81, no. 3, pp. 848–52, Feb. 1984.

[196] A. Gragerov, E. Nudler, N. Komissarova, G. A. Gaitanaris, M. E. Gottesman, and V. Nikiforov, “Cooperation of GroEL/GroES and DnaK/DnaJ heat shock proteins in preventing protein misfolding in Escherichia coli.,” *Proc. Natl. Acad. Sci. U. S. A.*, vol. 89, no. 21, pp. 10341–4, Nov. 1992.

[197] A. Zhuravleva and L. M. Gierasch, “Allosteric signal transmission in the nucleotide-binding domain of 70-kDa heat shock protein (Hsp70) molecular chaperones.,” *Proc. Natl. Acad. Sci. U. S. A.*, vol. 108, no. 17, pp. 6987–92, Apr. 2011.

[198] M. E. Feder and G. E. Hofmann, “Heat-shock proteins, molecular chaperones, and the stress response: evolutionary and ecological physiology.,” *Annu. Rev. Physiol.*, vol. 61, pp. 243–82, Jan. 1999.

[199] R. K. Siegenthaler and P. Christen, “The importance of having thermosensor control in the DnaK chaperone system.,” *J. Biol. Chem.*, vol. 280, no. 15, pp. 14395–401, Apr. 2005.

[200] Y. Groemping, D. Klostermeier, C. Herrmann, T. Veit, R. Seidel, and J. Reinstein, “Regulation of ATPase and chaperone cycle of DnaK from Thermus thermophilus by the nucleotide exchange factor GrpE.,” *J. Mol. Biol.*, vol. 305, no. 5, pp. 1173–83, Feb. 2001.

[201] A. Marada, P. K. Allu, A. Murari, B. PullaReddy, P. Tammineni, V. R. Thiriveedi, J. Danduprolu, and N. B. V Sepuri, “Mge1, a nucleotide exchange factor of Hsp70, acts as an oxidative sensor to regulate mitochondrial Hsp70 function.,” *Mol. Biol. Cell*, vol. 24, no. 6, pp. 692–703, Mar. 2013.

[202] S. F. Altschul, W. Gish, W. Miller, E. W. Myers, and D. J. Lipman, “Basic local alignment search tool.,” *J. Mol. Biol.*, vol. 215, no. 3, pp. 403–10, Oct. 1990.

[203] S. Dutta, K. Burkhardt, G. J. Swaminathan, T. Kosada, K. Henrick, H. Nakamura, and H. M. Berman, “Data deposition and annotation at the worldwide protein data bank.,” *Methods Mol. Biol.*, vol. 426, pp. 81–101, Jan. 2008.

[204] A. Sali and T. L. Blundell, “Comparative protein modelling by satisfaction of spatial restraints.,” *J. Mol. Biol.*, vol. 234, no. 3, pp. 779–815, Dec. 1993.

[205] R. A. Laskowski, M. W. MacArthur, D. S. Moss, and J. M. Thornton, “PROCHECK: a program to check the stereochemical quality of protein structures,” *J. Appl. Crystallogr.*, vol. 26, no. 2, pp. 283–291, Apr. 1993.

[206] I. Ilinkin, J. Ye, and R. Janardan, “Multiple structure alignment and consensus identification for proteins.,” *BMC Bioinformatics*, vol. 11, p. 71, Jan. 2010.

[207] W. van Gunsteren, S. Billeter, A. Eising, P. Hünenberger, P. Krüger, A. Mark, W. Scott, and I. Tironi, “Biomolecular Simulation: The {GROMOS96} manual and userguide,” 1996.

[208] T. Darden, D. York, and L. Pedersen, “Particle mesh Ewald: An N·log(N) method for Ewald sums in large systems,” *J. Chem. Phys.*, vol. 98, no. 12, p. 10089, Jun. 1993.

[209] U. Essmann, L. Perera, M. L. Berkowitz, T. Darden, H. Lee, and L. G. Pedersen, “A smooth particle mesh Ewald method,” *J. Chem. Phys.*, vol. 103, no. 19, p. 8577, Nov. 1995.

[210] G. Bussi, D. Donadio, and M. Parrinello, “Canonical sampling through velocity rescaling.,” *J. Chem. Phys.*, vol. 126, no. 1, p. 014101, Jan. 2007.

[211] B. Hess, H. Bekker, H. J. C. Berendsen, and J. G. E. M. Fraaije, “LINCS: A linear constraint solver for molecular simulations,” *J. Comput. Chem.*, vol. 18, no. 12, pp. 1463–1472, Sep. 1997.

[212] N. Schülke, N. B. Sepuri, and D. Pain, “In vivo zippering of inner and outer mitochondrial membranes by a stable translocation intermediate.,” *Proc. Natl. Acad. Sci. U. S. A.*, vol. 94, no. 14, pp. 7314–9, Jul. 1997.

[213] T. Bender, I. Lewrenz, S. Franken, C. Baitzel, and W. Voos, “Mitochondrial enzymes are protected from stress-induced aggregation by mitochondrial chaperones and the Pim1/LON protease.,” *Mol. Biol. Cell*, vol. 22, no. 5, pp. 541–54, Mar. 2011.

[214] A. Nakamura, K. Takumi, and K. Miki, “Crystal structure of a thermophilic GrpE protein: insight into thermosensing function for the DnaK chaperone system.,” *J. Mol. Biol.*, vol. 396, no. 4, pp. 1000–11, Mar. 2010.

[215] C.-C. Wu, V. Naveen, C.-H. Chien, Y.-W. Chang, and C.-D. Hsiao, “Crystal structure of DnaK protein complexed with nucleotide exchange factor GrpE in DnaK chaperone system: insight into intermolecular communication.,” *J. Biol. Chem.*, vol. 287, no. 25, pp. 21461–70, Jun. 2012.

[216] Y. Sanchez, J. Taulien, K. A. Borkovich, and S. Lindquist, “Hsp104 is required for tolerance to many forms of stress.,” *EMBO J.*, vol. 11, no. 6, pp. 2357–64, Jun. 1992.

[217] S. Nwaka, B. Mechler, O. von Ahsen, and H. Holzer, “The heat shock factor and mitochondrial Hsp70 are necessary for survival of heat shock in Saccharomyces cerevisiae.,” *FEBS Lett.*, vol. 399, no. 3, pp. 259–63, Dec. 1996.

[218] M. Schmitt, W. Neupert, and T. Langer, “The molecular chaperone Hsp78 confers compartment-specific thermotolerance to mitochondria.,” *J. Cell Biol.*, vol. 134, no. 6, pp. 1375–86, Sep. 1996.

[219] C. Harrison, “GrpE, a nucleotide exchange factor for DnaK.,” *Cell Stress Chaperones*, vol. 8, no. 3, pp. 218–24, Jan. 2003.

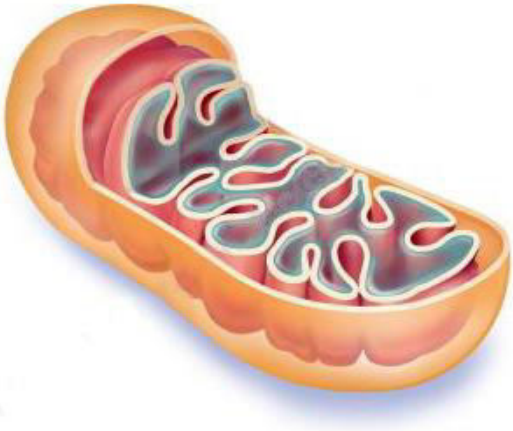

PUBLICATIONS

MBoC | ARTICLE

Mge1, a nucleotide exchange factor of Hsp70, acts as an oxidative sensor to regulate mitochondrial Hsp70 function

Adinarayana Marada, Praveen Kumar Allu, Anjaneyulu Murari, BhoomiReddy PullaReddy, Prasad Tammineni, Venkata Ramana Thiriveedi, Jayasree Danduprolu, and Naresh Babu V. Sepuri
Department of Biochemistry, School of Life Sciences, University of Hyderabad, Hyderabad 500046, India

ABSTRACT Despite the growing evidence of the role of oxidative stress in disease, its molecular mechanism of action remains poorly understood. The yeast *Saccharomyces cerevisiae* provides a valuable model system in which to elucidate the effects of oxidative stress on mitochondria in higher eukaryotes. Dimeric yeast Mge1, the cochaperone of heat shock protein 70 (Hsp70), is essential for exchanging ATP for ADP on Hsp70 and thus for recycling of Hsp70 for mitochondrial protein import and folding. Here we show an oxidative stress–dependent decrease in Mge1 dimer formation accompanied by a concomitant decrease in Mge1–Hsp70 complex formation in vitro. The Mge1-M155L substitution mutant stabilizes both Mge1 dimer and Mge1–Hsp70 complex formation. Most important, the Mge1-M155L mutant rescues the slow-growth phenomenon associated with the wild-type Mge1 strain in the presence of H_2O_2 in vivo, stimulation of the ATPase activity of Hsp70, and the protein import defect during oxidative stress in vitro. Furthermore, cross-linking studies reveal that Mge1–Hsp70 complex formation in mitochondria isolated from wild-type Mge1 cells is more susceptible to reactive oxygen species compared with mitochondria from Mge1-M155L cells. This novel oxidative sensor capability of yeast Mge1 might represent an evolutionarily conserved function, given that human recombinant dimeric Mge1 is also sensitive to H_2O_2.

Monitoring Editor
Ramanujan S. Hegde
National Institutes of Health

Received: Oct 5, 2012
Revised: Jan 8, 2013
Accepted: Jan 14, 2013

INTRODUCTION

Mitochondria are essential organelles involved in many cellular processes, such as energy metabolism and apoptosis. Although the mitochondrion has its own genome, it depends on the nucleus for optimal functioning (Chacinska *et al.*, 2009). Based on their signal sequence, mitochondrial proteins encoded by nuclear DNA are targeted to different subcompartments of mitochondria through a translocase system present on outer and inner mitochondrial membranes known as the translocase of outer membrane (TOM) and translocase of inner membrane (TIM) complexes, respectively (Schulke *et al.*, 1997, 1999; Endo *et al.*, 2003; Kutik *et al.*, 2007; Neupert and Herrmann, 2007). Targeting of precursor protein to the matrix involves an interplay among many proteins; however, the final step of this process is mediated by Tim44 and a translocation motor that contains mitochondrial heat shock protein 70 (mHsp70), Pam16, Pam18, and the nucleotide exchange factor Mge1 (Azem *et al.*, 1997; Mokranjac *et al.*, 2007; Stojanovski *et al.*, 2007; Schiller *et al.*, 2008). Hsp70, in combination with Tim44, binds to the emerging end of the transit peptide from the TIM channel in an ATP-dependent manner, and the ATPase cycle of mHsp70 leads to pulling or vectorial translocation of preproteins across the inner mitochondrial membrane (Matouschek *et al.*, 2000; Okamoto *et al.*, 2002; Liu *et al.*, 2003). Mge1, a component of this translocation motor, accelerates the exchange of ATP for ADP on mHsp70 and promotes a change from the high–substrate affinity conformation of mHsp70 to a lower–substrate affinity form with a concomitant release of precursor protein from mHsp70 to begin the next round of translocation

This article was published online ahead of print in MBoC in Press (http://www.molbiolcell.org/cgi/doi/10.1091/mbc.E12-10-0719) on January 23, 2013.

Address correspondence to: Naresh Babu V. Sepuri (nareshuohyd@gmail.com or nbvssl@uohyd.ernet.in).

Abbreviations used: Ccpo, cytochrome *c* peroxidase; DHFR, dihydrofolate reductase; HSP 70, heat shock protein 70; ROS, reactive oxygen species; Tim, translocase of inner membrane; Tom, translocase of outer membrane.

Supplemental Material can be found at:
http://www.molbiolcell.org/content/suppl/2013/01/21/mbc.E12-10-0719v1.DC1.html

MBoC | ARTICLE

Methionine sulfoxide reductase 2 reversibly regulates Mge1, a cochaperone of mitochondrial Hsp70, during oxidative stress

Praveen Kumar Allu, Adinarayana Marada, Yerranna Boggula, Srinivasu Karri, Thanuja Krishnamoorthy, and Naresh Babu V. Sepuri
Department of Biochemistry, School of Life Sciences, University of Hyderabad, Gachibowli, Hyderabad 500046, India

ABSTRACT Peptide methionine sulfoxide reductases are conserved enzymes that reduce oxidized methionines in protein(s). Although these reductases have been implicated in several human diseases, there is a dearth of information on the identity of their physiological substrates. By using *Saccharomyces cerevisiae* as a model, we show that of the two methionine sulfoxide reductases (MXR1, MXR2), deletion of mitochondrial MXR2 renders yeast cells more sensitive to oxidative stress than the cytosolic MXR1. Our earlier studies showed that Mge1, an evolutionarily conserved nucleotide exchange factor of Hsp70, acts as an oxidative sensor to regulate mitochondrial Hsp70. In the present study, we show that Mxr2 regulates Mge1 by selectively reducing MetO at position 155 and restores the activity of Mge1 both in vitro and in vivo. Mge1 M155L mutant rescues the slow-growth phenotype and aggregation of proteins of *mxr2*□ strain during oxidative stress. By identifying the first mitochondrial sub- strate for Mxrs, we add a new paradigm to the regulation of the oxidative stress response pathway.

Monitoring Editor
Thomas D. Fox
Cornell University

Received: Sep 13, 2014
Revised: Nov 17, 2014
Accepted: Nov 20, 2014

INTRODUCTION

Persistent oxidative stress is responsible for several neurological disorders, heart failure, and ageing (Finkel and Holbrook, 2000; Orrenius *et al.*, 2007). To combat oxidative stress, cellular systems have evolved several antioxidant defensive mechanisms. Methionine sulfoxide reductases (Msrs) are among the important regulators of oxidative stress (Levine *et al.*, 2000). These enzymes reduce either free or protein-bound oxidized methionine in a thioredoxin and thioredoxin reductase–dependent mechanism to prevent the accumulation of oxidized proteins and amino acids. In yeast, they are three methionine sulfoxide reductases, known as fRMsr, Mxr1/MsrA, and Mxr2/MsrB. The first is responsible for reducing free methionine sulfoxide (free Met-SO), and the last two are involved in the reduction of oxidized methionine present in proteins (Boschi-Muller *et al.*, 2008; Le *et al.*, 2009). Oxidation of methionine can produce a diastereomeric mixture of R and S methionine sulfoxide forms. Mxr1 apparently plays a role in reducing the S form of sulfoxide, whereas Mxr2 acts specifically on R sulfoxides. The mechanism of action of these enzymes has been well characterized in vitro using reconstitution assays containing purified Mxrs (Boschi-Muller *et al.*, 2008; Tarrago *et al.*, 2012). Homologues of Mxr proteins are present across evolution and have been found to play an essential role in the prevention of oxidative damage to proteins mediated by reactive oxygen species (ROS) in bacterial, plant, and animal cells (Zhang and Weissbach, 2008). These enzymes have been implicated in ageing and age-related disorders such as Alzheimer and Parkinson disease, cataract development, and insulin resistance (Gabbita *et al.*, 1999; Kantorow *et al.*, 2004; Glaser *et al.*, 2005; Styskal *et al.*, 2013). Despite their clinical relevance, there is a paucity of information on the identity of the physiological substrates of Mxrs and their regulation. Several reports suggest NF-κBα, potassium channel, and calmodulin as possible substrates of Mxrs (Ciorba *et al.*, 1997; Midwinter *et al.*, 2006; Erickson *et al.*, 2008). In a recent report, SelR, a homologue of MsrB in *Drosophila*, was shown to reduce the oxidized R form of methionine in actin and thereby regulate actin polymerization (Hung *et al.*, 2013). In mammals, MsrA has two isoforms present

This article was published online ahead of print in MBoC in Press (http://www.molbiolcell.org/cgi/doi/10.1091/mbc.E14-09-1371).
Address correspondence to: Naresh Babu V. Sepuri (nareshuohyd@gmail.com, nbvssl@uohyd.ernet.in).
Abbreviations used: